

THE DEVELOPMENT OF A PROTOTYPE
CROP RESIDUES BURNING MACHINE

By

NI NYOMAN SULASTRI

Bachelor of Science in Agricultural Engineering
Universitas Gadjah Mada
Yogyakarta, Indonesia
2004

Master of Agriculture in Environmental and Agricultural
Science
Tokyo University of Agriculture and Technology
Tokyo, Japan
2010

Submitted to the Faculty of the
Graduate College of the
Oklahoma State University
in partial fulfillment of
the requirements for
the Degree of
DOCTOR OF PHILOSOPHY
December 2019

THE DEVELOPMENT OF A PROTOTYPE CROP
RESIDUES BURNING MACHINE

Dissertation Approved:

Dr. John Long

Dissertation Adviser

Dr. Michael Buser

Dr. Ajay Kumar

Dr. Rodney Holcomb

ACKNOWLEDGEMENTS

I would like to show my sincere gratitude toward my advisor, Dr. John Long and my previous advisor Dr. Michael Buser, for their wisdom, patience, technical advice, and for all the manual labor they put into this project. I would also like to show my appreciation for the members of my committee, Dr. Ajay Kumar and Dr. Rodney Holcomb for their guidance and support.

I would like to thank my family for their love and support. I would also like to thank Collin and Jordan and the rest of my friends for their help as well as the welcome distraction they provided.

I greatly acknowledge the funding received toward my Ph.D. from Fulbright Program and Indonesia Government. The project would not have been possible without Mr. Wayne Kiner and Mr. Joe Preston and all the staff at the BAE laboratory. I would also like to thank Dr. Paul Funk and Mr. John Weir for their expert advice throughout this project. Finally, I would like to thank the faculty, staff and students of Biosystems and Agricultural Engineering Department for providing me with an academic home for last few years.

Name: NI NYOMAN SULASTRI

Date of Degree: DECEMBER, 2019

Title of Study: THE DEVELOPMENT OF A PROTOTYPE CROP RESIDUE BURNING MACHINE

Major Field: BIOSYSTEMS ENGINEERING

Abstract: The purpose of this study was to design, develop and evaluate a prototype crop residue burning machine that burns the largest area while maintaining burn uniformity. Additionally, the concentration of air pollutants and the machine cost was determined.

Three types of burners were assessed mainly in term of the generated flame temperature. Two of the burners were forced draft burners and the other was a natural draft burner. The burner that generated the best flame temperature for agricultural residue burning was then used for developing the prototype. Six burners were placed in a pyramidal shape combustion chamber. The effect of burner angle, crop residue loading rate on burned area percentages and burned uniformity were determined. Both burned area percentage and burned area uniformity were analyzed using image processing. Moreover, a control system was designed to ensure the machine operates in a safe manner. To evaluate the combustion conditions of the experimental system, CO₂, O₂, CO, NO and NO₂ concentrations were measured using an ECOM-EN2 flue gas analyzer. A Windows application was developed to systematically estimate the cost of the developed burning machine.

Six forced draft burners with 3/8" mixing tubes were used to develop the machine prototype. This burner generated a flame temperature of 800-840°C at 20 PSI. This temperature range was recorded at 5" from the burner flare. The burner angle of 67°, fuel loading of 2.9 ton/acre and travel speed of 1.9 mph had the highest percentage of burned area and relatively a higher burned area uniformity. The designed control system was able to maintain flame temperature in between 100 to 1000 °C and the LPG working pressure of ±10% from the set pressure. The gas emission study shows a high concentration of O₂ in the flue gas that suggests there was too much air was supplied for the combustion resulting in heat loss through flue gas. The cost of prescribed burning and the machine burning were comparable when the size of burn unit for prescribed burning was 134 acres. It indicates the potency of machine burning for small scale usage.

TABLE OF CONTENTS

Chapter	Page
SIGNATURE APPROVAL.....	ii
ACKNOWLEDGEMENTS.....	iii
ABSTRACT.....	iv
TABLE OF CONTENTS.....	v
LIST OF TABLES.....	viii
LIST OF FIGURES.....	ix
CHAPTER I.....	1
INTRODUCTION.....	1
CHAPTER II.....	4
OBJECTIVES.....	4
CHAPTER III.....	5
REVIEW OF LITERATURE.....	5
Grain harvesting.....	5
Post-harvest residue management.....	8
Crop residue burning.....	10
Fire effects on livestock production.....	13
Influence on technical factors.....	14
Burner type.....	14
Burner angle and height.....	18
Burner operating pressure.....	20
Speed of application.....	21
Orifice type.....	21
Flame type.....	22
Prescribed burning.....	23
Other means of thermal weed control.....	26
Environmental impact of biomass burning.....	27

CHAPTER IV	32
METHODOLOGY	32
LPG burner performance assessment	32
The burners	32
The burners experiment set up	34
Orifice discharge coefficient determination	39
The prototype of crop residue burning machine experiments	41
The prototype of crop residue burning machine development	41
Safety and fuel control system development	42
The machine components and configurations	45
Combustion chamber temperature measurement	47
Experimental set up and design to assess the machine performance	47
Burned area and burned uniformity determination	48
Gas emission measurement	52
The cost estimation determination	53
CHAPTER V	58
FINDINGS	58
Single burner performance assessment	58
Flame temperature	58
Discharge coefficient determination	60
Air flow rate estimation	62
Machine prototype performance assessment	64
Overview	64
The best burner angle determination	66
The best crop residue loading rate determination	72
The machine gas emission	77
The machine cost estimation	84
CHAPTER VI	93
CONCLUSIONS AND RECOMMENDATIONS	93
Conclusions	93
Recommendations	94
REFERENCES	96
APPENDICES	106
Appendix A1. Arduino codes for temperature measurements	106
Appendix A2. Arduino codes for safety fuel and control system	114
Appendix A3. MATLAB® codes for single burner temperature pattern	119

Appendix A4. MATLAB® codes for the prototype machine temperature pattern	120
Appendix A5. MATLAB® codes for image processing	126
Appendix A6. Microsoft Visual Studio® codes for the machine cost estimation.....	127
Appendix B1. Travel speed calibration	151
Appendix B2. Adjustable speed motor specification.....	151
Appendix B3. Blower motor specification	152
Appendix B4. Variable frequency drive specification.....	152
Appendix B5. Air compressor performance	152
Appendix C1. LPG pressure readings during the determination of the best burner angle study	152
Appendix C2. LPG pressure readings during the determination of the best crop loading rate study	153
Appendix C3. Air flowrate during the determinations of the best burner angle study	153
Appendix C4. Air flow rate during the determinations of the best crop loading rate study.	154
Appendix C5. Stack flowrate and velocity data	154
Appendix D1. One set of burner with 3/8” mixing tube.....	156
Appendix D2. The prototype crop residue burning machine.....	157
Appendix D3. Burner plumbing drawing	158
Appendix D4. The trolley system drawing.....	161
Appendix D5. Rectangular tray drawing	165
Appendix D6. Individual box drawing	166

LIST OF TABLES

Table	Page
Table 1. Category day classification (Bidwell et al., 2003).....	24
Table 2. Biomass burning emission in Asia	28
Table 3. Emission factors for open burning of wheat residue (g/kg).....	29
Table 4. Main characteristics of the burners.....	33
Table 5. Burner types tested for flame temperature.....	37
Table 6. Remaining salvage value as percent of new list price (Edward, 2015).	54
Table 7. The ANOVA table of flame temperature for.....	58
Table 8. Estimation of burner discharge coefficient (Cd).	61
Table 9. The Anova table of air flow rate.....	63
Table 10. The result of Kruskal-Wallis Test and Tukey HSD for burner angle's effect on the percentage of burned area.....	69
Table 11. The result of Kruskal-Wallis Test and Tukey HSD for burner angle's effect on the Uniformity coefficient of burned area.	71
Table 12. The result of Kruskal-Wallis Test and Tukey HSD for crop residues loading rate's effect on the percentage of burned area.....	73
Table 13. The results of Kruskal-Wallis Test and Tukey HSD for crop residues loading rate on the Uniformity coefficient of burned area.	75
Table 14. The results of Kruskal-Wallis test and Tukey HSD for CO emission factors.	80
Table 15. Kruskal-Wallis test and Tukey HSD for NO emission factor.....	82

LIST OF FIGURES

Figure	Page
Figure 1. Process diagram of a combine harvester (Srivastava et al., 1993)	5
Figure 2. Combine system(Xie et al., 2011)	7
Figure 3. Schematic section view of an early model of Oregon State University mobile field incinerator (John R. Hardison, 1976).....	11
Figure 4. Smokeless mobile field incinerator (Patent No. 3,606,877, 1971).....	12
Figure 5. Mobile field burner (Patent No. 3,802,020, 1974).	13
Figure 6. Vapor burners used in (Laguë et al., 1997). Left: flat burner, right: tubular burner.....	15
Figure 7. Three types of burners tested by (Kang, 2001).....	16
Figure 8. A box-shaped burner and flamer hood and burner mounting system (Neilson et al., 2017).....	17
Figure 9. Top view of atmospheric burner (A) and industrial burner (B) (Berry et al., 1921; US Bureau of Standards, 1931).....	18
Figure 10. Self-propelled flaming machine (M. Raffaelli et al., 2013)	20
Figure 11. Side view of an open burner set at an angle of 67° aimed backwards. The arrow shows the operating direction (Ascard, 1998)	20
Figure 12. Design of orifices. 1,2,3,4 are designated as sharp edge type and 5 is channel type....	22
Figure 13. Fire prescription planner (OK-Fire)	25
Figure 14. Burner 1 and 2	34
Figure 15. Burner 3	34
Figure 16. A fan-shaped flare	34
Figure 17. The burner experimental set up (A) Thermocouples, (B) Burner, (C) Propane line, (D) Airline, (a) Solenoid Valve, (b) Manual Shut-off valve, (c) Pressure gauges, (d) Air Flowmeter, (e) Globe valve, (f) Excess air valve.....	35
Figure 18. Temperature measurement data logging wiring	36
Figure 19. Thermocouple placing arrangement to determine the flame temperature pattern	39
Figure 20. The prototype of crop residue burning machine. The arrow shows the operating direction.	42
Figure 21. A set of three LPG burner.....	42
Figure 22. Safety and fuel control system flow chart.	43
Figure 23. Pressure sensor calibration curve	44
Figure 24. Temperature measurements and safety gas train wiring. (A) K-type thermocouple, (B) Solenoid valve, (C) Power source, (D) Pilot gas ignition control, (E) Transformer 24 V 1A, (F) 9V 1A Switching power supply, (G) Arduino Uno, (H) Pressure sensor (I) SD card module, (J) RTC DS1307, (K) MAX31856, (L) Solid State Relay.	45
Figure 25. The machine prototype components and configurations	46
Figure 26. Thermocouples arrangement for measuring combustion temperature in the combustion chamber. The red arrow shows the operating direction.	47
Figure 27. Flame temperature interaction plot of burner type (BT) and pressure (PL).	59
Figure 28. Flame temperature pattern of burner 1.	62
Figure 29. The blue flame generated by the burners.....	63
Figure 30. Air flow interaction plot of BT and PL.	64
Figure 31. The burners were set at four different angle (α).	65
Figure 32. The flame generated by the three set of burners in the combustion chamber.....	65
Figure 33. Temperature recorded inside the combustion chamber.	66

Figure 34. The image after the burn, where (A) is the original image and (B) is the binary image.	67
Figure 35. (A) The highest burned area percentage as a result of burner angle 67° Treatment, (B) the lowest burned area percentage as a result of burner angle of 22.5°)	68
Figure 36. The effect of burner angle treatment on burned area percentage.	69
Figure 37. The burned area uniformity determination by splitting each individual tray into two zones. (A) The original image (B) One of individual sand tray, B1 and B2 (The binary image that separated into two zones).	70
Figure 38. The effect of burner angle treatment on uniformity coefficient.	71
Figure 39. The effect of crop residue loading rate on burned are percentage.....	73
Figure 40. The binary images of a higher crop residues loading rate. (A) The after-burn surface image, (B). The after-burn image after flipping crop residues manually.....	74
Figure 41. The effect of crop residues loading rate treatment on uniformity coefficient.	75
Figure 42. The binary image comparison of (A) 3Low (B) 4Low.....	76
Figure 43. Combustion temperature recorded in the combustion chamber during gas emission measurement experiment gas emission. (A) 1 SET (B) 2 SET.....	77
Figure 44. The concentration of O ₂ , CO ₂ and CO in dry flue gas.....	78
Figure 45. CO emission factors (lb/acre).....	80
Figure 46. The CO concentrations in the flue gas (ppm).....	81
Figure 47. NO emission factors (lb/acre).....	82
Figure 48. NO concentrations in the flue gas (ppm).....	83
Figure 49. NO ₂ emission factors (lb/acre).....	84
Figure 50. NO ₂ concentrations in the flue gas (ppm).....	84
Figure 51. Windows app layout for determining fixed cost for the developed burning machine..	85
Figure 52. Window app for determining variable cost and total annual cost for the developed burning machine (\$/year).....	86
Figure 53. The machine's fixed cost calculation scenario.	87
Figure 54. The machine's variable cost calculation scenario.	91
Figure 55. Vegetable bed flamer's variable cost and total calculation scenario.....	91
Figure 56. The effect of increasing more acres of use and the machine size on machine cost.....	92
Figure 57. The effect of increasing field efficiency on machine total cost.....	92

CHAPTER I

INTRODUCTION

Fire is commonly used to remove a large amount of the residue (greater than 4-5 Mg per ha) typically left by harvesting machines, which makes soil tillage for the next planting difficult when there has been insufficient time for residue to decay (Valzano, Greene, & Murphy, 1997). In some cases, a late harvest can further complicate matters, leaving less time for farmers to till their fields and incorporate the residue before freezing soil temperatures make tillage difficult. If producers are unable to complete tillage operations in the fall, seeding can be delayed in the spring, which has the potential to negatively affect the next season's crop. As a result, many choose burning as a residue management option. Furthermore, fire can be used to reduce the intensive use of chemicals, especially for livestock operations where the application of herbicides is needed to control weeds in pastures. However, the intensive application of broadcast herbicides can kill plants, such as forbs, valuable to livestock production systems

Nowadays, liquefied propane gas (LPG)-fueled burner application in agriculture system is an increasingly attractive method for straw removal and maintaining crop and soil health. It is because LPG is non-toxic and does not leave chemical residue in or on soil, air and water (Knezevic, Datta, Bruening, & Gogos, 2014). Crop residue burning maintains a soil microclimate that is unfavorable to the development of plant diseases. The burning avoids residue toxicity as the result of large quantities of unweathered residues especially in non-inversion tillage systems. In this system, straw tends to be incorporated at shallow depth or left on the soil surface. The effect of residue on plant health leads to growth impairment, which is associated with emergence and growth rates or tillering (Morris, Miller, Orson, & Froud-Williams, 2009). In California, burning rice fields after harvesting eliminates straw and minimizes rice stem rot caused by *Sclerotium oryzae* (Webster, Bolstad, Wick, & Hall, 1976). Wheat stubble burning is a cultural practice used to control flag smut, twist disease, and wheat seed nematode. Flag smut and twist disease are caused by fungus species, *Urocystic agropyri* and *Dilophospora alopecuri*, respectively (Fuentes-Dávila, Goates, Thomas, Nielsen, & Ballantyne, 2002). Crop residue burning would remain an option, with the benefit of rapid, natural drying of the straw after rain and uniform distribution of the ash (Klinner, Neale, Arnold, Geikie, & Hobson, 1987). Furthermore, fire has been used to control weeds on rangelands. A frequent fire reintroduction has been conducted to control woody plants species that are invading rangelands throughout the United States. This practice has shown the most effective method to control invasive, nonsprouting native juniper. This juniper causes a drastic decline in forage production, which in turn affects carrying capacity, stocking rate and livestock performance (J. R. Weir, 2009).

In terms of promoting biodiversity, fire-based wildland management was compared to organic farming where both practices increase total organism abundance and evenness (Crowder, Northfield, Gomulkiewicz, & Snyder, 2012). Some experimental studies have shown biodiversity plays an

important role in biomass production, resource consumption, decomposition and other desirable ecosystem properties (Cadotte, Cardinale, & Oakley, 2008; Loreau et al., 2001).

While open field burning is a practical and economical practice for controlling insects, diseases, and weeds and improving soil nutrient health, the environmental risks of this activity are an issue. Open biomass burning is a major source of global air pollutants and aerosols. Approximately 40, 32, 20, and 50% of the annual global carbon monoxide, carbon dioxide, aerosols, and polycyclic aromatic hydrocarbons (PAHs) emissions were attributed to biomass burning (Yu, Lin, & Chang, 2012). For agricultural crop residue burning, it decreases air quality by producing greenhouse gases (CO₂, N₂O, CH₄), particulate matter (PM), and other air pollutants (CO, NH₃, NH_x, SO₂, NMHC, VOC) (Li et al., 2007). Those pollutants cause health issues, especially respiratory problems, and PAH particles smaller than 2.5µm can pose a human health hazard by entering the pulmonary alveoli (Jain, Bhatia, & Pathak, 2014; McCarty, Korontzi, Justice, & Loboda, 2009; H. H. Yang, Tsai, Chao, Su, & Chien, 2006). Even though LPG is a very clean burning, the combustion does emit carbon dioxide. Therefore, the propane consumption should be reduced as far as possible. It implies that it is important to improve burning equipment.

CHAPTER II

OBJECTIVES

The overall objective of this project was to develop a prototype machine for crop residue burning, which can effectively burn the crop residue left by harvesting machinery. Specifically, this project focuses on three research objectives:

- 2.1 To design, develop and evaluate a prototype crop residue burning machine that burns the largest area while maintaining burn uniformity.
- 2.2 To develop electronics, control systems and analyze pre- and post-burn image data
- 2.3 To estimate the concentration of air pollutants (CO, NO_x).
- 2.4 To determine several factors affecting the developed machine cost. Those factors were then used to develop a software for estimating the machine cost.

CHAPTER III

REVIEW OF LITERATURE

Grain harvesting

A combine harvester is a widely used mechanical harvesting method. There are three stages in the flow of the crop through a combine harvester including cutting and elevating, threshing, and separation (Bell, 1996). A modern combine performs many functional processes, including gathering and cutting or picking (in case of windrows), threshing, separation, and cleaning (Srivastava, Goering, & Rohrbach, 1993). Figure 1 shows the process diagram of a combine.

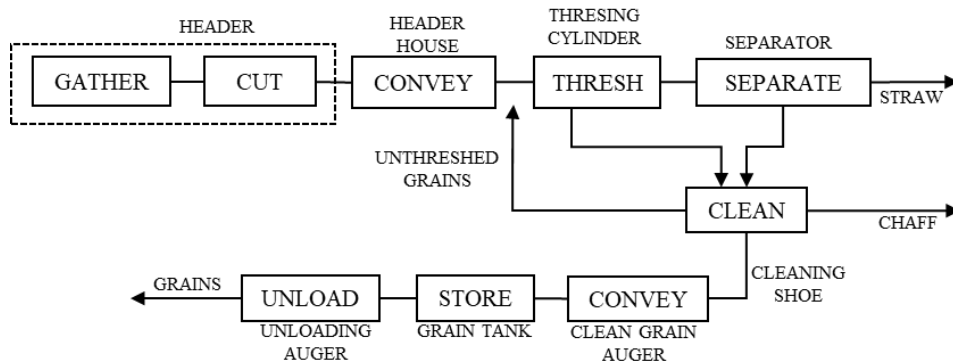


Figure 1. Process diagram of a combine harvester (Srivastava et al., 1993)

The height of the cut using a combine harvester varied in the range of 7.5-90 cm depending upon the plant density and forward speed of the combine harvester (Singh, 2016). Generally, a wheat crop is cut leaving approximately 100 mm stubble height (Špokas & Dainius Steponavičius, 2010). For optimum combine operation, the crop should be cut below the grain heads. Uneven crop height will result in losses (Srivastava et al., 1993).

The combine harvester has two major drawbacks. The first drawback is the increase in header losses as the increase of the crop maturity from the time combine ripeness is reached. The second drawback is the straw throughput; reduction in straw intake leads to higher potential work rates (Klinner et al., 1987).

Header loss contributes approximately 75% of harvesting process losses (Glancey, 1997).

(Glancey, 1997). Improper setting of header height causes a significant portion of the loss.

Header height is the distance between the cutting platform tip and ground. Figure 2 shows a schematic of a combine harvester system operating in the vertical plane. The header height can be adjusted by raising or lowering the header with an actuator. If the header height is too large, there is a reduction in harvest yield since much of the viable crop will be left unharvested. On the other side, if the header height is too low, it will damage the equipment and result in operator fatigue (Xie, Alleyne, Greer, & Deneault, 2011).

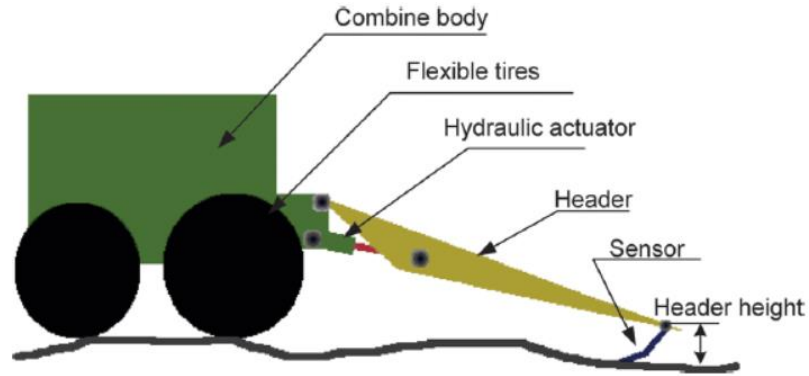


Figure 2. Combine system(Xie et al., 2011)

The header losses can be reduced to a minimum of about 80 kg/ha in winter wheat by stripping the seed off the crop in situ (Klinner et al., 1987; Tado, Wacker, Kutzbach, & Suministrado, 1998). The principle of stripping is taking the seeds from the plant without harvesting straw. As consequence, a stripper-header leaves standing stubble, which can dry out quickly after a rain (Klinner et al., 1987). In addition, harvesting with a stripper-header combine attachment maximizes soil and water conservation while minimizing harvest losses. Cutting height of a stripper-header was 0.3-0.5 m, which was higher compared to conventional a combine header. Taller stubble can capture more snow and reduced soil-water evaporation (Mcmaister, Aiken, & Nielsen, 2000).

Distribution of small grain residue produced by combines is evaluated using an uneven residue distribution ratio (URDR), dispersion index (DI) and shift index (SI). URDR is the ratio of the maximum total field residue concentration and the minimum total residue concentration. This ratio ranges from 1 for a uniform distribution to larger values for non-uniform distribution. DI is estimated by equation (1) with a lower limit of zero for a uniform distribution of cut residue; and an upper limit approaching one for a non-uniform distribution. SI is defined as the directional shift of the maximum residue concentration from the center of the header. The SI ranges from

zero to 1R or 1L when this distance is normalized by the parameter $\frac{x}{2}$ (Allmaras & Rasmussen, 1985; Douglas, Rasmussen, & Allmaras, 1989).

$$DI = \left(\frac{1}{2}\right)(X)(B)(A_+ + A_-) \quad (1)$$

Where,

X : the header width (m)

B : the field concentration (Mg/ha) of residue cut by the combine

A : the measured area enclosed by the residue distribution curve and the mean field residue concentration cut by the combine.

Combined with header widths ranging from 5.5 to 7.3 m yielded 4.8 to 7.1 Mg/ha of grain and 9 to 11.4 Mg/ha of straw plus chaff. URDR and DI were found varied to from 1.4 to 5.1, and 0.09 to 0.42 respectively (Allmaras & Rasmussen, 1985). The uniformity of residue distribution decreases as the header height lowers (Douglas et al., 1989).

Post-harvest residue management

Agricultural crop residues have several potential uses, for example for animal feed, animal bedding, soil erosion prevention, soil fertility maintenance and an energy source. They are also expensive to transport and store because of their low energy density (Dauve & Flaim, 1979).

Crop residue management/CRM (incorporation/retention) has been suggested as a non-chemical method to conserve soil nutrient reserves in the long term since the remaining stubble and straw incorporation returns most of the nutrients into the soil (Dobermann & Fairhurst, 2002).

Furthermore, incorporation/retention of crop residues into the soil improves physical, chemical and biological properties (Turmel, Speratti, Baudron, Verhulst, & Govaerts, 2014).

Even though, physical, chemical, and biological soil properties can be improved by crop residue management (residue retention, incorporation or surface retention), large quantities of un-weathered residues, especially for fall-seeded crops, can cause residue toxicity. In the Columbia Basin, disease problems found in annual winter wheat cropping systems are, potentially due to toxins and pathogens, found in un-weathered residues. These residues are often plowed under the surface where they are intercepted by the root (Wuest & Skirvin, 1999). The experimental study on rice residues submerged in soil showed the residues released phytotoxic substances that hinder radicle growth of rice seedlings (Chou & Lin, 1976).

In non-inversion tillage systems, crop residue management can lead to poor crop establishment. A study on crop residue incorporation for wheat suggests that crop establishment was mainly affected by the position of the residue in relation to the crop seed. The amount of crop residues (3.3 to 6.7 t ha⁻¹) did not show any consistent trends in reducing crop growth. However, there was an interaction between the residue position and its amount in affecting crop growth. Additionally, It is difficult to work in field situations with high levels of straw residue on the surface which in turn can increase slug populations that could potentially reduce the plant population (Morris et al., 2009).

In some environments, CRM can negatively affect crop production. In N limiting environments, CRM reduces N availability. In addition, in cooler temperatures, retaining crop residue on the soil surface can lower soil temperature. In regions with high rainfall, excess soil moisture incorporation/retention can result in waterlogging. Conversely, in semi-arid regions with light rain, crop residues can intercept rainfall and increase evaporation (Turmel et al., 2014).

Wheat stubble burning was proven more effective than stubble retention in maintaining a low incidence of crown rot infestation. Crown rot is a wheat soil borne disease that has become more prevalent as reduced tillage practices involving residue retention have been widely adopted. The

incidence of infection after stubble burning remained below 10%, while stubble retention was 34-36% through 1993 to 1994(Burgess, Backhouse, Swan, & Esdaile, 1996). Burning of the harvest residue would be an option, with the benefit of rapid, natural drying of the straw after rain and uniform distribution of the ash (Klinner et al., 1987).

Crop residue removal is also practiced through baling as a result of the recent advances in enzyme and bioprocessing technology for ethanol production(Carolan, Joshi, & Dale, 2007). Depending on the harvesting system, only 26 to 40% of total aboveground crop residue were removed with baling. Straw removal was greater with swathing and less using a stripper header (Lafond et al., 2009). Approximately 75% of straw (by weight) was removed after harvesting, while standing stubble was removed using flail mowers or rotary mowers (“Grass Seed Crops: Post Harvest Residue Management,” n.d.)

Even though baling did not significantly alter soil quality after 50 years, the high cost of handling and supplying biomass feedstock is still a main challenge (Kemmerer, 2012; Lafond et al., 2009). Prior to baling, a multiple-pass system is used to facilitate drying (mowing and raking). Additionally, bales are transported several kilometers, depending on the field location, for storage. The number of days needed for bale production depends on weather conditions. This operation from the time bale production starts until all the bales are stored needs approximately 15 to 30 days (Kemmerer, 2012). Baling is conducted before field burning in Central Oregon in order to reduce some of the smoke from field burning by removal of some of the straw load (“Grass Seed Crops: Post Harvest Residue Management,” n.d.).

Crop residue burning

Fire has been used in agriculture to clear land, remove weeds, waste removal and control disease from earliest time (Brandt, 1966). The effect of fire on vegetation and soil properties depends on fire severity. Fire severity consists of two components: intensity and duration (Certini, 2005).

Severe fires, such as wildfires, can cause removal of soil organic matter, loss of nutrients, leaching and erosion, structure and porosity degradation (Andreu, Rubio, Forteza, & Cerni, 1996; Certini, 2005; Mataix-Solera, Cerdà, Arcenegui, Jordán, & Zavala, 2011). However, light to moderate fire temperatures have shown to be beneficial in increasing soil nutrients i.e. $\text{NO}_3\text{-N}$, $\text{NH}_4\text{-N}$, P, Ca, Mg, Na and K, without significant difference in soil runoff and erosion (Badía & Martí, 2003; Kutiel & Inbar, 1993).

Field flaming and burning using oil or gas burners have been used since 1926 to control insects and weeds. This method has been chosen because of the public opposition to smoke and a lack of dry fuel in a wet climate (John R Hardison, 1976). In 1970, Oregon State University designed and built a mobile incinerator to remove straw and stubble with a minimum of smoke (Figure 3). Using this machine, the soil surface varied from 93 to 538 °C depending on fuel load. Although the treatment was almost completely removed and most weed seeds were killed, there were severe problems hindering the development of this machine, i.e. escaped fire, excessive temperatures, and smoldering crowns after the machine has pass (J R Hardison, 1976).

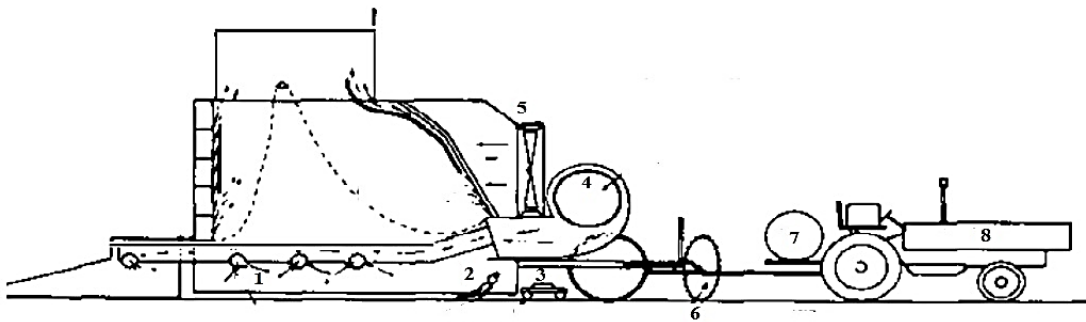


Figure 3. Schematic section view of an early model of Oregon State University mobile field incinerator (John R. Hardison, 1976)

- | | |
|-------------------|-----------------------------------|
| 1. Air | 5. Fans for secondary air cooling |
| 2. Propane flamer | 6. Windrow bale |
| 3. Mower | 7. Water |

4. Pressure blower

8. Propane

A concept of a smokeless mobile field-burning incinerator was developed in 1971 using two combustion stages (Figure 4). The first stage was de-volatilization and gasification and the second stage was gas burning. To discharge a clear combustion gas to the atmosphere, this oil incinerator was equipped with a water spray scrubber to remove cinder and fly ash (Patent No. 3,606,877, 1971).

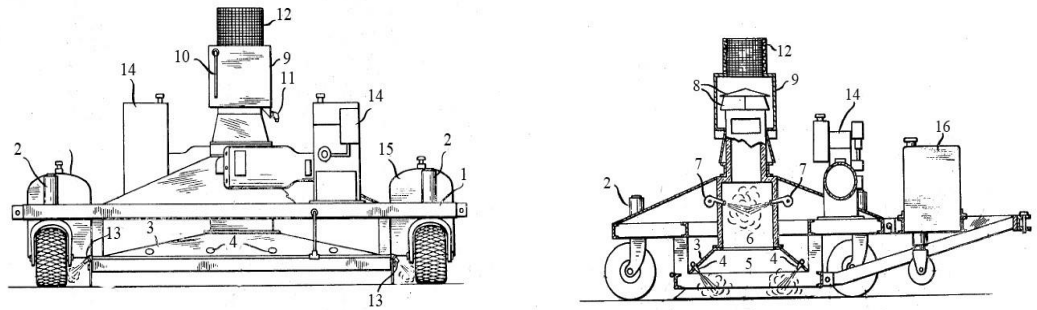


Figure 4. Smokeless mobile field incinerator (Patent No. 3,606,877, 1971)

- | | |
|---------------------------------|--|
| 1. Frame | 9. Scrubber chamber |
| 2. Vertical hydraulic cylinder | 10. Water pipe nozzles |
| 3. Hood | 11. Water and solid drain |
| 4. Burner nozzles | 12. Spark arrester screen |
| 5. Primary combustion chamber | 13. Water spray nozzles |
| 6. Secondary combustion chamber | 14. Gasoline engine driven electric power plants |
| 7. Burner nozzles | 15. Fuel tank |
| 8. Deflector plate | 16. Water tank |

A vehicular combustion chamber to burn loose seed grass was also developed in 1974 (Figure 5). This mobile burner consisted of a combustion chamber and means for collecting and conveying the loose seed grass on the ground. This burner was coupled with flue gas cleansing and an impingement system directing the hot gas combustion gases into the soil (Patent No. 3,802,020, 1974).

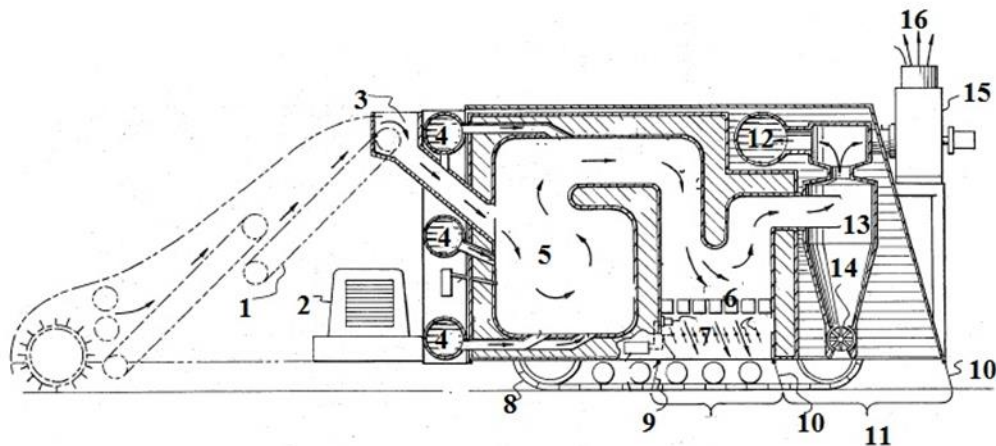


Figure 5. Mobile field burner (Patent No. 3,802,020, 1974).

- | | |
|--------------------------------|---------------------------|
| 1. Conveyor | 9. Skirts |
| 2. Engine | 10. Additional skirts |
| 3. Fuel inlet port | 11. Impingement area |
| 4. Combustion air inlet | 12. Recirculating conduit |
| 5. Combustion chamber | 13. Cyclones |
| 6. Perforated refracting grate | 14. Rotary valves |
| 7. Temperature sensor | 15. Fans |
| 8. Crawler tracks | 16. Exhaust port |

Postharvest field burning of Kentucky Bluegrass was also used to control germination sclerotia of *Claviceps purpurea*. The germination on the soil surface was significantly ($P=0.05$) reduced by machine and open field burning treatments. This burning was compared to non-burn control and sclerotia germination burying at 1 and 3 cm. In addition, the machine burner provided a more consistent temperature and reduced more sclerotia, even with higher moisture in the residue, compared to open field burning (Johnston, Golob, Sitton, & Schultz, 1996).

Fire effects on livestock production

Fire has been used to produce better habitat for livestock, which will lead to an increase in individual animal performance and carrying capacity. One way to accomplish this is through woody species suppression (J. R. Weir, 2009). Texas and the Southern Plains states are

dominated by eastern redcedar (*Juniperus virginiana*), redberry juniper (*Juniperus pinchotii*), and Ashe juniper (*Juniperus asheii*). In Oklahoma, the distribution of eastern redcedar has increased remarkably from 1.4 million to 2.4 million ha, from 1985 to 1995 (Ansley & Rasmussen, 2005).

Fire has also been used to successfully control a number of other brushes, i.e. oaks, sumac, mesquite which can cause significant problems on rangeland. These shrubs can reduce overall forage quantity and quality (DiTomaso, 2000; J. R. Weir, 2009). The timing of fire reintroduction should be considered. The best time to burn is following seed dispersal and senescence of desirable grasses and forbs or before viable seed production by the noxious weed. The use of fire in rangeland can also stimulate annual and perennial grass growth and enhance native forb diversity (Ditomaso et al., 1999).

Conducting prescribed burning on rangelands will reduce dependence on herbicide. Even though the application of herbicide to control weeds is common practice, this method often does not provide long-term weed control. Continuous herbicide application leads to environmental problems, including off-site chemical movement, injury to desirable plants and reduction in plant diversity. Biodiversity has been proposed as a source of stability in a managed ecosystem (DiTomaso, 2000). A study conducted on mixed prairie of the North American Southern Great Plains did not recommend the application of herbicide for increasing forage for livestock production because of its negative impact on biodiversity and ecosystem services (Fuhlendorf, Engle, O'Meilia, Weir, & Cummings, 2009).

Influence on technical factors

Burner type

Burners for flaming are commonly classified according to the shape of the burner (flat or tubular/round) and according to whether they have a vapor chamber or not (liquid or gas phase)(Ascard, 1995).

Flat type burners generate broad flames while tubular types generate very long and narrow flames. These two types of burners were tested using the same operating pressure of 380 kPa (55 psi). Using this operating pressure, the flat burner reached a maximum temperature of 1300 °C and a slightly higher temperature of 1400 °C for the tubular burner (Laguë, Gill, Lehoux, & Péloquin, 1997).

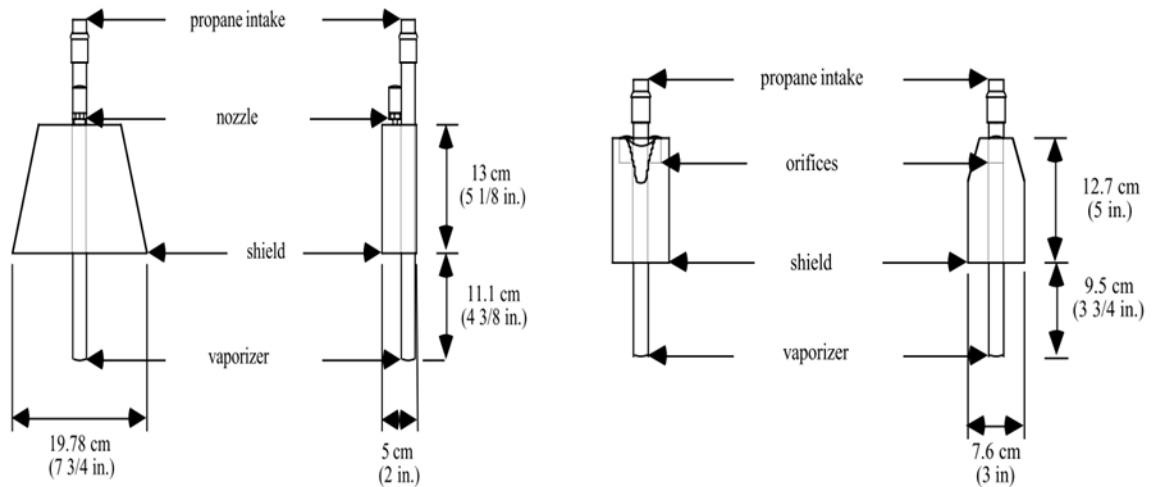


Figure 6. Vapor burners used in (Laguë et al., 1997). Left: flat burner, right: tubular burner
 A recent study on the development of a flame weeder tested four types of burners. They were cone, cylinder, rectangular, and gun-barrel type (Figure 7). For a distance up to 300 mm, the gun barrel burner produced the hottest flame (above 840 °C), and a longer flame than any other burner type. However, this burner consumed more gas(Kang, 2001).

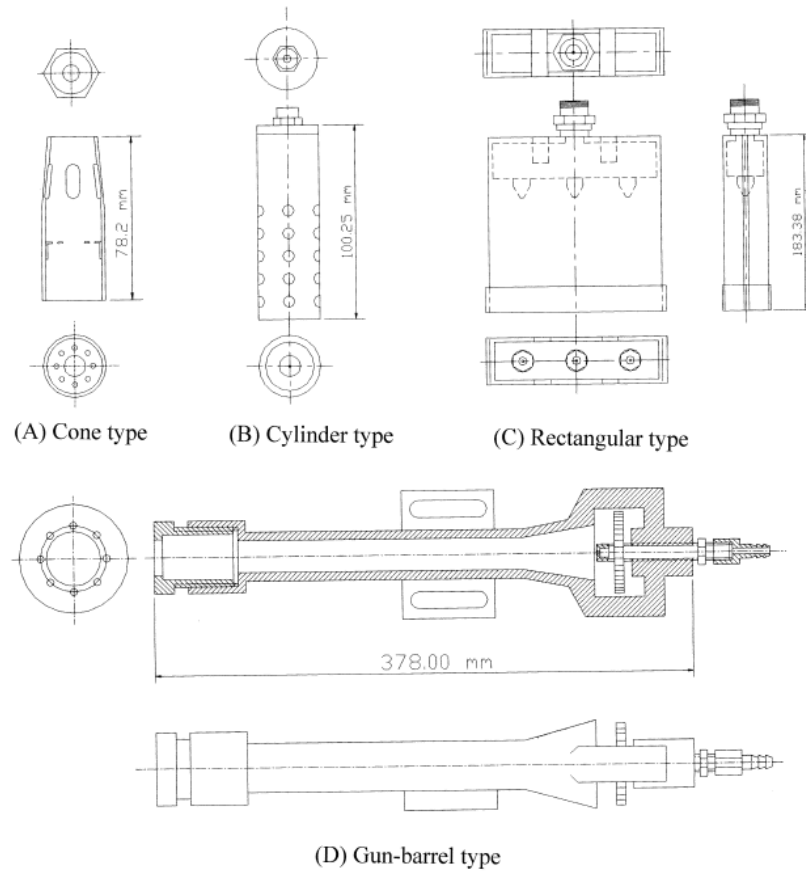


Figure 7. Three types of burners tested by (Kang, 2001).

A box-shaped burner was developed at the University of Nebraska-Lincoln for weed flaming, utilizing a U-shaped vaporizer tube and had one nozzle. This burner used two square U-bolts to securely clamp its hood for the high-vibration application (Figure 8). The highest temperature recorded was 645°C at operating pressure 172 kPa (25 PSI) (Neilson et al., 2017).

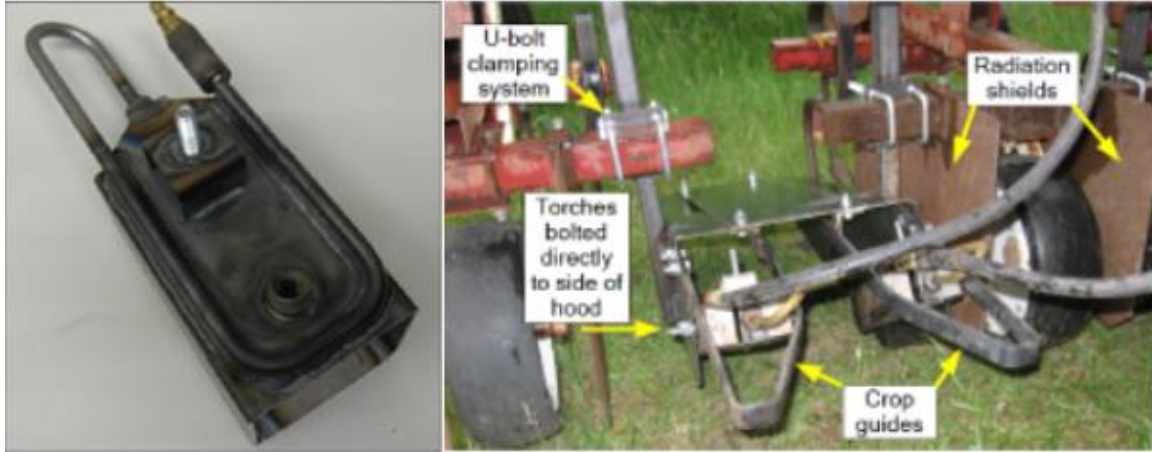


Figure 8. A box-shaped burner and flamer hood and burner mounting system (Neilson et al., 2017).

Commercial burners for flame weeders are usually standard atmospheric burners without forced air assistance. These propane burners commonly generate flame temperatures of 1200-1350 °C. Air-assisted burners are typically not used in practice, as this addition would make the burners even more expensive (Ascard, 1995).

Generally, a burner with a cover (shielded burner) is more energy-efficient, requiring 40% to 50% less fuel than an open burner. A shielded burner is also more tolerant to variations in burner angle relative to the ground (Ascard, 1995; Neilson et al., 2017). The burner cover (hood) provides safety by keeping the hot gasses underneath the shield and provides a more consistent treatment by blocking much of the effect of wind (Neilson et al., 2017).

In addition, burners are classified based on their application, whether it is for domestic (range burner) or industrial applications (atmospheric pipe burner) (Figure 9). After passing the gas cock, a high velocity gas flows out through the orifices and the momentum of the gas stream causes air to be injected into the burner. The injection tube (mixing tube) design affects the volume of air injected. There are some considerations for designing the injecting tube, including (Berry, Brumbaugh, Moulton, & Shawn, 1921):

1. the diameter change of the inlet to the outlet should be gradual,
2. the outlet angle should be about two degrees,
3. the length of the outlet should be about six times the throat diameter,
4. the area of the throat should be about 43 per cent of the area of the ports

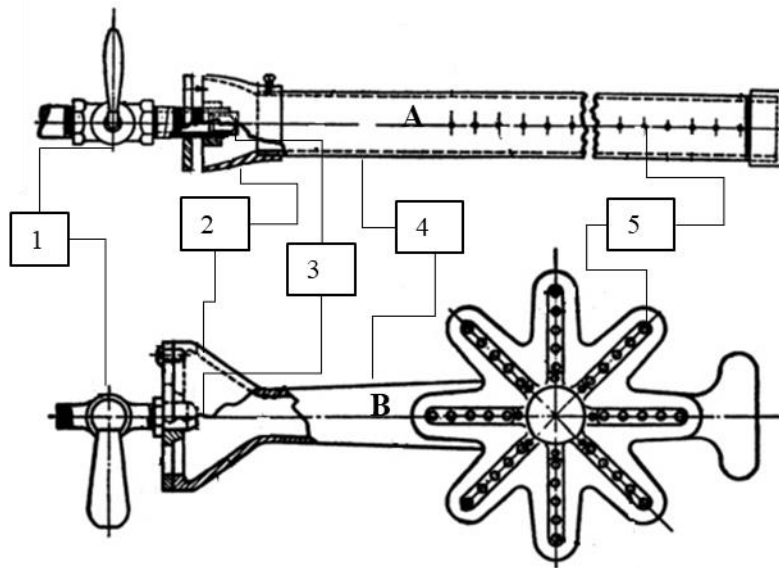


Figure 9. Top view of atmospheric burner (A) and industrial burner (B) (Berry et al., 1921; US Bureau of Standards, 1931)

- | | |
|----------------|-----------------|
| 1. Gas cock | 4. Mixing tube |
| 2. Air mixer | 5. Burner ports |
| 3. Gas orifice | |

Burner angle and height

Burner settings affect how the flame reaches the plant residue and for how long a high temperature is maintained. The appropriate combination of height and angle are influenced by several factors, including burner type, operating pressure, flame length, surface condition, weed height, ground speed and wind (Ascard, 1995).

Burner performance was assessed using a utilization factor, as shown in equation (2) (Storeheier, 1994):

$$Utilization\ Factor = \frac{\sum(T \times t)}{G} \quad (2)$$

Where,

T : temperature, °C

t : time, s

G : gas consumption per unit area (dose), kg/ha

For shielded burners, utilization factor for both flat and tubular burner types was considerably higher than unshielded burners and was highest at small angles. At the small angles, the flame spread along the soil surface and covered a larger area than steep angles. The shielded burners were found to be less dependent on burner angle because the shield kept the flame close to the ground for a longer period, regardless of angle. It was recommended to set the burner angle at 22.5 ° to 45°(Storeheier, 1994).

Other studies in Italy found that normally flat burners (Figure 10) set at an angle of 30° to 45° and at height 7 cm, guarantees maximum effectiveness in weed flaming (M. Raffaelli, Martelloni, Frasconi, Fontanelli, & Peruzzi, 2013). Additionally, burner height doesn't affect burner performance unless the burner is set at a steep angle (approximately 67.5°) (Storeheier, 1994).



Figure 10. Self-propelled flaming machine (M. Raffaelli et al., 2013)

There were considerable discrepancies between field tests and laboratory experiments on the effect of burner angle to weed reduction. A burner angle of 67° , aimed backward (Figure 11) gave the highest reduction of weeds during field experiments. However, this burner angle caused flame deflection upwards. A test that was conducted in the laboratory showed a burner angle of 45° aimed backward generated a higher maximum pattern than the other angle (Ascard, 1998).

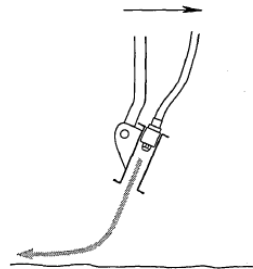


Figure 11. Side view of an open burner set at an angle of 67° aimed backwards. The arrow shows the operating direction (Ascard, 1998)

Burner operating pressure

A higher burner operating pressure improves flame penetration, especially for dense weed areas (Ascard, 1995). However, increasing the gas pressure can also cause a decrease in efficiency.

Below optimal combustion, which is visualized by yellowish flame, usually occurs at a minimum pressure of 250 kPa (Carter, Colwick, & Tavernetti, 1960; Storeheier, 1994). In addition, the maximum flame temperature does not vary with the operating pressure, even though in some cases the higher operating pressure produces a wider and longer high temperature zone within the flame (Laguë et al., 1997; M. Raffaelli et al., 2013). The working pressure for flat type burners usually varies from 200 to 400 kPa (Peruzzi, Ginanni, Fontanelli, Raffaelli, & Bàrberi, 2007; M. Raffaelli, Frasconi, Fontanelli, Martelloni, & Peruzzi, 2015; Storeheier, 1994).

Speed of application

Generally, effective ground speed increases as burner power increases (Ascard, 1995). However, a study on weed control in cotton showed the most controlling factor in plant damage was the duration of heat exposure compared to fuel input. Little or no adverse effect on tall cotton plants could be seen when fuel rates varied between 2.9 to 6.5 kg h⁻¹ at a ground speed of 4.8 km h⁻¹. At this speed, individual cotton plants were exposed to the high temperature for approximately one-tenth of a second. When the ground speed reduced to 3.2 km h⁻¹, serious damage to plants occurred at all fuel rates (Carter et al., 1960). Similar results were also shown in flame weeding in maize; weed control is significantly higher at the lowest travel speed (0.5 m/s). This could be attributed to the greater exposure time weeds were subjected to at lower travel speed (Loghavi, 2012).

Orifice type

The flow gas through an orifice under the small pressure is presented for practical purposes by following equation (3) (US Bureau of Standards, 1931):

$$q = aK \sqrt{\frac{h}{d}} \quad (3)$$

Where q is the quantity of gas delivered per unit of time, a is the area of the orifice, h is the pressure through the orifice, d is the specific gravity of the gas relative to air and K is an orifice constant that depends on the orifice design.

There are two types of orifices commonly used for domestic and industrial gas burners, namely channel and sharp-edge orifice designs (Figure 12). The channel type has a cylindrical hole through a metal plate of appreciable thickness or a cylindrical hole opening at one end into a cone which is concentric with the hole, while the sharp-edge orifice is the channel type with zero length (Berry et al., 1921; US Bureau of Standards, 1931). The effect of the channel length causes a large variation in the rate of flow as the length of channel is increased, from the conical edge. At a certain point, this effect is a maximum and as the length of the channel is further increased the friction increases and reduces the flow. Channel type orifices produces less burner pressure than the sharp-edge type under equal gas rate. This is because the sharp-edge type has a greater maximum velocity than the channel orifice; hence, its air entraining power is greater (Berry et al., 1921). However, the mechanical difficulty of manufacturing orifices of accurate size with no channel is costly (US Bureau of Standards, 1931).

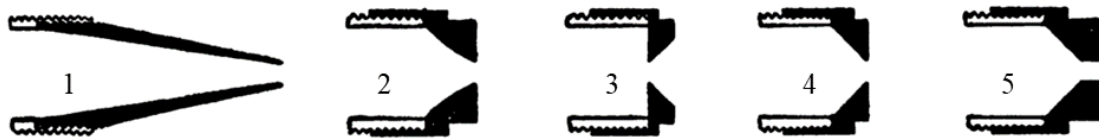


Figure 12. Design of orifices. 1,2,3,4 are designated as sharp edge type and 5 is channel type

Flame type

A combustion system consists of two reactants, a fuel and oxidizer. When the complete mixing occurs before the combustion begins, the mixture is known as a premixed fuel-air mixture, generating premixed flames. Turbulent premixed flames are more common in the various

practical application compared to laminar flames because it increases the ignition of fuel with the reduction in the emission of gases. The turbulent premixed flames results in a flame length reduction and a mixing process acceleration thus enhancing combustion. A non-premixed flame or diffusion flame results when the fuel and oxidizer are not mixed prior to reacting. This type of flames typically produces longer and cooler flames than premixed flames as the mixing step limits the overall combustion (Baukal Jr, 2003).

Prescribed burning

Prescribed burning has been used to manage smoke hazards and public complaints of reduced visibility. Prescribed burning is defined as a burning activity set under planned conditions to achieve a specific management goal. In Western Oregon, for example, prescribed burning has been used to reduce fire hazards through the implementation of smoke management plans. The smoke management plan includes the types of land that can be subjected to prescribed burning, allowable burning periods, and when alternative treatments, such as the use of herbicide or manual clearing, should be applied (US EPA, 1992). The main goal for smoke management is to minimize fire emission, improve the dispersion of smoke columns and ensure the smoke plume does not affect smoke-sensitive areas (J. R. Weir, 2009). The Oklahoma dispersion model classifies the dispersion condition into five category days (Table 1). The category day is determined by ventilation rate. The ventilation rate (VR) is calculated using equation (4) below (Bidwell et al., 2003).

$$VR = H \times W \tag{4}$$

Where,

VR : ventilation rate (m²/s)

H : afternoon mixing height (m)

W : transport wind speed (m/s)

Table 1. Category day classification (Bidwell et al., 2003)

Category day	Ventilation rate (m ² /s)	Burning guidelines
I	<2,000	No burning
II	2,000-4,000	No burning until 11 am and not before surface inversion has lifted. Fire should be out by 4 pm
III	4,000-8,000	Day time burning only after inversion lifted
IV	8,000-16,000	Burn anytime. For night burns, use backfires with surface winds greater than 1.8 m/s
V	>16,000	Unstable and windy. Excellent smoke dispersion, burn with caution.

A burn plan is critical for safety and legal purposes to determine the weather under which the burn will be conducted, number of personnel, the duties of each and the type and amount of crop residue. All this information will be useful to determine actions prior to the burn, to reduce problems and ensure safe operation. In order to increase safety, the prescribed burning is conducted at a low ambient temperature, high relative humidity and low windspeed (Bidwell, Weir, Masters, & Engle, 2018; J. R. Weir, 2009).

The Oklahoma Mesonet provides “Fire Prescription Planner” ([OK-Fire](#)) to specify the lower and the upper limits for various variables pertaining to weather, dispersion conditions, dead fuel moisture and fire danger. OK-Fire utilizes the Oklahoma Mesonet for current and recent conditions, and the North American Model (NAM) of the National Weather Service for forecast conditions (Figure 13)(J. R. Weir, 2009).

Figure 13. Fire prescription planner (OK-Fire)

To reduce the possibility of escaped fire, firebreaks are essential to set out the burn unit boundary. There are several types of firebreaks, such as natural (creeks, streams, river), existing (roads and cultivated fields), constructed and mowed line/wet line. The type of firebreak required depends on fuel load, fuel type, topography and weather conditions for each burn unit (J. R. Weir, Bidwell, Stevens, & Mustain, 2017).

Prescribed burning is a risky fuel load management tool because of the possibility of escaped fire even with appropriate burn plans; equipment and material; preparations; and labor (Stevens et al., 1996; Yoder, 2008). Legal liability for escaped fires is a major concern for those using prescribed burning (Cleaves, Martinez, & Haines, 1999). Most basic farm owner's policies can cover legal liability aspects of prescribed burning. General policy limits range from \$25,000 to \$500,000 (Stevens et al., 1996). The escaped fire and smoke interference risk in surrounding areas

directly affect prescribed burning costs. Additionally, fuels, topography, weather, management objective, and unit size and shape were important influences on the prescribed burning cost (Cleaves & Brodie, 1990).

The cost of prescribed burning is affected by several factors, such as fuel type, treatment method, area to be treated, steepness of slopes, fire regime type, site elevation, management objectives, whether the site is a designated protection area (DPA) and whether the site is in the wildland-urban interface (WUI) (Fight & Barbour, 2004). Commonly, burning costs range from \$0.50 to \$10 per acre, with firebreak preparation believed to be the greatest direct cost of prescribed burning (Bidwell et al., 2003). Burning costs for timber and grass in 1996 were estimated at \$4.64/acre and \$0.23/acre, respectively (Stevens et al., 1996).

Based on data analysis of FASTRACS (Fuel analysis, Smoke Tracking, and Report Access Computer System) program of the Pacific Northwest Region of the USDA Forest Service from 2000-2002, the highest price for prescribed burning was \$174 for 200-acre area of mixed conifer and the lowest was \$12 for 100-acre area of Douglas-fir (Fight & Barbour, 2004).

A survey from 1985 to 1994 of the USDA Forest Service's National Forest System showed the slash reduction burning had the highest estimated cost per acre (\$167.04), while the brush, range and grassland burns were the least costly, averaging \$57.09 (Cleaves et al., 1999).

Other means of thermal weed control

In addition to flame type machines, lasers have been used for non-chemical weed control. In contrast to flame treatments, the application of laser energy is selective (Marx, Barcikowski, Hustedt, Haferkamp, & Rath, 2012). Lasers discharge high density energy to selected plants, increasing the water temperature in the plant cells which stops or delays growth (Mathiassen, Bak, Christensen, & Kudsk, 2006).

A study on heat treatment on monocotyledonous and dicotyledonous weeds using a CO₂ laser with a wavelength of 10.6 μm and a diode laser with a wavelength of 9.4 μm showed the CO₂ laser needed lower doses (approximately 0.1 J mm⁻²) compared to the diode laser (approximately 1 J mm⁻²) to reduce weed fresh weight (Wöltjen, Haferkamp, Rath, & Herzog, 2008). The application of hand-held laser system to irradiate weed species indicated that the optimization of targeting accuracy, laser spot size, and energy density may improve the laser application (Mathiassen et al., 2006).

To treat weeds effectively using vehicle-based laser systems, several fundamental technical issues should be addressed. The first is a quick orientation towards the target coordinates which takes the motion speed of the agricultural machine into account. The second is decent techniques for weed detection and the last is heating of the weeds within a few milliseconds (Langner et al., 2006).

Environmental impact of biomass burning

Biomass combustion is a complex process that consists of consecutive heterogeneous and homogeneous reactions. The main steps of the combustion process are drying, devolatilization, gasification, char combustion, and gas-phase oxidation. The biomass combustion emits relatively high nitrogen oxides (NO_x; collective term for NO and NO₂) and particulates matter in the ambient air (B. Jenkins, Baxter, & Miles, 1998; Nussbaumer, 2003). This emission is derived from several routes in combustion processes, which potentially comes from oxidation of nitrogen in the fuel (fuel nitrogen), conversion of nitrogen in the air (air nitrogen) and the formation of thermal NO_x (Houshfar et al., 2012; Tariq & Purvis, 1996). Elevated thermal NO_x commonly occurs at combustion temperatures above 1300°C (Werther, Saenger, Hartge, Ogada, & Siagi, 2000). A low combustion temperature of 800° to 900°C in fuel-bed combustion resulted in a lower NO_x emission (Johnsson, 1994b). It is recommended for agricultural residues that the

combustion temperature remain below 1000°C so that the emission of NO would be mainly from the fuel nitrogen (Werther et al., 2000). NO_x contributes to environmental issues i.e. rain, photochemical smog formation and depletion of stratospheric ozone (Houshfar et al., 2012; Tariq & Purvis, 1996). The large amount of unburnt pollutants (CO, Hydrocarbon (HC), tar, polycyclic aromatic hydrocarbons (PAHs), C_xH_y and char particles) depends on combustion temperature, mixing of fuel with combustion air and short residence time (Werther et al., 2000).

Open biomass burning is a major source of global air pollutants and aerosols. A study reported that about 40, 32, 20, and 50% of the annual global carbon monoxide, carbon dioxide, aerosols, and PAHs emissions were attributed to biomass burning (Yu et al., 2012). Forest, crop residue, and grassland/savanna burning were reported to have contributed to about 45%, 34%, and 20% of the total air emissions from biomass burning in Asia, respectively. The estimation of biomass burning emission is shown in Table 2 (Streets, Yarber, Woo, & Carmichael, 2003).

Table 2. Biomass burning emission in Asia

Atmospheric emission	Yield (Tg)
SO ₂	0.37
NO _x	2.8
CO ₂	1100
CO	67
CH ₄	3.1
NMVOC	12
BC	0.45
OC	3.3
NH ₃	0.92

A study on particulate and trace gas emissions from open burning of wheat straw and corn stover was conducted by setting up sampling instruments on an agricultural vehicle at a sampling height of about 2.5 m. The vehicle was moved to collect smoke with a sampling time of 35 to 45 minutes. The sampling site was 5-10 m away from the fire; far enough for smoke emissions to dilute and cool to ambient temperature before sampling (Li et al., 2007). PM emissions for wheat

and rice straw burning had a unimodal accumulated particle size distribution with peaks between 0.26-0.56 μm (Hays, Fine, Geron, Kleeman, & Gullett, 2005; Li et al., 2007).

Several studies estimated daily average $\text{PM}_{2.5}$ and $\text{PM}_{2.5-10}$ concentrations emitted during open crop residue burning. In China, the daily average $\text{PM}_{2.5-10}$ concentration was $266 \mu\text{g m}^{-3}$, while in Taiwan the $\text{PM}_{2.5}$ and $\text{PM}_{2.5-10}$ concentrations during open rice straw burning was 123.6 and $31.5 \mu\text{g m}^{-3}$ and 32.6 and $21.4 \mu\text{g m}^{-3}$ during non-burning periods. The $\text{PM}_{2.5}$ concentrations during these burning periods exceeded the U.S. Environmental Protection Agency (EPA) $\text{PM}_{2.5}$ National Ambient Air Quality Standards (NAAQS) (Cheng et al., 2009; S. Yang, He, Lu, Chen, & Zhu, 2008).

Rice straw burning was a primary source of fine polycyclic aromatic hydrocarbons (PAH). During the straw burning in Taiwan, the average PAH concentration in the particulate phase was 33 ng m^{-3} and the PAH concentration in the gaseous phase was 1160 ng m^{-3} , which were higher than PAH levels reported during non-burning periods. In addition the emitted PAH particles were smaller than $2.5 \mu\text{m}$ (H. H. Yang et al., 2006).

Several studies have reported emission factors of PM and gaseous pollutants emitting from wheat crop residue burning as shown in Table 3. Some of these gases are set by EPA NAAQS as criteria pollutants which are or could be harmful to people.

Table 3. Emission factors for open burning of wheat residue (g/kg)

References	Pollutant					
	PM	$\text{PM}_{2.5}$	PM_{10}	CO	NO_x	SO_2
(B. M. Jenkins et al., 1996)		5.05	5.3	61.8	2.15	0.45
(Dennis, Fraser, Anderson, & Allen, 2002a)	4.8	4.55	4.7	38.2	2.9	
(Gaffney, 2000)		5.05	5.3	51.8	2.15	0.45
(Hays et al., 2005b)		4.7 ± 0.04				
(Dhammapala et al., 2006a)		3 ± 0.6		52.9 ± 8.0		

Laboratory studies to estimate emissions from agricultural burning are mostly preferred to control some variables since the field experiments are not easily conducted or replicated (Dhammapala, Claiborn, Corkill, & Gullett, 2006; Dhammapala, Claiborn, Simpson, & Jimenez, 2007). The laboratory studies provide information on the entire fire process because sampled emissions are well mixed over the entire burning process, while field studies offer only a snapshot in time, space and combustion phase (Chen et al., 2007; McMeeking et al., 2009). The primary drawback of a field study is the lack of direct knowledge of the mass of fuel burned (B. M. Jenkins et al., 1993).

The emission factor of crop and forest residue commonly burned in California was determined using controlled laboratory simulations in a combustion wind tunnel. The wind tunnel allowed a relatively large amount of mass to combust, while controlling wind speeds to mimic different field conditions (B. M. Jenkins, Turn, Williams, Goronea, & Abd-el-Fattah, 1996). The reported emission factors of PM_{2.5}, PM₁₀, NO_x and SO₂ are recommended by California Air Resources board since these emission factors were quality control checked (Gaffney, 2000).

Compilation of air emission factors by EPA, AP-42, provides emission factors for wheat crop residue PM and CO, which are 6 and 54 g/kg, respectively. These emission factors were measured using a burning tower simulation as proposed by Darley (1974). In addition, the emission factors for agricultural burning provided by AP-42 is rated D (below average) (EPA, 1995).

The study to determine emission factor of PM_{2.5} for agriculture crop residue and agriculture fire was also simulated in an enclosure. The crop residues were arranged to mimic field conditions with respect to fuel array, density, and airflow characteristics. The sample probe was inserted in the enclosure near the fire zone. The resulting mean emission factors from replicate burns of the wheat and rice residuals were 4.7±0.04 and 13.0±0.3 g kg⁻¹ (Hays et al., 2005).

The greenhouse gases, air pollutants and PM emitted from agricultural burning causes health issues especially respiratory problems(Jain et al., 2014; McCarty et al., 2009). PAH particles smaller than 2.5 μm can pose human health by entering the pulmonary alveoli(H. H. Yang et al., 2006). A study reported that a 10 $\mu\text{g}/\text{m}^3$ increase in two-day mean $\text{PM}_{2.5}$ was associated with a 1.5% increase in total daily mortality in six eastern U.S. cities during 1976 to 1987. The deaths were mostly caused by chronic obstructive and Ischernic heart disease (Klemm, Mason, Heilig, Neas, & Dockery, 2000; Schwartz, Dockery, & Neas, 1996).

CHAPTER IV

METHODOLOGY

LPG burner performance assessment

The burners

Three prototypes of burners were developed using three different size of steel pipes for their mixing tubes, there are 3/8", 1/2" and 3/4", henceforth called burner 1, burner 2 and burner 3. Main characteristics of the burners are shown in Table 4. All the developed burners are a premixed type burner, where propane and air are mixed prior to the passage in to the reaction zone. This type of burner produces shorter and more intense flames compared to diffusion flames. This intense flame is expected to enhance the heating rates.

Burner 1 and 2 were designed as a forced-draft burner where the air is supplied by a blower/pump. These two burners were equipped with an orifice of 0.038" (Figure 14). Burner 3 was developed based on burner that was designed by [Lionel Oliver](#) in 2002 with some modifications (Figure 15).

The burner 3 has two 0.6” inch diameter air inlets allowing air enter the combustion chamber. A rolled sheet metal plate was added for obtaining air input area variation. This sheet metal was slid to close and open the air inlets. The fuel pipe was 1/8” steel pipe with a 0.043” diameter hole drilled in the center. To improve flame coverage area, a fan shaped-flare was installed on the tip of the burner pipe (Figure 16).

Table 4. Main characteristics of the burners

Parameter		Burner Type		
		1 (inch)	2 (inch)	3 (inch)
Mixing Tube (b)	Length	7	7	7
	ID	0.493	0.622	0.824
	OD	0.675	0.824	1.05
Orifice location (c)	Diameter	0.038	0.038	0.043
Air Line (d)	ID	0.493	0.622	0.824
	OD	0.675	0.824	1.05
Fuel line (e)	ID	0.324	0.324	0.324
	OD	0.54	0.54	0.54
Secondary Air Inlet (f)	Diameter	NA	NA	0.6
Flare	a		5	
	b		0.2	
	c		1.2	
	d		5	
	e		1.2	

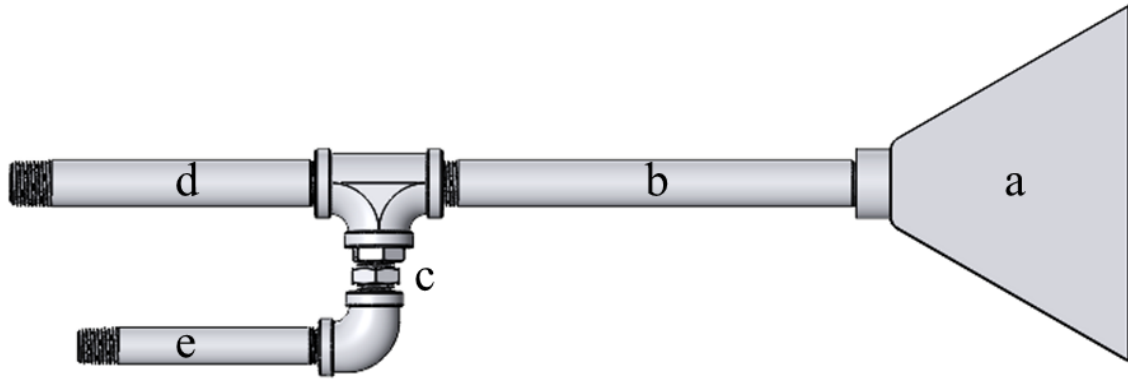


Figure 14. Burner 1 and 2

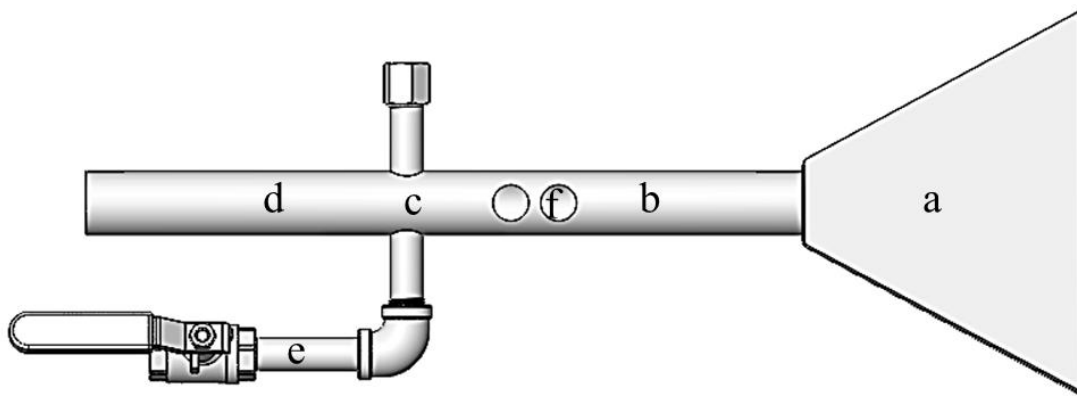


Figure 15. Burner 3

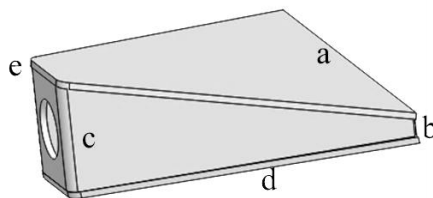


Figure 16. A fan-shaped flare

The burners experiment set up

The performance of the three burners were assessed mainly in terms of flame temperature. To achieve that goal, the burners were mounted on a specific test bench and connected to a 20 lb. LPG tank. The feed line from LPG tank to the burner was equipped with a pressure regulator,

manual valve to open and close the gas flow and solenoid valve. The solenoid valve was used for auto on/off switch based on thermocouple and pressure sensor feedback. To quantify the amount of air needed for the combustion by burner 1 and 2, a flowmeter and a globe valve were added in the air pipe (Figure 17).

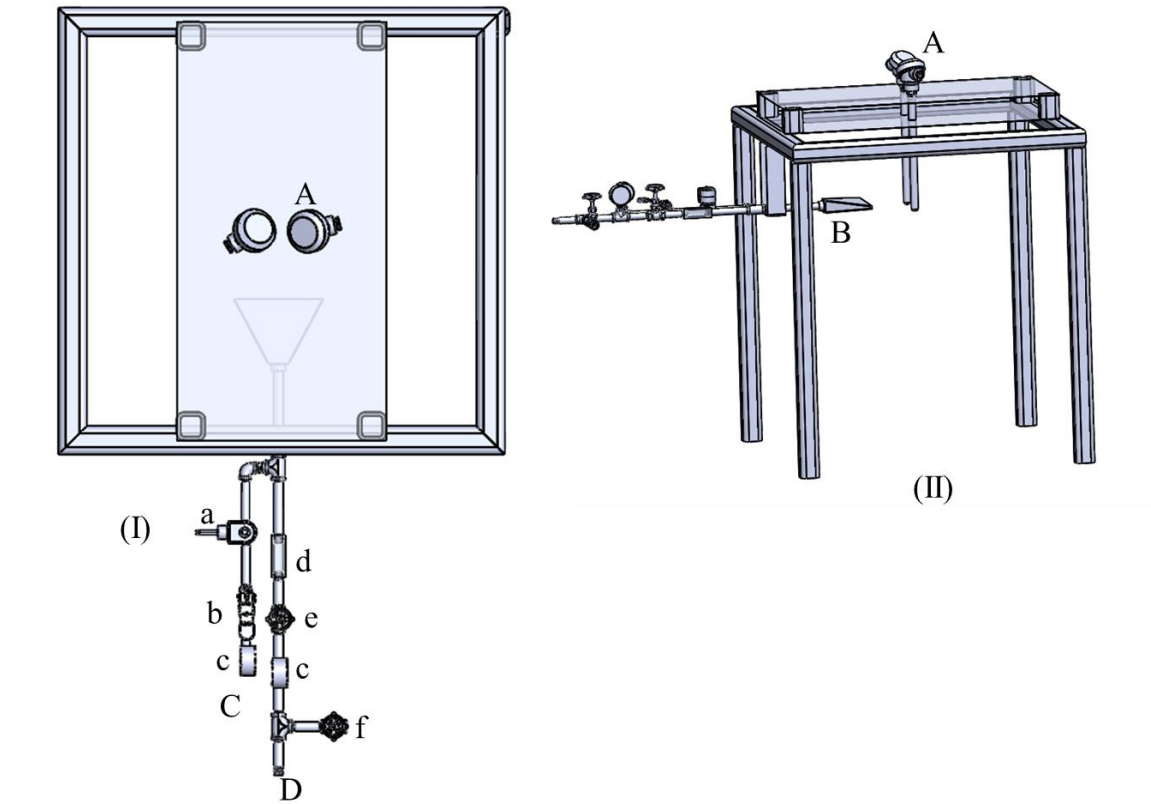


Figure 17. The burner experimental set up (A) Thermocouples, (B) Burner, (C) Propane line, (D) Airline, (a) Solenoid Valve, (b) Manual Shut-off valve, (c) Pressure gauges, (d) Air Flowmeter, (e) Globe valve, (f) Excess air valve.

Flame temperature was measured using two K-type thermocouples placed 5" from the edge of burner flare as shown in Figure 17. Each thermocouple was connected to MAX31856 and Arduino Uno. The MAX31856 provides an integrated amplifier with cold junction compensation. Arduino Uno, which was used as a data logger, has 14 digital I/O. Pin SDO, SCK, and SDI on

each MAX31856 were wired in parallel and connected to the Arduino Uno, while pin CS was wired to individual pins on the Arduino. For data logging purposes, a MicroSD breakout board and Real time clock (RTC) DS1307 were added (Figure 18). The Arduino codes for temperature measurements can be seen in [Appendix A1](#).

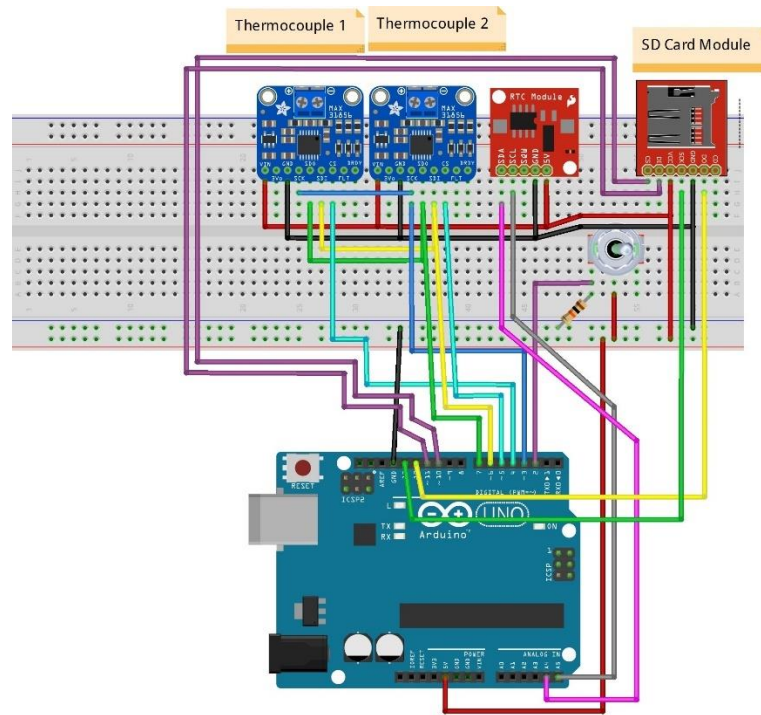
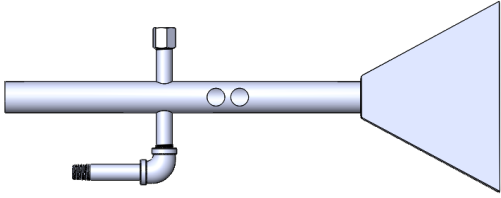
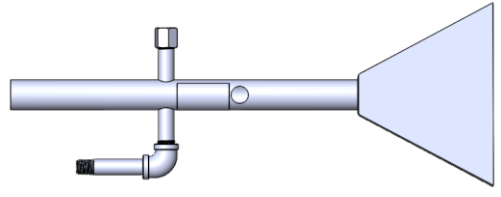
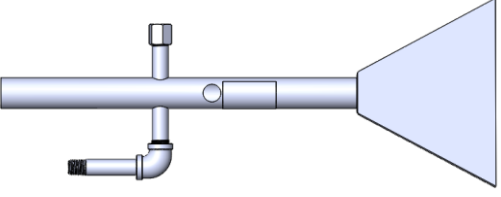
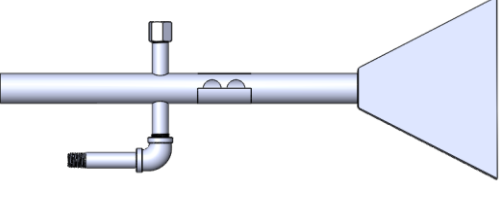
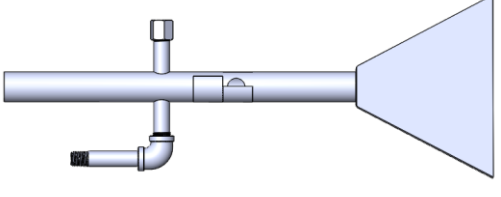


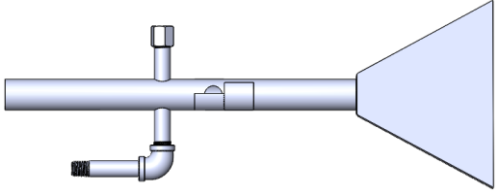
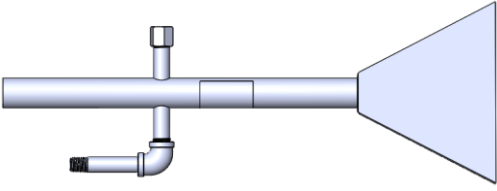
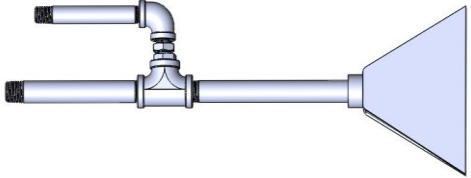
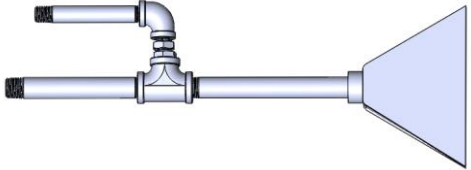
Figure 18. Temperature measurement data logging wiring

The experimental design was a completely randomized 3 X 9 factorial treatment structure with factor A, Operation pressure having 3 levels (20, 25 and 30 PSI) and factor B, burner type having 9 levels. The description of burner type level can be seen in Table 5. There were three replications of the 27 factor-level combination of the two factors. The first letter of the labelling system for the burner type 3 is whether the air inlet was fully open/close (F) or half open/close (H). The combination of number and letter after the F or H label (10 and 1C) indicates whether the first and second air inlet open or close. The first air inlet is located closer to the burner flare

and LPG. For example, H1O2C means the first air inlet was half open while the second air inlet was close.

Table 5. Burner types tested for flame temperature

Mixing tube size (inch)	Hole opening picture	Label
$\frac{3}{4}$		F1O2O
$\frac{3}{4}$		F1O2C
$\frac{3}{4}$		F1C2O
$\frac{3}{4}$		H1O2O
$\frac{3}{4}$		H1O2C

Mixing tube size (inch)	Hole opening picture	Label
3/4		H1C2O
3/4		F1C2C
1/2		HALF
3/8		THREEI

Three more replications of the experiments were conducted only for the burner that generated the best flame temperature for burning agriculture residues. This additional experiment was to understand the flame temperature pattern. This information is essential for the application of the burner in the field to set the distance limit between the burner and the ground. The temperature pattern were plotted using Matlab® ([Appendix A3](#)).

Six K-type thermocouples were placed a fixed distance from the burner (Figure 19). The wiring of these thermocouples is similar to Figure 18 with the addition four more thermocouples. The

three flame temperature values in each measurement spot was then averaged. The pattern was generated using MATLAB®.

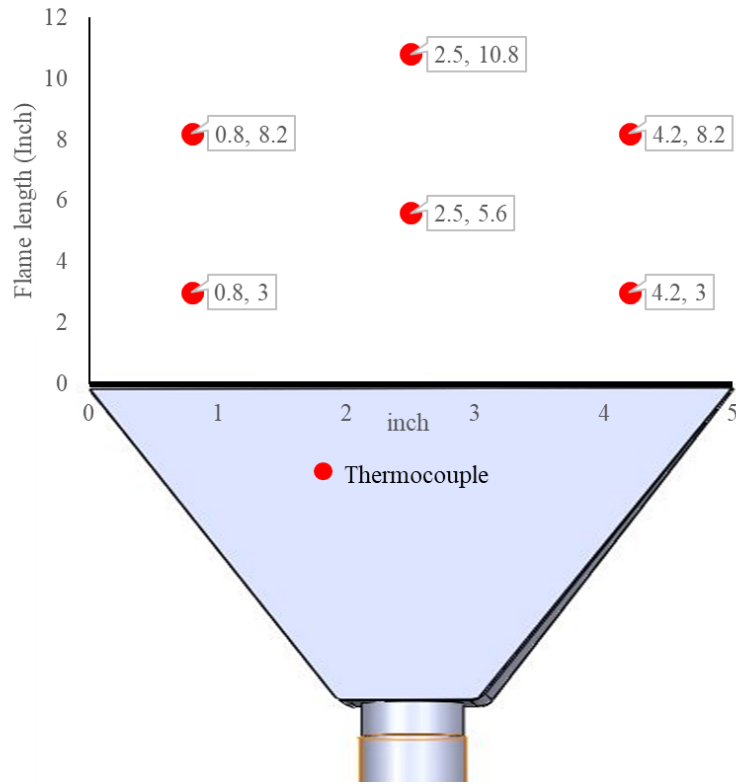


Figure 19. Thermocouple placing arrangement to determine the flame temperature pattern

Orifice discharge coefficient determination

The orifice discharge coefficient was determined by using the ideal gas law and the assumption of ideal flow. The first step in calculating the coefficient was to determine whether it operates above or below critical pressure P_c . P_c can be determined as follows.

$$P_c = \left[\frac{2}{k+1} \right]^{k/(k-1)} \quad (5)$$

Where k is the ratio of specific heats of propane (i.e. 1.13). If $P_c > P_b/P_t$, the propane exits the orifice at sonic conditions. If $P_c < P_b/P_t$, the propane exits the orifice at subsonic conditions. P_b and P_t represent atmospheric pressure and fuel pressure in absolute, respectively.

The second step is to calculate mass flow rate of the propane through the orifice. For sonic flow conditions, the flow rate is determined using the equation (6) below.

$$\dot{m} = \frac{c_d P_t g_c A}{\sqrt{T_t \bar{R} g_c / MW}} k^{\frac{1}{2}} \left[\frac{2}{k+1} \right]^{\frac{k+1}{2(k-1)}} \quad (6)$$

Where c_d is the orifice discharge coefficient. A is the area of the orifice (1.13×10^{-3} in²), T_t is the total temperature of the propane. \bar{R} is the universal gas constant equal to 8314.34 J/kmol/K = 1545 (ft-lbf)(lb-mole-R). MW is the molecular weight of propane (44.10 g/mol), and g_c is the gravitational constant equal to 32.2(lbm.ft)(lbf.s²). If the LPG discharges through the orifice at subsonic flow conditions, Equation (7) is used to determine the flow rate.

$$M_e = \sqrt{\frac{2}{k-1} \left[\left(\frac{P_t}{P_b} \right)^{\frac{k-1}{k}} - 1 \right]} \quad (7)$$

$$c_e = \left[\frac{k T_e \bar{R}}{MW} \right]^{\frac{1}{2}} \quad (8)$$

$$\rho_e = \frac{P_b}{\frac{T_e \bar{R}}{MW}} \quad (9)$$

$$T_e = \frac{T_t}{1 + \frac{k-1}{2} M_e^2} \quad (10)$$

In the experiment, the discharge coefficient was determined by using eight different pressures for each different burner type. The pressure ranged from 5 PSI to 40 PSI in steps of 5 PSI. The atmospheric pressure was considered as 14.7 PSI. The orifice diameter for 3/4", 1/2", and 3/8" inch pipe burners were 0.043", 0.038", and 0.038", respectively. For all the treatments, the LPG consumption was determined by weighing the propane tank before and after 30 minutes of the burner working.

The data then subjected to non-linear regression using the two models of gas discharging through an orifice as described in equations (6) and (7). The regression was performed using the model of subsonic outflow for values of working pressure lower than 20 PSI and using the model of sonic outflow for values of working pressure higher than or equal to 20 PSI. The limit value of working pressure was identified according to equation (5). Non-linear regression analysis statistically verifies whether the consumption data collected follows the physical model of chosen outflow and can determine the value of the discharge coefficient (C_d). The non-linear regression was performed with the SOLVER function in Microsoft excel adopting two different models of gas outflow.

The prototype of crop residue burning machine experiments

The prototype of crop residue burning machine development

Six burners were placed in a pyramidal shaped hood (Figure 20). The hood has a square top base with dimension of 25"x25" and the bottom base is a rectangular base with dimension of 65"x25". The height of the chamber is 20" and the stack diameter is 7". The prototype burning machine ([Appendix D2](#)) was developed based on smokeless mobile burner that was designed in 1921 (Patent No. 3,606,877, 1971) and self-propelled flaming machine (M. Raffaelli et al., 2013). Those six burners consist of two sets of three burners (Figure 21). The spacing of each burner in a set of burners was designed in order to cover burned area that lies in between the burner space. All burners can be easily adjusted by varying the inclination with respect to the soil surface and angle difference. Furthermore, difference angle between the three set of burners on one side with the other three set on the other side of the hood will allow staged combustion to occur ensuring high combustion efficiency and low emission of unburnt pollutants. The drawing of one set of burners can be seen in [Appendix D1](#) and [Appendix D3](#).

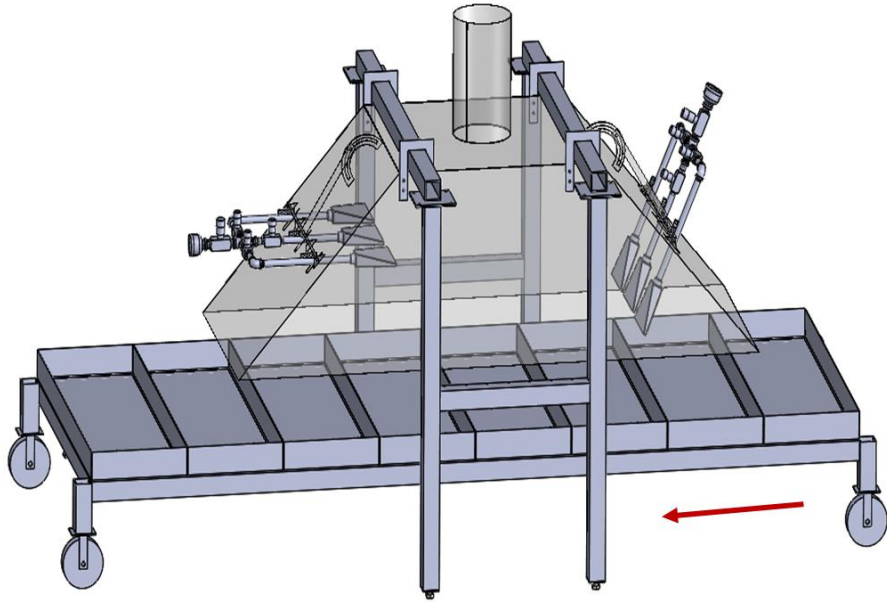


Figure 20. The prototype of crop residue burning machine. The arrow shows the operating direction.

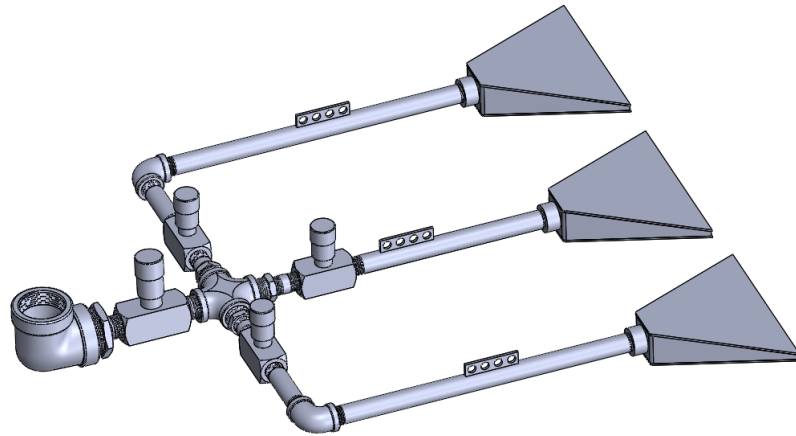


Figure 21. A set of three LPG burner

Safety and fuel control system development

A control system was designed to ensure the burner operates in a safe condition. The system avoids gas leaking and explosion. The flowchart of the safety and fuel control system is shown in Figure 22. The system maintains the flame temperature in between 100-1000 °C and the LPG

pressure within $\pm 10\%$ from the set pressure. In addition, the system is equipped with an emergency shutdown switch that can be activated in the event of malfunctioning burner. The Arduino codes for the safety and fuel system control can be seen in [AppendixA2](#).

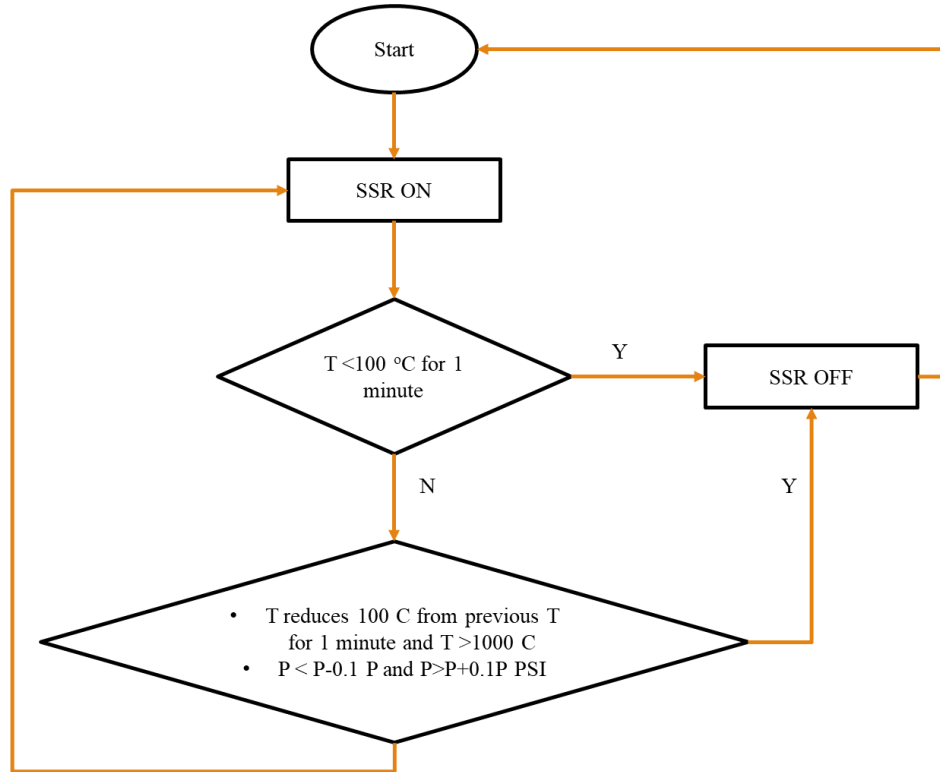


Figure 22. Safety and fuel control system flow chart.

The pressure sensor was an analog pressure sensor with a maximum pressure range of 30 PSI. The pressure sensors were located along the pipeline on either side of the orifice. The recorded pressure data were then used to determine propane flow rate using equation (6). Both pressure sensors and thermocouples were connected to an Arduino Uno. The analog values of the pressure sensor are converted into digital binary values by an analog to digital converter (ADC). Since the ADC reports a ratiometric value of input signal and reference voltage, the measured voltage was calculated using this equation (11).

$$\text{Measured Voltage} = \frac{\text{Reference Voltage} \times \text{ADC Reading}}{\text{ADC Resolution}} \quad (11)$$

Since Arduino Uno has a 10-bit ADC on a 5 V voltage reference, therefore equation (12) is obtained.

$$\text{Measured Voltage} = \frac{5V \times \text{ADC reading}}{1023} \quad (12)$$

Figure 23 shows pressure sensor calibration curved was generated by using equation. The uploaded program controlled a solid-state relay (SSR) acting as an electronic switch to turn on or off the AC solenoid valve.

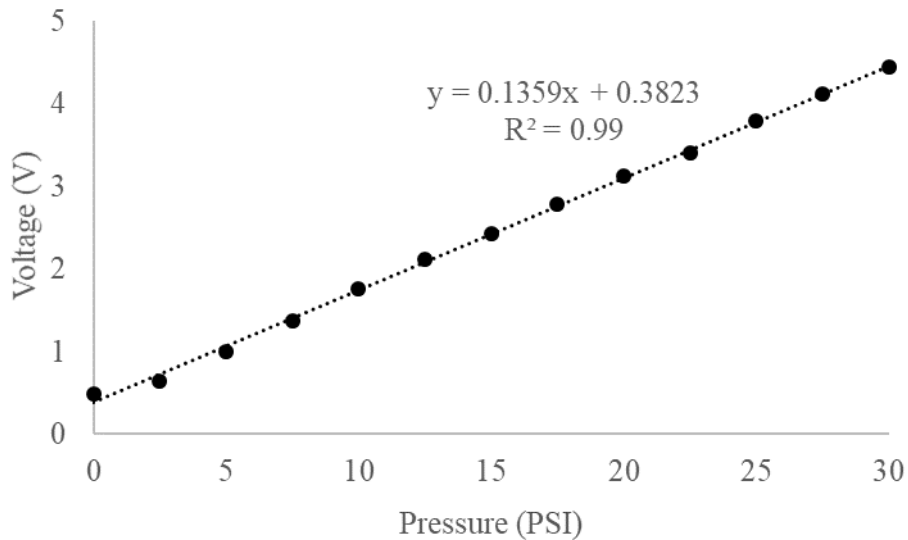


Figure 23. Pressure sensor calibration curve

[Honeywell S8610U](#) module was used to provide ignition sequence, flame monitoring and safety shut-off for the pilot flame. The pilot gas and spark would automatically shut-off if the pilot flame fails to light. A new trial for ignition is initiated after a five-minute delay. This sequence continues until the pilot lights or the call for heat is removed. In case the established flame is lost, trial for ignition restarts immediately. The wiring of the safety and fuel control system and temperature measurement can be seen in Figure 24.

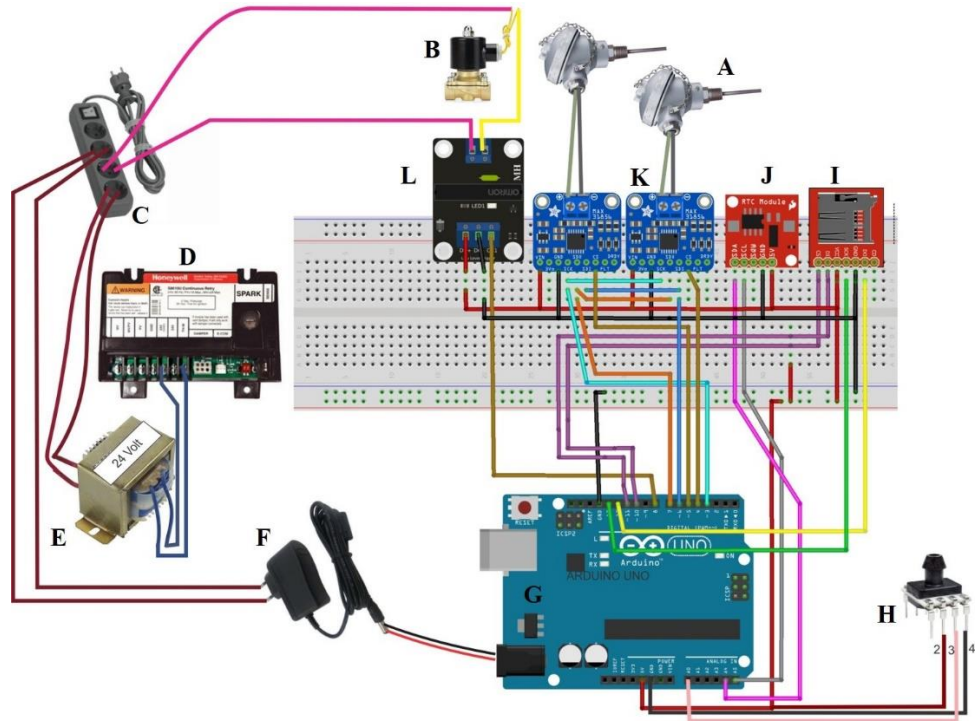


Figure 24. Temperature measurements and safety gas train wiring. (A) K-type thermocouple, (B) Solenoid valve, (C) Power source, (D) Pilot gas ignition control, (E) Transformer 24 V 1A, (F) 9V 1A Switching power supply, (G) Arduino Uno, (H) Pressure sensor (I) SD card module, (J) RTC DS1307, (K) MAX31856, (L) Solid State Relay.

The machine components and configurations

The LPG was supplied from a 250-gallon tank and it was controlled and distributed by a supply network. The supply network consists of manual valves, solenoid valves and pressure regulators. The pressure regulators were used to reduce the pressure of the propane tank to the operating pressure (Figure 25). The operating pressure was set at 23 PSI and the operating pressure for the pilot flame was 10 PSI. Propane-compatible hard piping and flexible hose rated for the required pressure supplied the propane from the tank to the burners.

Since the burners are a forced-draft burner design, air was supplied by an air compressor ([Appendix B5](#)). The amount of air supplied, and its static pressure were monitored using a flowmeter and pressure gauge.

The combustion gases from the combustion chamber pass upward by a centrifugal blower with adjustable speed drive through a 7" flue pipe ([Appendix B3](#) and [B4](#)). In addition, the blower pulled the fresh air into the chamber, to provide more oxygen for the combustion process. The air velocity, static pressure, and temperature in the stack were monitored using a digital thermo anemometer, a digital pressure transmitter and a thermocouple, respectively.

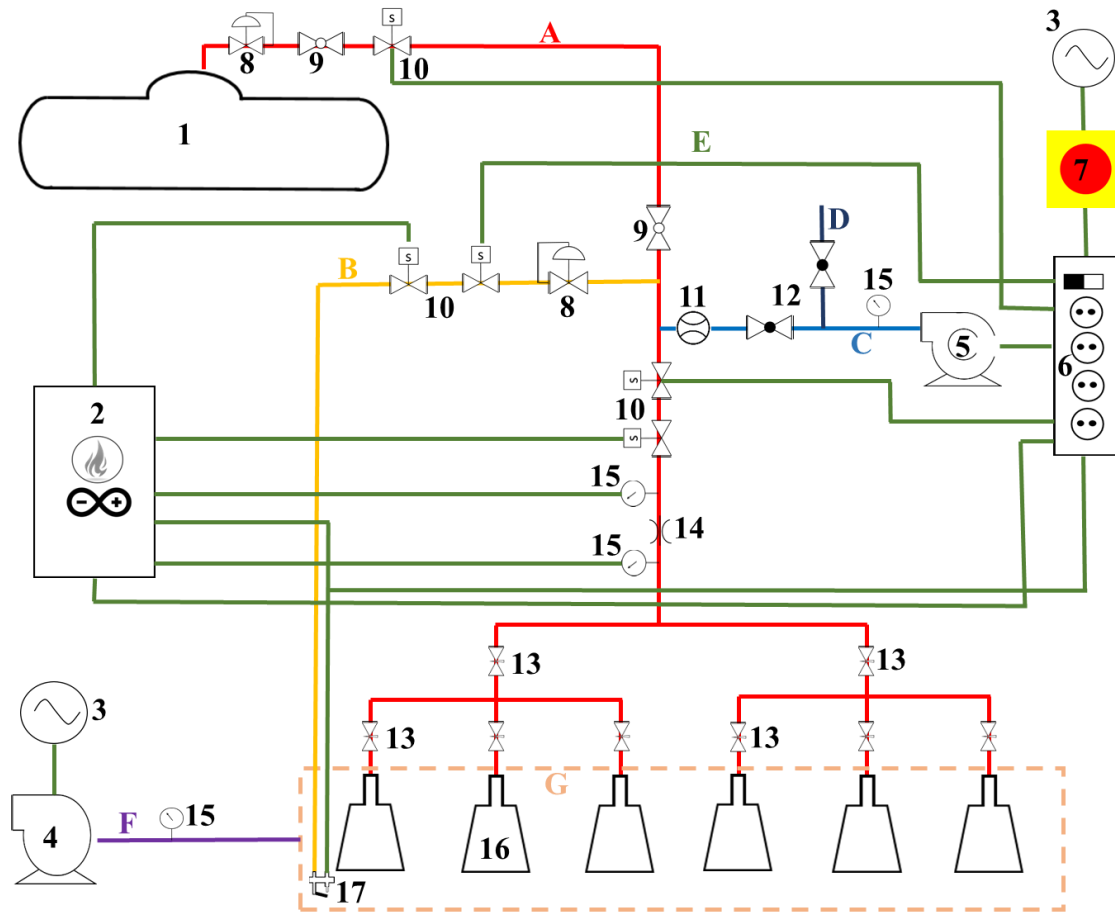


Figure 25. The machine prototype components and configurations

- | | |
|--|--------------------|
| 1. Supply tank | 13. Needle valve |
| 2. Safety fuel and control system and temperature data logging electronics | 14. Orifice/Nozzle |
| 3. AC power source | 15. Pressure gauge |
| 4. Blower | 16. The burner |
| 5. Air compressor | 17. Pilot burner |

- | | |
|--------------------------|----------------------|
| 6. Power strip | A. LPG main line |
| 7. Emergency stop button | B. LPG pilot line |
| 8. Pressure regulator | C. Air supply line |
| 9. Manual ball valve | D. Excess air line |
| 10. Solenoid valve | E. Electronic wiring |
| 11. Flow meter | F. Flue gas |
| 12. Globe valve | G. Hood boundary |

Combustion chamber temperature measurement

Temperature inside the combustion chamber was measured using eight K-type thermocouples (Figure 26). The wiring of the thermocouples is shown in Figure 18. The temperature on the surface of the hood was also recorded by taking a measurement at every vertex of the hood (A, B, C, D, E, F, G, H) using a digital infrared thermometer. The combustion temperature in the combustion chamber was then illustrated using MATLAB® ([Appendix A4](#)).

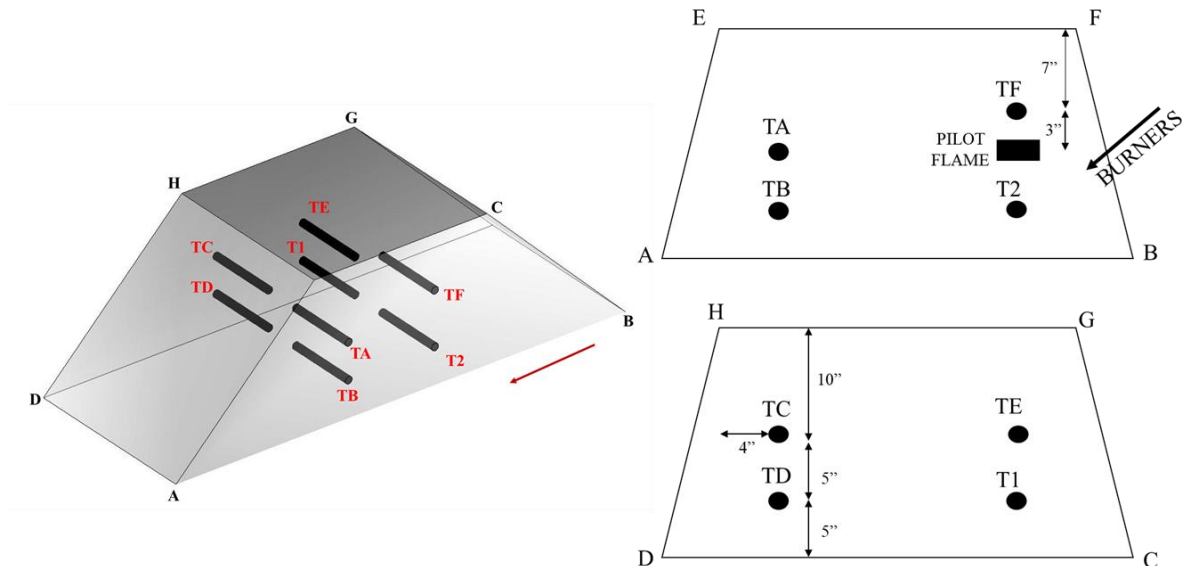


Figure 26. Thermocouples arrangement for measuring combustion temperature in the combustion chamber. The red arrow shows the operating direction.

Experimental set up and design to assess the machine performance

The first experimental study was conducted to determine the best burner angle that burns the largest area while maintaining burn uniformity. To achieve the goal, switchgrass residues were placed on a rectangular tray, which has eight 37"x12" boxes filled with sand ([Appendix D5](#) and

[D6](#)). The distance between the bottom edge of the hood and the tray was 3”, which resulted in the distance between the edge of the burner flares and crop residues was approximately 5”.

Additionally, the moisture content of the crop residues was determined according to the American Society of Agricultural and Biological Engineers (ASABE) standard ANSI/ASAE S358.3. The treatments consisted of four different level of angles, 22.5°, 30°, 45° and 67°, with three replications. The travel speed and crop loading rate were constant at 2.2 mph and 2.9 tons/acre. The tray was driven by adjustable speed motor ([Appendix B2](#)) in a trolley system ([Appendix D4](#)). The data were statistically analyzed using a Kruskal-Wallis test. This test is used to compare three or more independent samples.

After determining the best burner angle, a second experiment was conducted to determine the best crop residue loading rate that could be burnt by the best burner angle. The burning practice is commonly conducted when the farm has a high crop residue load (≥ 2.9 tons/acre). Thus, two levels of crop residue loading rates (2.9 and 3.5 tons/acre), and two levels of travel speed (1.9 and 2.2 mph) were tested resulting in four crop loading rate levels with three replications. The travel speed was calibrated using three replications ([Appendix B1](#)). The data were then statistically analyzed in R using a Kruskal-Wallis test.

Burned area and burned uniformity determination

The percentage of burned area is calculated using equation (13)

$$\% \text{ burned} = \left(\frac{IA - FA}{IA} \right) \% \quad (13)$$

Where:

IA = Initial area before burning,

FA = Final area after burning.

IA and FA were determined using digital image processing techniques. The image processing programs were developed in MATLAB® ([Appendix A5](#)).

There were four steps carried out for image processing: image acquisition, image conversion to grayscale image, image segmentation and noise reduction. A GoPro Hero 5 Black was used for image acquisition. In order to capture a whole tray, the distance between the camera and the tray was set at 67". Acquisition was carried out twice, first to determine IA and the second for FA. In addition, a reference object with a known area was captured to translate pixel count area. The images produced by the camera were then stored in an external memory card for further analysis.

The pseudocode for digital image processing techniques as follows

```
Start
    Detect the image resolution (320 x 1530 or 663 x 1275 for uniformity
    analysis)
        Get the snapshot of image
        Store the captured image as a variable
        Convert the color image into grayscale image
            Gray = 0.2989 Red + 0.5870 Green + 0.1141 Blue
        Convert the grayscale image into a binary image
            Read the image size
                [height,width]= size of image
            Determine threshold
            For row = 1 to height of image
                For column =1 to width of image
                    If image(row , column)>= threshold
                        Binary(row , column)=1
                    Else
                        Binary(row , column)=0
            Count all the white pixels in the binary image
            Read the image size
                [height,width]= size of image
            WhitePixel=0
            For row = 1 to height of image
                For column =1 to width of image
                    If image(row , column)== 1
                        WhitePixel =WhitePixel+1
End
```

Pseudocode for FA is similar to the IA, except for determination of white as a background.

```

BlackPixel=0
For row = 1 to height of image
For column =1 to width of image
    If image(row , column)= 1
        BlackPixel =BlackPixel+1

```

RGB image generated by the camera was converted to grayscale image using equation (14) (Jyothi, Sushma, & Veeresh, 2015).

$$Gray = 0.2989Red + 0.5870Green + 0.1141Blue \quad (14)$$

A thresholding method was used for image segmentation. The grayscale images produced by equation (14) has values ranging from 0 to 255. These images were converted to a binary image that has values 0 (black) and 1 (white). The first step of the thresholding method was to determine the threshold value (T). If the grayscale level was greater than T, the pixel was converted to 1 (white). Conversely, the grayscale level was less than T; the pixel color was converted to 0 (black) (equation (15)). The T was determined by trial and error and it was found that 0.1 was the best luminance threshold for the image before burn and 0.2 was the value for the image after burn.

$$g(x, y) = \begin{cases} 1 & f(x, y) \geq T \\ 0 & f(x, y) < T \end{cases} \quad (15)$$

For IA determination, zero value (black) was background and white was the crop residues. On the contrary, for FA determination, zero value was burned crop residue, while white was used as a background.

After the image segmentation process, images that had noises were removed. In this case, the small objects less than 100 pixels were detected as a noise and were removed.

The reference object was the sand tray which has an area of 3552 in². One-pixel value was calculated using equation (16)(Patil & Bodhe, 2011).

$$1 \text{ Pixel value} = \frac{\text{Area of reference object}}{\text{Sand tray total pixel count}} \quad (16)$$

Burned area both IA and FA were calculated using equation (17).

$$\text{Burned Area} = \text{crop residues pixel count} \times 1 \text{ Pixel value} \quad (17)$$

Since the determination of object reference was using sand trays filled with crop residues, there were additional steps performed after the image segmentation process. The first was image morphological reconstruction by filling binary image (Soille, 1999). The second was image dilation for transforming binary images that produces the same shape as the original but is a different size (Gonzalez, Woods, & Eddins, 2009).

To determined burned area uniformity, each sand box was divided into two zones, so that there are 16 zones per treatment. Zone area was determined using digital image processing. Burn uniformity is calculated using Christiansen's uniformity coefficient (UC) as shown in equation (Christiansen, 1942).

$$UC = 100 \left[1 - \frac{\sum_{i=1}^n |z_i - \bar{z}|}{\bar{z}} \right] \quad (18)$$

Where:

- z_i : total pixel count at zone I,
- \bar{z} : mean total pixel count,
- n : number of zone ($n = 16$).

Gas emission measurement

The experimental design for gas emission measurement consisted of two levels of burner settings and two levels of travel speed. The first burner setting used only one set of burners that made up of three single burners, while the other set of burners remained off. The burner angle was at 67° with respect to the ground (1 SET). The second setting used two sets of burners consisting of six single burners. One set of burners was at angle of 67°, while the other burner set was parallel to the ground (2 SET). The amount of gas emission captured was also determined at 1.9 mph (MOVING) and 0 mph of travel speed (STANDSTILL).

To evaluate the combustion conditions of the experimental system CO₂, O₂, CO, NO and NO₂ concentrations were measured using ECOM-EN2. The gas velocity, static pressure and gas concentration were sampled at 28” from the top of the hood. The average sampling time for “MOVING” treatment was 0.55 minute and for “STANDSTILL” treatment was 1.7 minutes. Combustion efficiency (CE) is determined using modified combustion efficiency (MCE), which assumes all the carbon is released as CO or CO₂(19).

$$MCE = \frac{\Delta[CO_2]}{\Delta[CO_2] + \Delta[CO]} \quad (19)$$

$\Delta[CO]$ and $\Delta[CO_2]$ are the mass concentrations of CO and CO₂ in excess of the background. Previous studies have demonstrated that over 95% of carbon is released as CO and CO₂. Therefore, it is accurate to estimate CE without considering hydrocarbons or PM (Chen et al., 2007; Gupta et al., 2001).

Emission Factor (EF) was calculated using equation (20) (Dhammapala et al., 2007).

$$EF = \frac{\Delta C_x \times Q \times t}{A_{burned}} \quad (20)$$

ΔC_x is the measured pollutant concentration minus the ambient concentration. Q is the flowrate through the chamber ([Appendix C5](#)), t is the sampling time and A_{burned} is the area of biomass burned. The velocity, static pressure and temperature in the stack were also monitored.

The cost estimation determination

The prototype machine cost is categorized into two categories: ownership cost (fixed cost) and operating cost (variable cost). Fixed costs include depreciation, interest (opportunity cost), taxes, insurance and maintenance facilities (Edward, 2015). Depreciation was calculated using a straight-line depreciation. The assumption of economic life of the machine and a salvage value is needed for annual depreciation calculation. Salvage value and total depreciation was calculated using equation (21) and (22) (Edward, 2015; Field & Long, 2018).

$$D = P_p - S_v \quad (21)$$

$$S_v = L_p \times R_v \quad (22)$$

Where:

D : total depreciation, \$

P_p : purchase price, \$

L_p : current price list, \$

R_v : remaining value factor,

S_v : salvage value, \$.

The current price list, which is used to determine the salvage value, is assumed that a new machine is purchased at a discount from purchase price (Huhnke & Bowers, 1990).

$$L_p = \frac{P_p}{0.9} \quad (23)$$

Where L_p : list price, \$
 P_p : purchase price for a new machine, \$
0.9 : discount factor for a new machine.

Remaining value was determined using a table for “other machine” as reported in Table 6.

Table 6. Remaining salvage value as percent of new list price (Edward, 2015).

Machine Age (Year)	Remaining Value (%)	Machine Age (Year)	Remaining Value (%)
1	69	11	33
2	62	12	31
3	56	13	29
4	52	14	28
5	48	15	26
6	45	16	25
7	42	17	24
8	40	18	22
9	37	19	21
10	35	20	20

The joint cost of depreciation and interest was calculated by using a capital recovery factor (R). A capital recovery was calculated using equation (24) (ASAE, 1999; Field & Long, 2018).

$$R = \left\{ Dx \left[\frac{\left(\frac{i}{q}\right) x \left(1 + \frac{i}{q}\right)^{nq}}{\left\{\left(1 + \frac{i}{q}\right)^{nq} - 1\right\}} \right] \right\} + \frac{S_v}{q} \quad (24)$$

Where:

R : one of series of equal payments due at the end of each compounding period, \$

D : Total depreciation, \$

- i : interest rate as compounded q times per year, decimal
- S_v : salvage value, \$
- n : life of the investment in year.

The ASAE standard EP496.2 provides the estimate value of taxes, insurance and housing (TIH) as percentages of the purchase price. To simplify the calculation, the TIH was calculated as 2% of purchase price.

Another approach to estimate fixed cost is to combine salvage value factor, machine life, interest rate and TIH cost into an annual fixed cost percentage as shown in equation (25). The fixed annual cost was determined by multiplying the purchase price of the machine by this equation (25)(ASAE, 1999; Field & Long, 2018).

$$C_o = 100 \left[\frac{1 - S_{vf}}{L} + \frac{1 + S_{vf}}{2} i + K_2 \right] \quad (25)$$

Where,

- C_o : ownership cost percentage, %
- S_{vf} : salvage value factor, % (percent of salvage value compared to purchase price)
- L : machine life, year
- K_2 : ownership cost for taxes, housing and insurance, decimal

Variable costs are associated with the operation of a machine and occur only when the machine is used. Repair and maintenance costs depend on hours of annual use and length of ownership.

Annual hours of use were determined by dividing the total acres of operation with effective field capacity (C_a). C_a was calculated using (26) (ASAE, 1999; Field & Long, 2018).

$$C_a = \frac{swE_f}{8.25} \quad (26)$$

Where,

- s : field speed, mile/h
 w : working width, ft
 E_f : field efficiency, decimal.

The accumulated repair and maintenance cost were estimated using equation (27) that based on ASAE standard EP496.2 (ASAE, 1999; Field & Long, 2018)

$$C_{rm} = (RF1)P_{p-inf} \left[\frac{h}{1000} \right]^{(RF2)} \quad (27)$$

Where,

- C_{rm} : Accumulated repair and maintenance cost, \$
 P_{p-inf} : Adjusted purchase price for inflation, \$
 h : accumulated use of machine, hour

RF1, RF2 : repair and maintenance factors. These factors can be found in ASAE standard D497.7 clause 5 (ASAE, 2015).

To adjust the price of the machine for inflation equation (28) was used (Field & Long, 2018).

$$P_{p-inf} = P_p (1 + inf)^n \quad (28)$$

Where,

- P_p : purchase price, \$
 inf : inflation, decimal
 n : machine life, year

Fuel cost depends on the hours of operation (h) and the size of the tractor or power unit. Hourly fuel consumption was determined by multiplying the tractor PTO by a constant (m) that provided a value in gallon per hour. The value was 0.06 for gasoline engines and 0.044 for diesel engines. The annual fuel cost (\$/year) was calculated using equation (29)(Edward, 2015). This annual fuel cost was also including the annual fuel cost for burning operation.

$$\text{Fuel Cost} = \text{Gas Consumption} \times \text{Gas Price} \times h \quad (29)$$

The total cost to own and operate the machine is the total ownership cost per hour and operation cost per hour. In addition, A software was developed to estimate the cost of this machine.

CHAPTER V

FINDINGS

Single burner performance assessment

Flame temperature

Flame temperature analyzed data shows there was significant interaction between burner types (BT) and operating pressure (PL) ($P_{value} = 0.00119$) as shown in Table 7. The interaction is displayed in Figure 27. The Tukey HSD post hoc was carried out between each of interaction of two factors.

Table 7. The ANOVA table of flame temperature for

	D _f	Sum Square	Mean Square	F-value	P-value	
BT	8	653725	81716	71.68	2.0e-16	***
PL	2	53815	26907	23.6	4.30e-08	***
BT:PL	16	55258	3454	3.03	0.00119	**
Residuals	54	61559	1140			

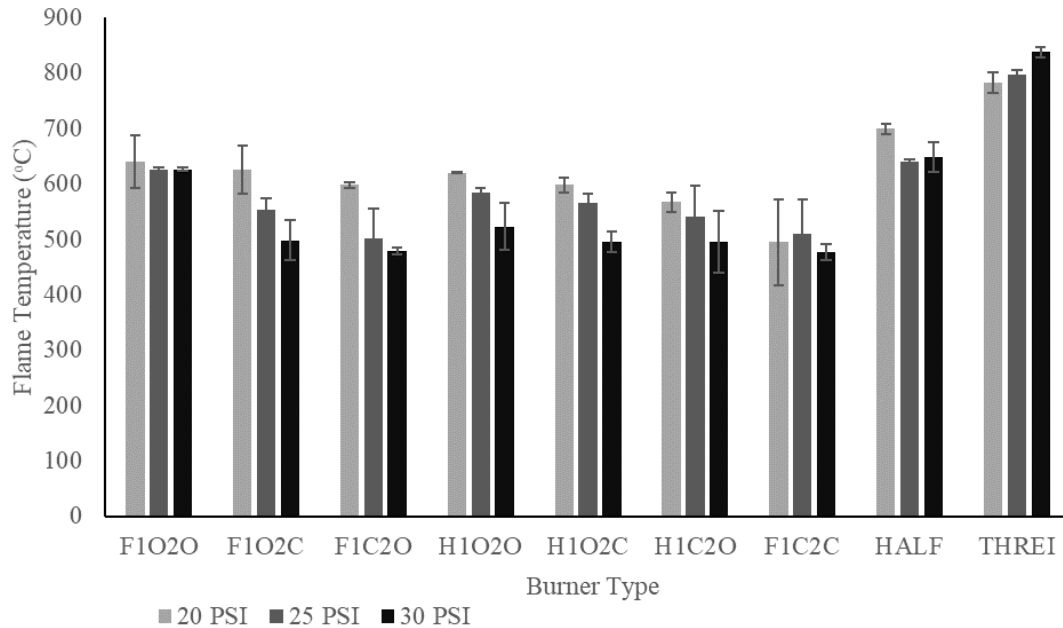


Figure 27. Flame temperature interaction plot of burner type (BT) and pressure (PL).

The operation pressure for burner 3 worked best at 20 PSI, which produced flame temperatures ranging from 509-610 °C (**Error! Reference source not found.**). This result agrees with the experiment carried out by Oliver, 2000 stating that the burner seems to burn best at 20 PSI. The addition of air inlets significantly produced a higher temperature ($P < 0.05$). The flame temperature generated by the addition of two 0.6" air inlets and two 0.3" air inlets were not significantly different ($P < 0.05$). Moreover, TukeyHSD shows the placing of air inlets (F1O2C, F1C2O, H1O2C, and H1C2O) whether it is closer or farther from the fuel orifice did not seem to have a significant effect on the flame temperature ($P > 0.05$).

The performance of burner 2 with the operating pressure of 25 and 30 PSI shows insignificantly different with F1O2O (in all operating pressure setting) and H1O2O (operating pressure of 20).

The highest temperature was generated using an operating pressure of 20 PSI, which was 699.5 °C.

Burner 1 produced significantly the highest flame temperature among the tested burners. The flame temperature generated by operating pressures of 20 and 25 were not significantly different. This burner burned best at 30 PSI in term of flame temperature. The flame temperature range produced by this burner at all pressures was approximately 800-840 °C. The temperature range from 800 to below 1000 °C is recommended for agricultural residue burning to reduce the NO_x emission (Johnsson, 1994a; Werther et al., 2000).

Flame temperature pattern was generated using burner 1 temperature data, since this burner produced the highest temperature in all pressure treatments (Figure 28). At a working pressure of 30 PSI, the flame temperature ranging from 800 to below 1000 °C is maintained at the flame length of approximately 5.5 inches. This flame length is the largest for this temperature range compared to the 20 and 25 PSI treatments that only can maintained 800-1000 °C flame temperatures for up to 4 to 4.5- inch flame lengths.

Discharge coefficient determination

Table 8 reports the results of the non-linear regression analysis on the values of the LPG consumption, recorded for the different working pressures with different burner types, according to the mixed gaseous outflow model. Non-linear regression for the two different orifices provided R² values very close to 1 for the fit of the LPG consumption to the adopted outflow model.

The values of coefficient of determination (R²) in **Error! Reference source not found.** are very close to one suggesting that the model proposed for the gaseous outflow is suitable for describing the LPG consumption. The relatively low standard error values for most analysis support the curve fit of the estimated discharge coefficient of each burner. The standard error in non-linear regression analysis should not be taken too seriously because of linearizing assumption. This

assumption underestimates the true uncertainty of any non-linear equation (Brown, 2001). The estimated C_d values are in agreement those in Baukal Jr, (2003), according to which the value coefficient for a gas nozzle can vary from 0.75 to 0.95(Baukal Jr, 2003) .

Table 8. Estimation of burner discharge coefficient (C_d).

	F1O2O	F1O2C	F1C2O	H1O2O	H1O2C	H1C2O	F1C2C	HALF	THREI
C_d	0.929	0.926	0.929	0.923	0.937	0.911	0.919	0.909	0.909
R^2	1.000	0.993	0.996	0.999	0.998	1.000	0.998	0.999	0.999
SE	0.088	0.162	0.112	0.082	0.105	0.102	0.093	0.095	0.067

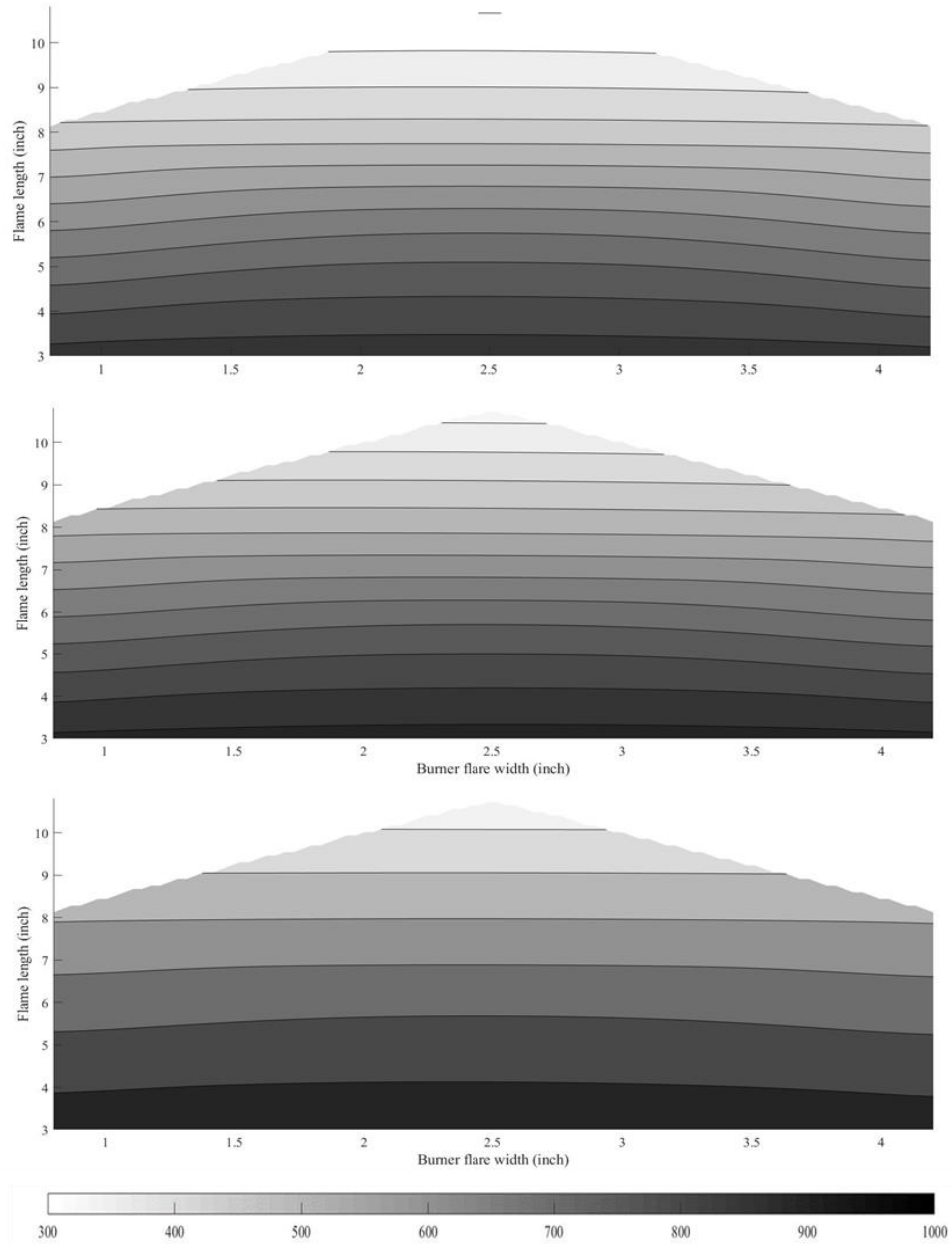


Figure 28. Flame temperature pattern of burner 1.

Air flow rate estimation

The addition of air for the burning operation was meant to improve combustion efficiency and reduce NO_x emissions. The amount of air supplied was based on visual observation. The opening of air valve was set when the flame appeared blue. The blue flame was generated because the

complete combustion creates enough energy to excite and ionize the gas molecule in the flame (Figure 29).



Figure 29. The blue flame generated by the burners

There is an interaction between operating pressure and burner type as shown in Table 9 and Figure 30. Tukey HSD post hoc shows the combustion air needed by burner 3 at operating pressure of 20 and 25 is significantly different ($P < 0.05$). In general, the air combustion needed at the same operating pressure are relatively constant. Based on the interaction plot, the highest amount of air combustion was in burner 3 and the lowest was in both burner 1 and 2.

Table 9. The Anova table of air flow rate.

	D _f	Sum Square	Mean Square	F-value	P-value	
PL	2	0.0354	0.0177	333.3	<2.0e-16	***
BT	8	0.0321	0.0040	75.55	<2.0e-16	***
PL:BT	16	0.0146	9.15e-4	17.23	9.88e-16	***
Residuals	54	0.0029	5.3e-5			

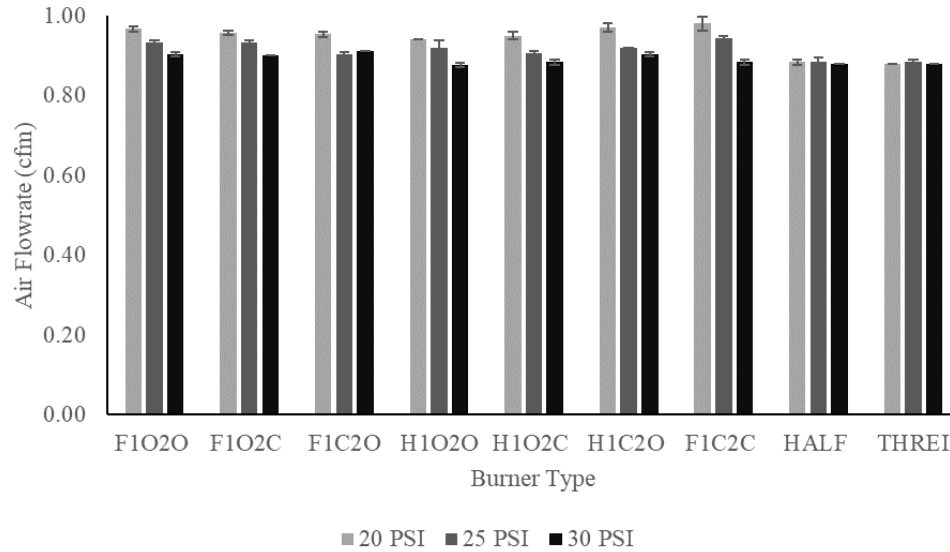


Figure 30. Air flow interaction plot of BT and PL.

Machine prototype performance assessment

Overview

The burner angle was set at certain angle (α) relative to the ground (Figure 31). The air supply flow rate and its static pressure were relatively constant at 4.3 CFM and 23 PSI, respectively ([Appendix C3](#) and [Appendix C4](#)). Those settings were obtained by flame visual observation. At those settings, the flame generated a relatively blue flame (Figure 32). In addition, the average of static pressure in the stack was 0.22 inch of water. The air velocity in the stack was at 4.5 *m/s* in order to be able to draw the gas emission out while maintaining the flame. The moisture content of the crop residues ranged from 13.5-15.2% wb.

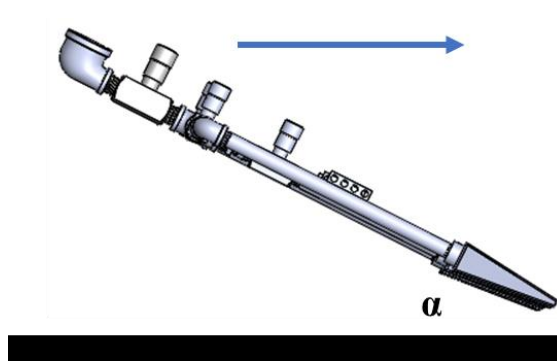


Figure 31. The burners were set at four different angle (α).



Figure 32. The flame generated by the three set of burners in the combustion chamber. The temperature inside the combustion chamber was recorded and plotted using MATLAB® (Figure 33). The higher temperature mostly recorded at T1 and T2. The highest temperature was 657 °C at burner angle of 22.5°. This occurred because the burner at this angle was closer to the thermocouples. In most treatment, the temperature at T1 and TE were higher compared to T2 and TF, it because the flame generated at the side closer to T1 and TE was longer and narrower than the other two burners.

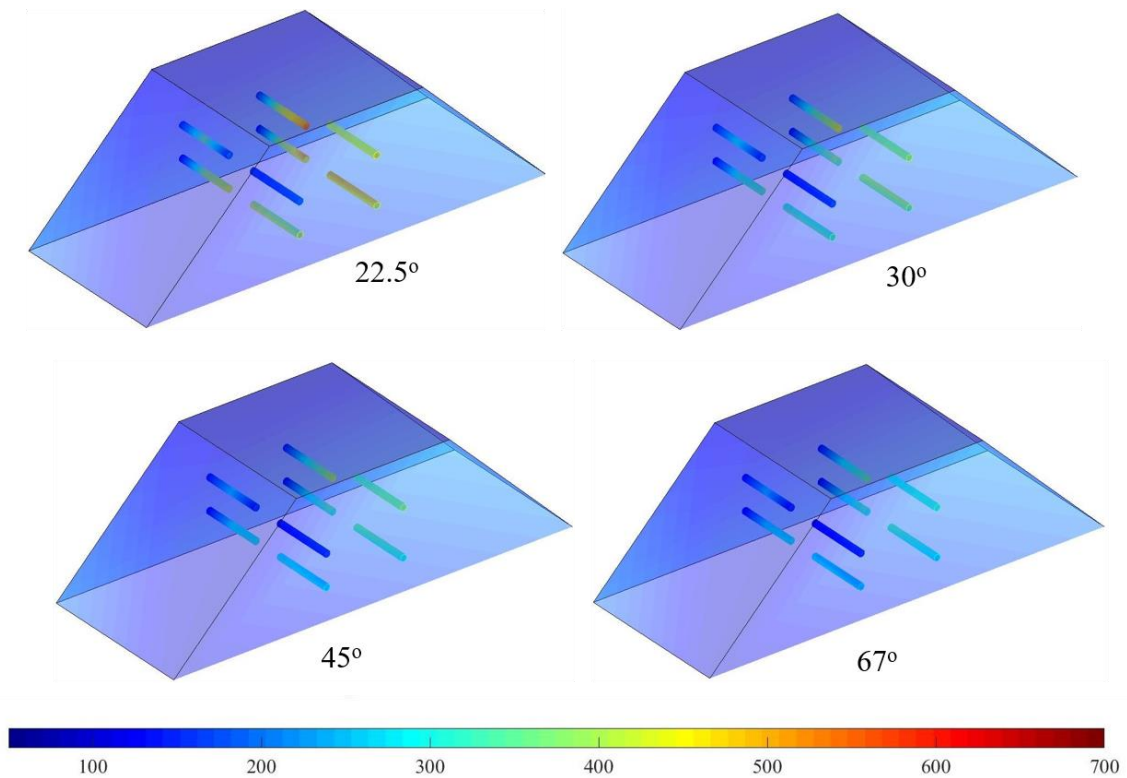


Figure 33. Temperature recorded inside the combustion chamber.

The best burner angle determination

The percentage of burned area was obtained by analyzing the image data. Figure 34 shows, the images taken after burning, where (A) is the original image and (B) is the binary image. The total count of white pixel before and after the burn was calculated to determine the area of burned area. The crop residues on the sand tray was not burned evenly. Figure 34 shows that in most cases, the unburned crop residue primarily located at the bottom portion. Based on visual observation, the flame generated by the burners were not uniform in length and width (Figure 32).

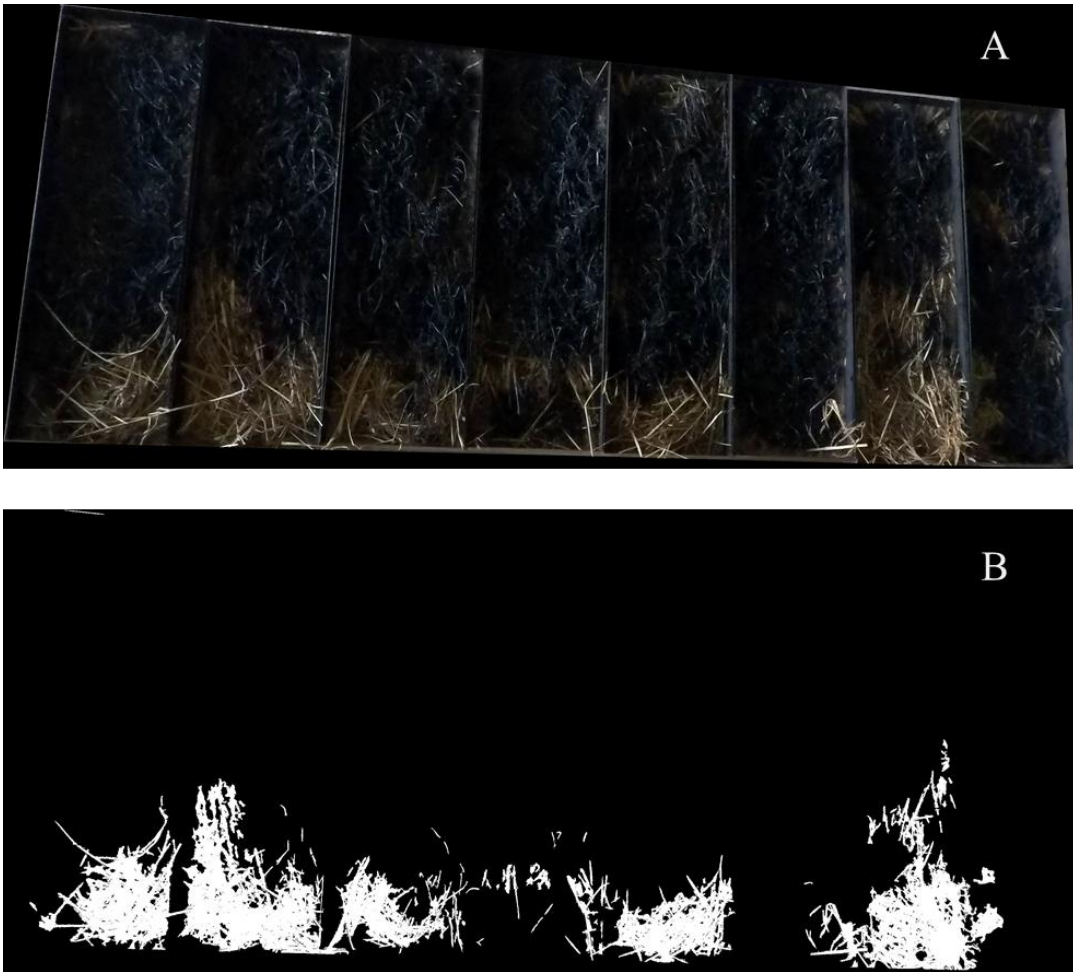


Figure 34. The image after the burn, where (A) is the original image and (B) is the binary image.

Figure 35 shows one example of the comparison between the highest (92.5%) and the lowest (48.2%) burned area percentage, which were produced by burner angle of 67° and 22.5° treatments, respectively.

The percentage of burned area were plotted in a graph as shown in **Error! Reference source not found.** It was found that burner angle of 67° burned more area compared to other burner angle treatments. This result confirms the previous research that found a burner angle of 67° gave the highest reduction of weeds during the field experiment, even though this burner angle caused

flame deflection upwards (Ascard, 1998). The burner angles of 22.5° and 30° gave a wider range of burned area (Figure 36). The inconsistent burned area percentages among the replications in these two angles treatments was likely due to the flame penetration issue. The burners at these angles were relatively farther from the crop residues, which caused the hot part of the flames did not reach the crop residues.

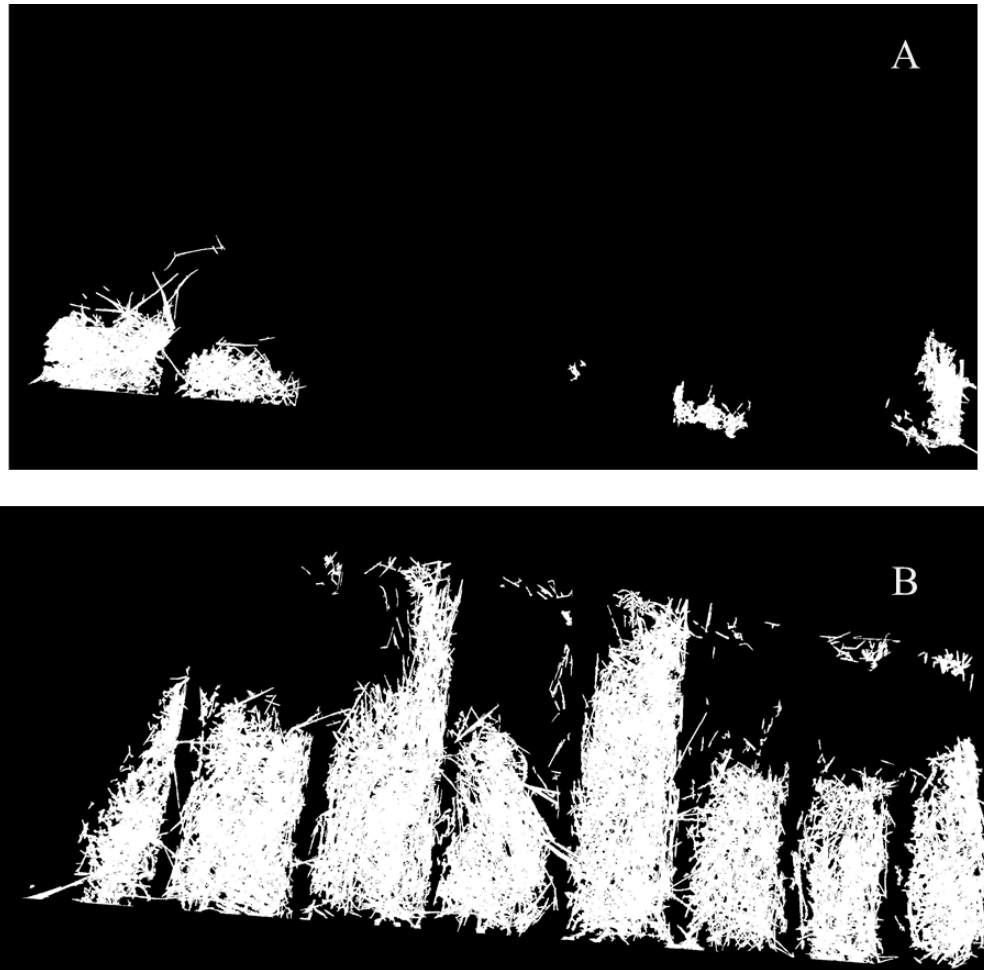


Figure 35. (A) The highest burned area percentage as a result of burner angle 67° Treatment, (B) the lowest burned area percentage as a result of burner angle of 22.5°

According Kruskal-Wallis test, there was significant difference in burned area percentage among the burners angle treatment at $\alpha = 0.05$. To determine which treatments, make this significant

difference, Tukey's HSD procedure was performed (Table 10). The percent burned area of burner angle 67° was found not significantly different compared to the percent burned area of 45° ($\alpha = 0.05$).

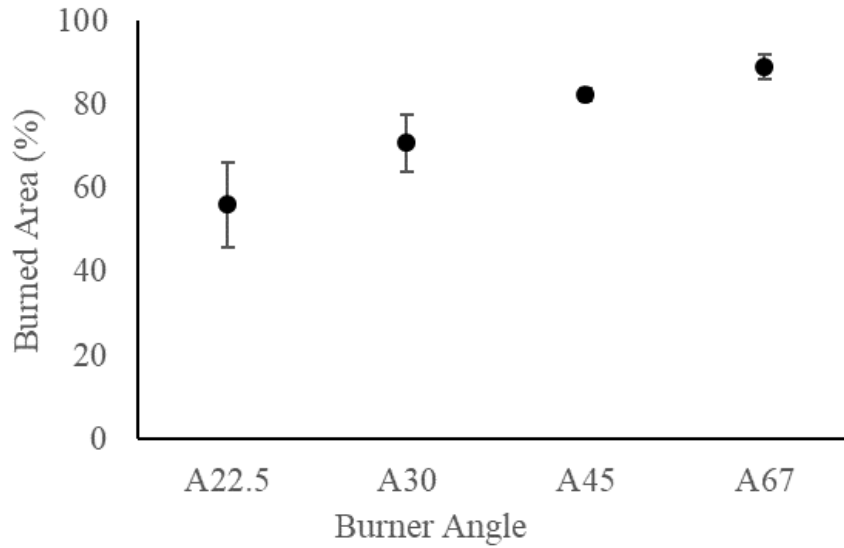


Figure 36. The effect of burner angle treatment on burned area percentage.

Table 10. The result of Kruskal-Wallis Test and Tukey HSD for burner angle's effect on the percentage of burned area.

Kruskal-Wallis Test	
X ²	9.84
Df	3
P-value	0.02
Tukey's HSD	
Interaction	P-value
30-22.5	0.34
45-22.5	0.01
67-22.5	0.00
45-30	0.06
67-30	0.00
67-45	0.10

The burned area uniformity was determined by dividing each individual sand tray into two zones (Figure 37). The total count of black pixel for each zone was then calculated, which would be the input data for the uniformity determination.

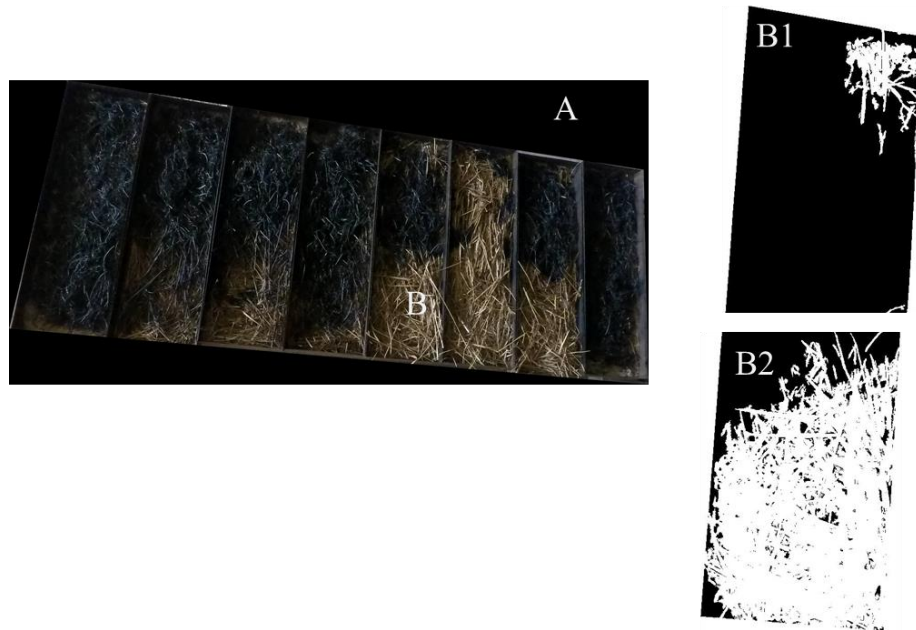


Figure 37. The burned area uniformity determination by splitting each individual tray into two zones. (A) The original image (B) One of individual sand tray, B1 and B2 (The binary image that separated into two zones).

Uniformity coefficient of burned area was determined by calculating the absolute difference of each zone from the mean divided by the mean. Burner angle of 67° has the highest uniformity which was 81.7%, while the lowest uniformity was produced by the burner angle of 22.5° (26.2%) (Figure 38). Burner angle of 22.5° treatment has a wide range of uniformity as well as the burned area percentage from the three replications. This is because the flame at this angle only reached the relatively taller crop residues (more than 5"). The fire would creep along the taller residues and slowly burned the shorter crop residues underneath. Kruskal-Wallis and Tukey's HSD test shows that there is a significant difference among the burner angle treatments (Table 11).

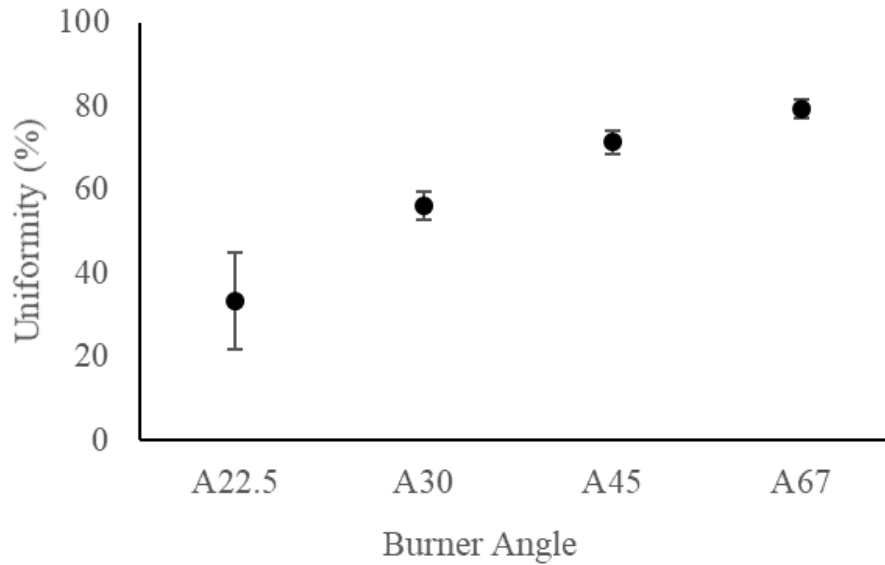


Figure 38. The effect of burner angle treatment on uniformity coefficient.

Table 11. The result of Kruskal-Wallis Test and Tukey HSD for burner angle's effect on the Uniformity coefficient of burned area.

Kruskal-Wallis Test	
X ²	10.39
Df	3
P-value	0.016
Tukey's HSD	
Interaction	P-value
30-22.5	0.03
45-22.5	0.00
67-22.5	0.00
45-30	0.03
67-30	0.00
67-45	0.03

Even though burned area percentage between burner angle of 67° and 45° treatments were not significantly different, according the post hoc test, the uniformity coefficient of burner angle of 67° treatment was significantly higher than other treatments. Based on those results, the following experiments focused on the effect of crop residue loading rate on percentage of burned area and coefficient uniformity, where the burner angle was at 67°.

The best crop residue loading rate determination

Four combinations of travel speed, and crop residues loading were tested, there are: 1.9 mph with 2.9 ton/acre, with 2.2 mph with 2.9 ton/acre, 1.9 mph with 3.5 ton/acre with and 2.2 mph with 3.5 ton/acre with. Those combinations are then called 3Low, 4Low, 3High and 4High, respectively.

Figure 39 depicts crop residue loading rate treatment of 3Low gave a higher than average of the percentage of burned area, while the lowest was 4Low treatment. Moreover, the standard deviation of 3High and 4High gave higher values compared to low crop residue loading rates.

Table 12 reports the combination of the crop residue loading levels within the same level of travel time gave insignificant difference on the percentage of burned area. In Addition, a slower travel time significantly increased the burned area percentage at a lower crop residue loading rate ($\alpha=0.05$).

Even though the high crop residue loading was seemingly able to burn well on the surface, the flame apparently had some difficulties to burn thicker in depth of the crop residue. The unburned crop residue underneath did not occur on a lower crop residue loading treatment. During the study, especially for high crop residue loading, the after-burn images were taken twice. The second images were captured by manually flipping the burned crop residues to see if the crop residues underneath were completely burn as the one on the surface. The extreme case occurred on 3High crop residues loading rate treatment where the surface area was completely burnt, however when the burned crop residues was flipped, there were some areas were still unburned (Figure 40).

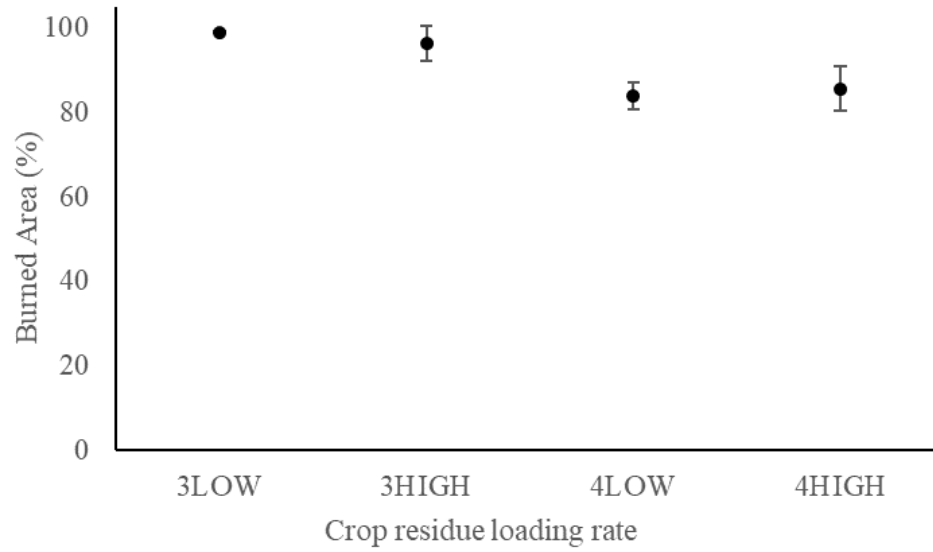


Figure 39. The effect of crop residue loading rate on burned area percentage.

Table 12. The result of Kruskal-Wallis Test and Tukey HSD for crop residues loading rate's effect on the percentage of burned area.

Kruskal-Wallis Test	
X^2	8.43
Df	3
P-value	0.04
Tukey's HSD	
Interaction	P-value
3Low-3High	0.93
4High-3High	0.05
4Low-3High	0.04
4High-3Low	0.02
4Low-3Low	0.02
4Low-4High	0.99

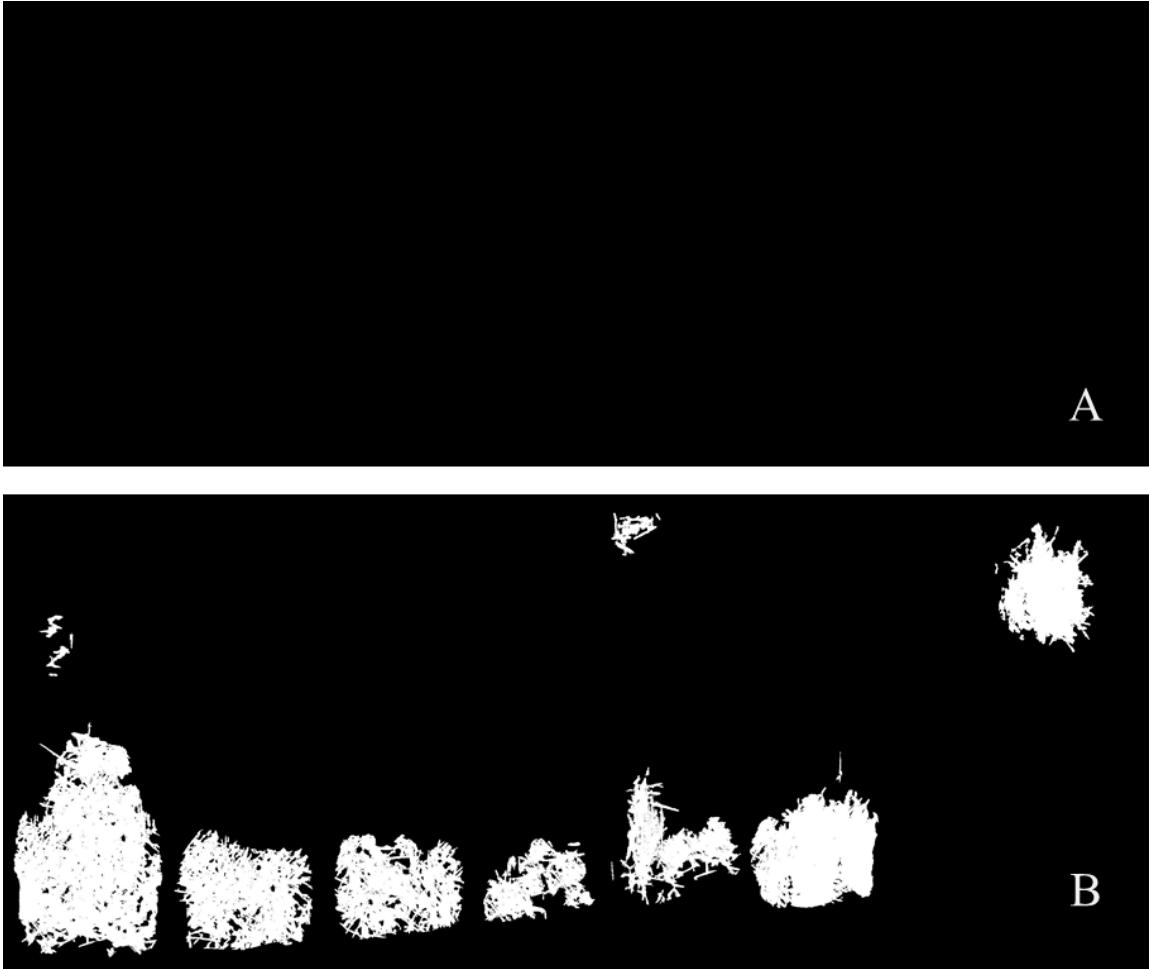


Figure 40. The binary images of a higher crop residues loading rate. (A) The after-burn surface image, (B). The after-burn image after flipping crop residues manually.

Figure 41 illustrates a higher average of uniformity coefficient was at 3High treatment (90.2%), however, at a certain depth in some areas were not burned completely because of the flame penetration issue. Even though, the combination of different travel time with lower crop residues loading rate shows insignificantly different on burned area uniformity (Table 13), the slower travel speed at lower crop residues loading treatment improve the burned area uniformity (Figure 42).

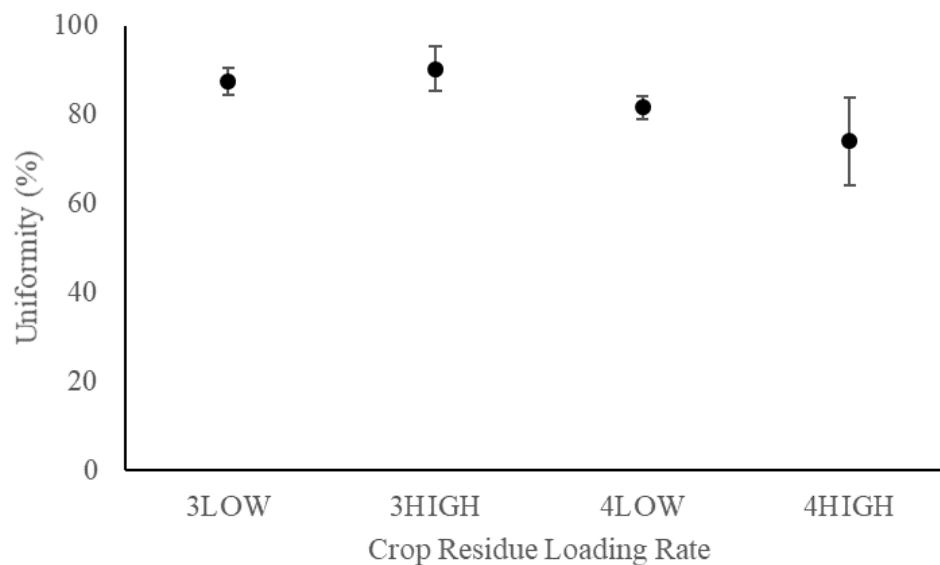


Figure 41. The effect of crop residues loading rate treatment on uniformity coefficient.

Table 13. The results of Kruskal-Wallis Test and Tukey HSD for crop residues loading rate on the Uniformity coefficient of burned area.

Kruskal-Wallis Test	
X ²	8.74
Df	3
P-value	0.038
Tukey's HSD	
Interaction	P-value
3Low-3High	0.92
4High-3High	0.01
4Low-3High	0.03
4High-3Low	0.02
4Low-3Low	0.07
4Low-4High	0.72

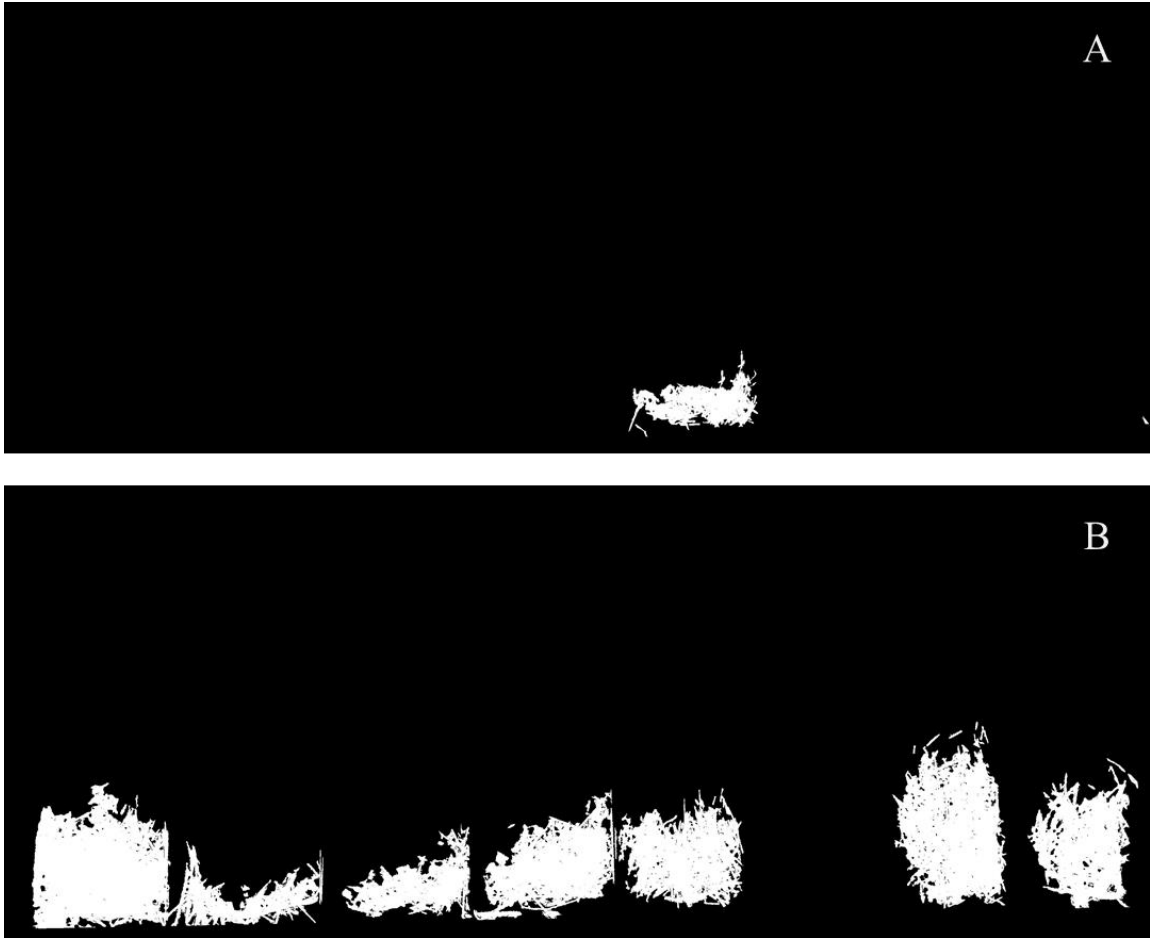


Figure 42. The binary image comparison of (A) 3Low (B) 4Low.

This machine prototype effectively burned crop residues at 1.9 mph of travel speed and crop residue loadings as high as 2.9 ton per acre. The working speed of the LPG flaming machine that was developed in Italy, was 2.2 mph with a working pressure of 29 PSI (Peruzzi et al., 2007; Michele Raffaelli et al., 2011). The working speed of the flaming machine is faster compared to this prototype because of the weed flaming only needs a brief heat for destroying plant tissue so that the weed dies, and the goal is not to burn up the weed. In addition, the working pressure higher than 20 PSI would extinguish the flame in the machine prototype because of the exit velocity exceeding the rate of burn of the gases.

The burner angle of 30° and 45° as it was recommended by a study on flaming machine in Italy (M. Raffaelli et al., 2013) did not work very well on this prototype burning machine. It was because the burners generated shorter flames. The burner angle of 30° and 45° worked with the strong burners with long flames and were usually set at a burner height of 6” to 7” (Ascard, 1995).

The machine gas emission

The temperature of combustion chamber for “1 SET” AND “2 SET” treatments was plotted and shown in Figure 43. The temperature of “1 SET” treatment was lower compared to “2 SET” treatment. The highest temperature that recorded by the thermocouple for “1 SET” and “2SET” was 457.29° and 638.84°.

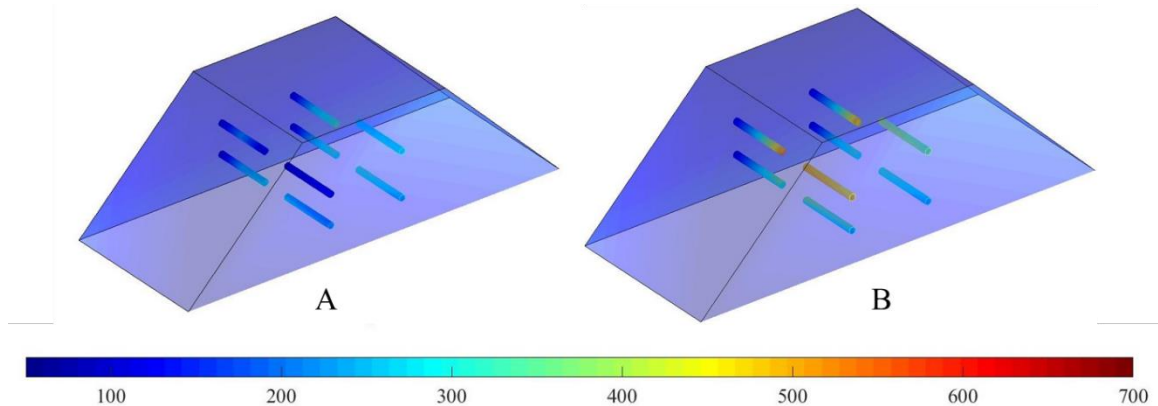


Figure 43. Combustion temperature recorded in the combustion chamber during gas emission measurement experiment gas emission. (A) 1 SET (B) 2 SET.

A high concentration of O₂ appeared in the flue indicates that more air was supplied than it was needed for complete combustion. For “MOVING” treatment, the concentrations were 15.82 (“1 SET”) and 14.86%-vol O₂ (“2 SET”) in dry flue gas, while “STANDSTILL” treatments were 11.10 and 12.7%-vol O₂ for “1 SET” and “2 SET”, respectively (Figure 44). Typically, for waste incineration systems, the standards are given for 10 to 11%-vol O₂, 6 to 12%-vol CO₂ and 0.001 to 0.06%-vol CO in dry flue gas (Zevenhoven & Kilpinen, 2001). The percentage of oxygen by

volume in the flue of a combustion process is directly related to excess air. For biomass fuels combustion, the concentration 3 to 8%-vol O₂ in the flue suggests the excess air supplied for the combustion is 15 to 40% (ABB, 2009). Figure 44 shows as O₂ concentration is higher, the concentration of CO is decreasing. Even though the concentration of O₂ in ‘STANDSTILL’ treatment is lower, the concentration of CO is increasing rapidly. The high concentration of O₂ and CO in the flue indicates the air supply was not utilized by the crop residues.

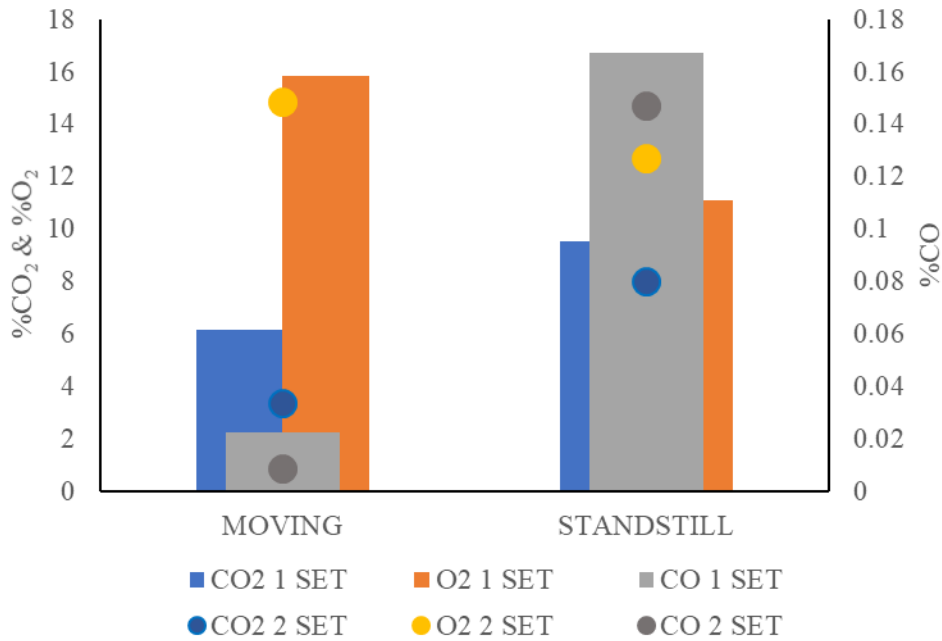


Figure 44. The concentration of O₂, CO₂ and CO in dry flue gas.

Using modified combustion efficiency equation, which assumes all the carbon is released as CO or CO₂, the combustion efficiency was 98.0±0.3%. The result agrees with the previous study on wheat stubble field burning that found the combustion efficiency for wheat stubble burning ranged from 92.2±0.5% to 97.7±0.3%. The lower combustion efficiency are partly due to higher stubble moisture content (Dhammapala et al., 2006).

The flue gas temperatures were 285.7±38.9 °C for ‘MOVING’ treatments and 480.7±21.4 °C for ‘STANDSTILL’ treatments. Kruskal Wallis rank sum and Tukey HSD shows the flue gas

temperature is not significantly different between “1SET” treatment and “2 SET” at $\alpha = 0.05$.

This excessive flue gas temperature is likely due to too much excess air was supplied for the combustion process. The excess air results in oxygen that is not consumed during combustion, and this oxygen absorb otherwise usable heat and carries it out of the flue. Furthermore, since air was used as oxidizer and most of the 79% of air is N, it absorbs heat from combustion of fuels.

CO emission factors (EF) for “MOVING” and “STANDSTILL” treatments are illustrated in Figure 45. The average EF for CO for “MOVING” treatments is 2.47 ± 0.6 lb/acre and “STANDSTILL” treatments is 54.19 ± 4.5 lb/acre. The more mass of crop residues was burned that resulted in the more flue gases were captured for “STANDSTILL” (S) treatments caused the EF was higher compared to “MOVING” (M) treatments. The statistical test (Table 14) shows that the EF for “1 SET” (1M and 1S) and “2 SET” (2M and 2S) are not significantly different ($\alpha = 0.05$).

EF results are difficult to compare against previous reports on biomass burning (CA ARB, 2000; Dhammapala et al., 2006; EPA, 1995; McMeeking et al., 2009) due to the difficulties to quantify the weight of the burned fuel by the machine. Additionally, when it is compared to EF for wildfires (US EPA, 1996), the EF value for wildfires is extremely high, which the lowest EF for CO was 1258 lb/acre. It is likely due to the difference in fuel type, activity rate and fuel moisture content.

The recorded CO concentration exceeds the CO concentration that regulated by EPA NAAQS. CO is one of EPA criteria air pollutant where its concentration in the ambient air should not exceed 35 ppm over a 1-hour period or 9 ppm over an 8-hour. During the study all the gas measured over at least a 0.5-minute period. The lowest CO concentration is 90.3 ppm and the highest is 1638.7 ppm (Figure 46).

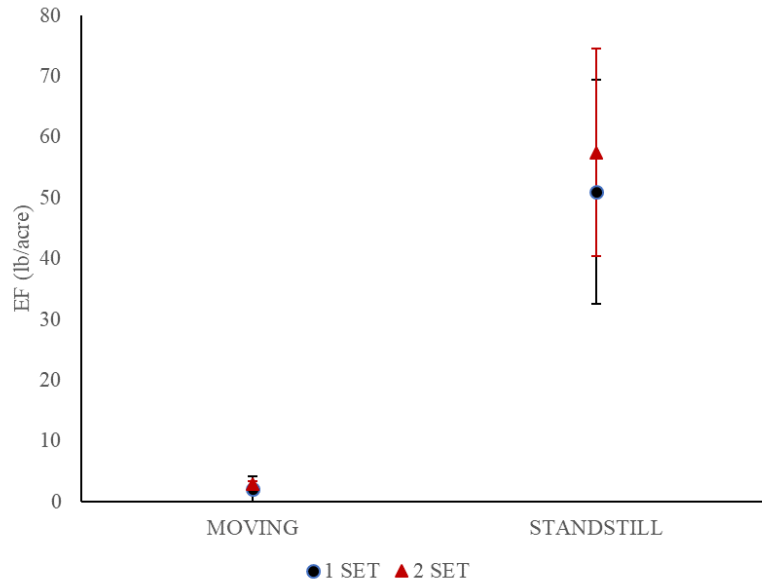


Figure 45.CO emission factors (lb/acre).

Table 14. The results of Kruskal-Wallis test and Tukey HSD for CO emission factors.

Kruskal-Wallis Test	
X ²	8.46
Df	3
P-value	0.04
Tukey's HSD	
Interaction	P-value
1S-1M	0.02
2M-1M	0.927
2S-1M	0.015
2M-1S	0.048
2S-1S	0.99
2S-2M	0.037

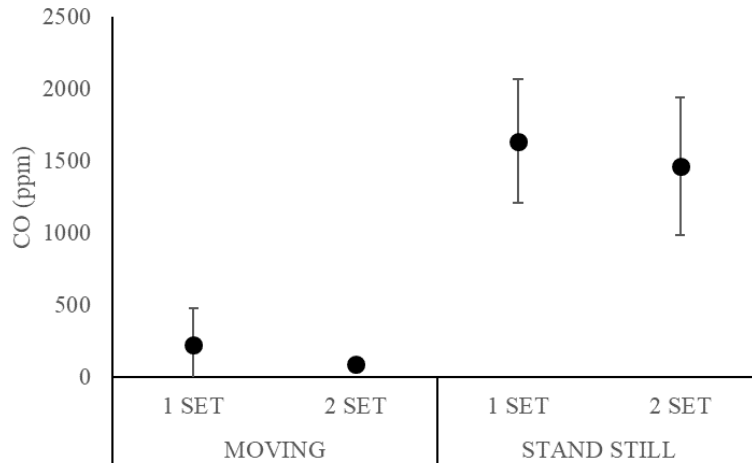


Figure 46. The CO concentrations in the flue gas (ppm).

Oxides of nitrogen are the main pollutants produced by combustions, nitric oxide (NO) and nitrogen dioxide (NO₂). NO is the major NO_x species that is emitted from a combustion process. Figure 47 illustrates the NO emission factors for each of four treatments. The average EF of NO for “MOVING” is 0.79± 0.34 lb/acre and for “STANDSTILL” is 3.31±0.50 lb/acre. Similar to CO EF, the NO EF for “1 SET” and “2SET” treatments is not statistically different at α=0.05 (Table 15). The concentration of NO for “1 SET” treatments is higher compared to “2 SET” treatments (Figure 48).**Error! Reference source not found.** It is likely due to the higher concentrations of O₂ in the flue gas for “1 SET” treatments. At temperature above 1300 °C, NO is generated to the limit of available oxygen (approximately 200,000 ppm), however at temperature below 760° is generated in much lower concentrations (EPA, 1999). Emission regulations refer to NO_x calculated as NO₂, because in the ambient atmosphere NO is oxidized within two hours (EPA, 1999).**Error! Reference source not found.**

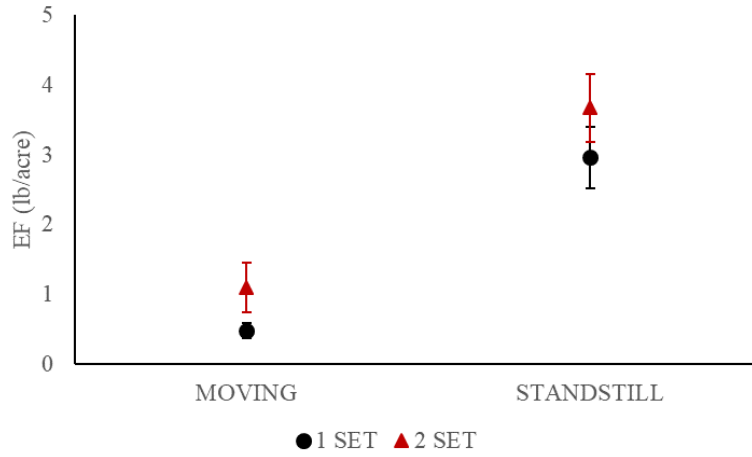


Figure 47. NO emission factors (lb/acre).

Table 15. Kruskal-Wallis test and Tukey HSD for NO emission factor.

Kruskal-Wallis Test	
X ²	9.97
Df	3
P-value	0.019
Tukey's HSD	
Interaction	P-value
1S-1M	0.001
2M-1M	0.083
2S-1M	0
2M-1S	0.053
2S-1S	0.199
2S-2M	0

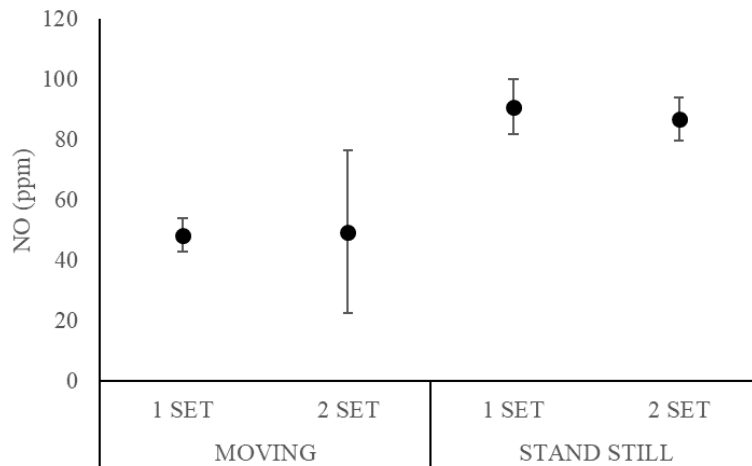


Figure 48. NO concentrations in the flue gas (ppm).

Nitrogen dioxide (NO₂) emission factor ranges from 0.24 to 0.54 lb/acre. Figure 49 shows NO₂ emission factor for the combination of “MOVING” and “2SET” treatments is slightly higher than the other treatments. However, the EF values among the treatments are not significantly different with p-value =0.24 at $\alpha=0.05$. NO₂ concentrations in the flue gas range from 5.7 to 16.2 ppm (Figure 50). The NO₂ concentrations are lower compared to previous study that found the NO₂ concentration for conventional burner was 221 ppm at air temperature of 500° (Flamme, 2001). However, this concentration exceeds the primary and secondary standard of EPA NAAQS, which is 0.053 ppm annual arithmetic mean concentration.

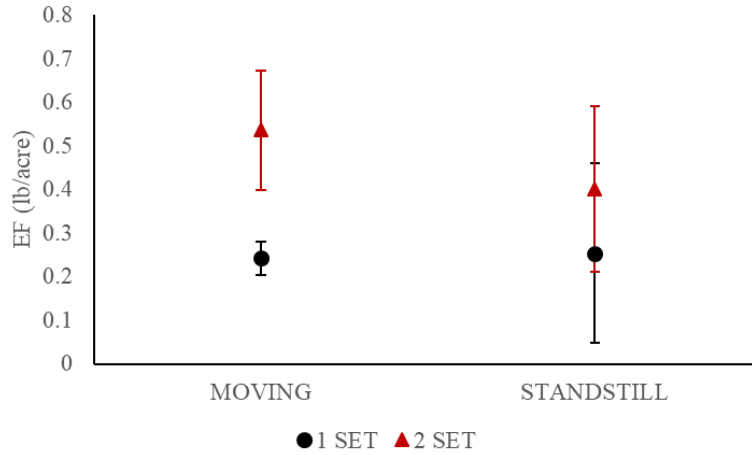


Figure 49. NO₂ emission factors (lb/acre).

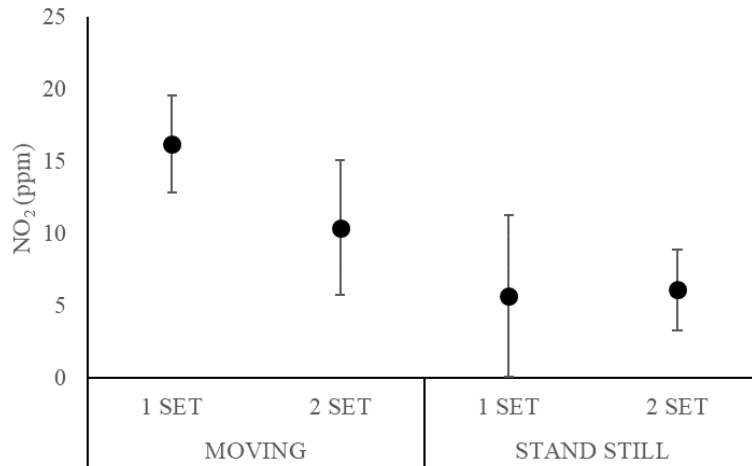


Figure 50. NO₂ concentrations in the flue gas (ppm)

The machine cost estimation

A Microsoft Windows® application was developed to systematically estimate the cost of the developed burning machine and to provide an additional tool for management decisions ([Appendix A6](#)). This application was built using Microsoft Visual Studio® 2017. Microsoft visual studio is an integrated development environment (IDE) that is used to develop computer programs for Microsoft Windows. Figure 51 and Figure 52 illustrate the application layout that

consists of two parts, fixed cost and variable cost. Each part has two columns, the first column is for data entry and the second column is the calculated results.

The screenshot shows a Windows application window titled "Burning Machine Cost Estimation". The window has a standard Windows title bar with minimize, maximize, and close buttons. Below the title bar, there are two tabs: "Fixed Cost" (which is selected) and "Variable Cost". The main area of the window is a light gray color and contains two columns of input fields. The left column contains fields for: "Purchase price for new machine (\$)", "Discount factor for new machine", "Economic Life (Year)" (with a dropdown menu showing "[Choose Year]"), "Remaining Value Factor (%)", "Inflation (%)", "Loan (Year)", "Interest Rate (%)", and "Number of times compounding will occur". The right column contains fields for: "Tax, Housing, Insurance (\$)", "List Price (\$)", "Salvage Value (\$)", "Salvage Value Factor", "Annual Depreciation (\$/Year)", "Total Depreciation (\$)", "Capital Recovery", "Ownership Cost Percentages", "Annual Ownership Cost 1 (\$/Year)", and "Annual Ownership Cost 2 (\$/Year)". At the bottom left of the window, there are two buttons: "CALCULATE" and "CLEAR".

Figure 51. Windows app layout for determining fixed cost for the developed burning machine.

Figure 52. Window app for determining variable cost and total annual cost for the developed burning machine (\$/year).

For the fixed cost, the purchase price was obtained by using the purchase price of Red Dragon[®] vegetable and bed flamer that was produced by Flame Engineering Inc. This bed flamer is used for burning down/pre-emerged treatment. The price of a 5 ft working width of the bed flamer is \$3700. Discount factor value, which is used to calculate the machine current price list, was set to 0.9 as the default value. User has the flexibility to change this factor value. The economic life was obtained based on the economic life of the mounted flaming machine which is 8 years (M. Raffaelli et al., 2013). Economic life value was designed as a dropdown menu. Each option of the economic life is assigned to a certain remaining salvage value as shown in Table 6. The annual inflation rate for the United State for 2019 was 1.7% and the interest rate for operating loans in Oklahoma based on Farm Service Agency USDA is 2.625% (FSA, 2019). The annual fixed cost was calculated based on two different approaches. The first approach was using capital recovery as shown in equation (24) and the second approach was using the ownership cost percentage in equation (25). Figure 53 reports the first approach gave a higher ownership cost,

which is \$561.21 compared to the second approach (\$401.09). It is because the extra \$160.12 for the first approach is assumed to be set aside each year to just repay the value lost due to depreciation and pay interest costs. In other words, the first approach takes into consideration the annual cost of ownership and the time value of money. While the second approach is a simple estimate of total annual ownership cost by multiplying the purchase price of the machine by the ownership cost percentage (ASAE, 2015).

Fixed Cost		Variable Cost	
Purchase price for new machine (\$)	3700	Tax, Housing, Insurance (\$)	74.000
Discount factor for new machine	0.9	List Price (\$)	4111.111
Economic Life (Year)	8	Salvage Value (\$)	1644.445
Remaining Value Factor (%)	40	Salvage Value Factor	0.444
Inflation (%)	1.7	Annual Depreciator (\$/Year)	256.944
Loan (Year)	5	Total Depreciation (\$)	2055.555
Interest Rate (%)	2.625	Capital Recovery	487.212
Number of times compounding will occur	1	Ownership Cost Percentages	10.840
		Annual Ownership Cost 1 (\$/Year)	561.212
		Annual Ownership Cost 2 (\$/Year)	401.090

Figure 53. The machine's fixed cost calculation scenario.

The estimation of variable cost was based on the developed burning machine mounted behind the tractor. The tractor for burning operation was assumed to be rented. Based on Oklahoma Farm and Ranch custom rates in 2017-2018, the tractor rent cost was categorized into two categories based on its rated power, less than 100 hp and 100-150 hp (Sahs, 2018). The rent cost was set to \$31.71 and \$32.16 as default for tractor power less than 100 hp and 100-150 hp, respectively. The rent cost can also be entered manually.

The determination of fuel consumption was divided into two groups. The first was fuel consumption for the tractor (gasoline or diesel) and the second was fuel consumption for machine burning (LPG). The fuel consumption data was obtained during the experiment. The average fuel consumption was 0.7 Gal/hour with working pressure and width 20 PSI and 25", respectively. If the prototype machine was manufactured with a working width of 5 ft, the fuel consumption would be approximately 1.75 Gal/hour.

The cost of site preparation for fireguard varies depends mostly on topographical region. The average cost for site preparation for burning purposes is \$36.51/acre (Myers, Powell, & Megalos, 2012). In most cases, the greatest direct cost of prescribed burning is preparing a firebreak around the perimeter of the burn unit. Often, firebreak preparation is a one-time cost, and can be maintained indefinitely to keep the long-term cost down (Bidwell et al., 2003). For a small farm, the site preparation for firebreak construction was assumed to be \$0. The \$0 cost assumption was based on the assumptions that for firebreak fixed costs are prohibitive for a small farm. The installation of a bare-ground firebreak of a minimum width of 15 feet around a 20-acre field using farm equipment (i.e. tractors, plows, disks or similar implements) is \$235.72. This cost was according to firebreak cost scenario that was developed by the USDA National Resources Conservation Service (NRCS, 2014). In addition, the firebreak would take up a larger percentage of the small farm's acreage; thereby taking away too much productive ground. Therefore, the burning practices using the developed burning machine would need a more labor to patrol the perimeter and spend less on constructing the firebreak. The backing fire techniques would need to implement first before conducting the actual burning practices to reduce the fuel along the burn unit perimeter and contain the fire within the boundary of the burn burning.

The total annual cost for the burning machine (\$/year) is shown on the same window as the variable cost. The two values of the total annual costs because of the two different methods in calculating the machine fixed cost as previously described (Figure 54).

The total cost of Red Dragon ® vegetable and bed flamer was also calculated using the same scenario as the burning machine (Figure 55). The LPG consumption for 5-ft working pressure and 36 PSI is 6.9 Gal/hour. Based on the calculation, the LPG consumption cost resulted in the total cost of the prototype burning machine being slightly lower (\$164.78/acre) than the bed flamer machine(\$172.23/acre).

The cost of prescribed burning is a lot lower compared to the cost of machine burning. The cost ranges from \$10 to \$15 per acre. Additionally, the minimum charge per contract is ranging from \$300 to \$350. For this amount, the tractor hours and hauling unit miles are not included. The actual tach hour would vary from \$72 to \$116, it depends on the tractor rated hours (CPNRD, 2019; NCFS, 2009).

Based on the survey from 1985 to 1994 of the USDA Forest Service's National Forests System, the average cost for all type of prescribed burning were \$101.48 per acre with 134 acres of average burn size. The unit size is the crucial factor to be used in calculating per-acre costs, where larger units have smaller costs. This cost included site preparation, ignition and maintenance, mop up, post-fire monitoring, contractor costs (Cleaves et al., 1999). Considering the inflation and consumer price index, the value of \$101.48 in 2019 is \$175.82.

The USDA NRCS provides financial assistance that covers part of the costs of prescribed burning activities through the Environmental Quality Incentives Program (EQIP). For Oklahoma payment schedule year of 2020, the financial assistance for prescribed burning of herbaceous fuel and firebreak construction is \$8.79 per acre and \$0.04 per feet (NRCS, 2019). Based on personal communication with John Weir, Oklahoma State University's prescribe burn specialist using a

20-acre of prescribed burning scenario, the average firebreaks needed is 0.75 miles (J. Weir, 2019). The total financial assistance would be up to \$334.2 or \$16.71 per acre.

Using the assumption of a 5-foot working width of burning machine, the machine field efficiency of 60%, the travel speed of 1.9 mph, and a 20-acre burn unit, the total cost of burning practice using the developed burning machine was comparable to prescribed burning cost on 134 acres of burn unit. Figure 56 illustrates the effect of burn acreage changes on the machinery cost. More acres of use lowers per acre costs as depreciation and interest costs are spread over more area. However, it might also mean that there would be some issues getting the burning practices done in a timely manner if the 5-ft working width of machine were used to burn large size farm. In general, the increase in machinery size would lower the machinery cost. However, Figure 56 shows a 15-ft working width of machine has the highest total cost, while the 10-ft working width has the lowest total cost. It is because of the assumptions of purchase price for different working width was not the same. It was assumed the purchase prices for a 10-ft and 15-ft working width were \$5,200 and \$7,700, respectively. This assumption was based on the purchase price of vegetable and bed flaming machine with the same working width.

Machine's Field Efficiency (FE) considers for failure to utilize the full operating width of the machine and many other interruptions such as turning, waiting, etc. Effective field capacity (EFC) is one of several factors affecting the EF values. The most accurate EFC data should be collected for a two-week period of operation (Hancock, Swetnam, & Benson, 1991). Figure 57 illustrates the increase of EF's effect on the machine total cost. As the EF increases, the annual hour of use decreases which in turn would lower the total cost.

Burning Machine Cost Estimation

Fixed Cost Variable Cost

Machine Width (ft)	5	Effective Capacity (Acre/hr)	0.691
Machine Speed (mph)	1.9	Annual Use (hr)	28.947
Field Efficiency (%)	60	Adjusted Price (\$) for Inflation	4163.401
Age of Machine (Year)	7	Total Tractor Rent (\$/Year)	634.200
Repair Factor 1	2	Accumulated Repair (\$/Year) and Maintenance	1632.369
Repair Factor 2	0.46	Fuel 1 Cost Diesel (\$/Year)	99.347
Tractor Rent (\$/hr)	<100 HP	Fuel 2 Cost (\$/Year)	50.658
Tractor Rent Cost (\$/hr)	31.71	Total Fuel Cost (\$/Year)	150.005
Tractor Rated Power (Pto)	20	Total Labor Cost (\$/Year)	477.921
Total Area (Acre)	20	Total Mechanical Site (\$/Year) Preparation	0.000
Purchase Price (\$)	3700	Annual Variable Cost (\$/Year)	2894.496
Inflation (%)	1.7	Total cost 1 (\$/Year)	3455.708
Fuel 1 Consumption (Gal/hr)	Diesel 0.88	Total cost 2 (\$/Year)	3295.586
Fuel 1 Price (\$/gallon)	3.9		
Fuel 2 Consumption (Gal/hr)	1.75		
Fuel Price 2 (\$/gallon)	2.36		
Labor Cost (\$/hr)	16.51		
Mechanical Site (\$/Acre) Preparation	0		

CALCULATE CLEAR

Figure 54. The machine's variable cost calculation scenario.

Burning Machine Cost Estimation

Fixed Cost Variable Cost

Machine Width (ft)	5	Effective Capacity (Acre/hr)	0.691
Machine Speed (mph)	1.9	Annual Use (hr)	28.947
Field Efficiency (%)	60	Adjusted Price (\$) for Inflation	4163.401
Age of Machine (Year)	7	Total Tractor Rent (\$/Year)	634.200
Repair Factor 1	2	Accumulated Repair (\$/Year) and Maintenance	1632.369
Repair Factor 2	0.46	Fuel 1 Cost Diesel (\$/Year)	99.347
Tractor Rent (\$/hr)	<100 HP	Fuel 2 Cost (\$/Year)	199.737
Tractor Rent Cost (\$/hr)	31.71	Total Fuel Cost (\$/Year)	299.084
Tractor Rated Power (Pto)	20	Total Labor Cost (\$/Year)	477.921
Total Area (Acre)	20	Total Mechanical Site (\$/Year) Preparation	0.000
Purchase Price (\$)	3700	Annual Variable Cost (\$/Year)	3043.574
Inflation (%)	1.7	Total cost 1 (\$/Year)	3604.786
Fuel 1 Consumption (Gal/hr)	Diesel 0.88	Total cost 2 (\$/Year)	3444.665
Fuel 1 Price (\$/gallon)	3.9		
Fuel 2 Consumption (Gal/hr)	6.9		
Fuel Price 2 (\$/gallon)	2.36		
Labor Cost (\$/hr)	16.51		
Mechanical Site (\$/Acre) Preparation	0		

CALCULATE CLEAR

Figure 55. Vegetable bed flamer's variable cost and total calculation scenario.

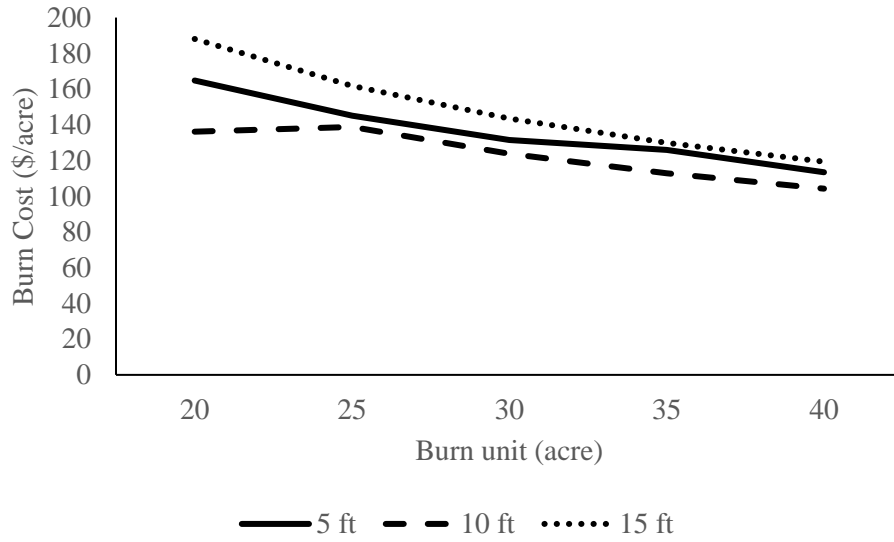


Figure 56. The effect of increasing more acres of use and the machine size on machine cost.

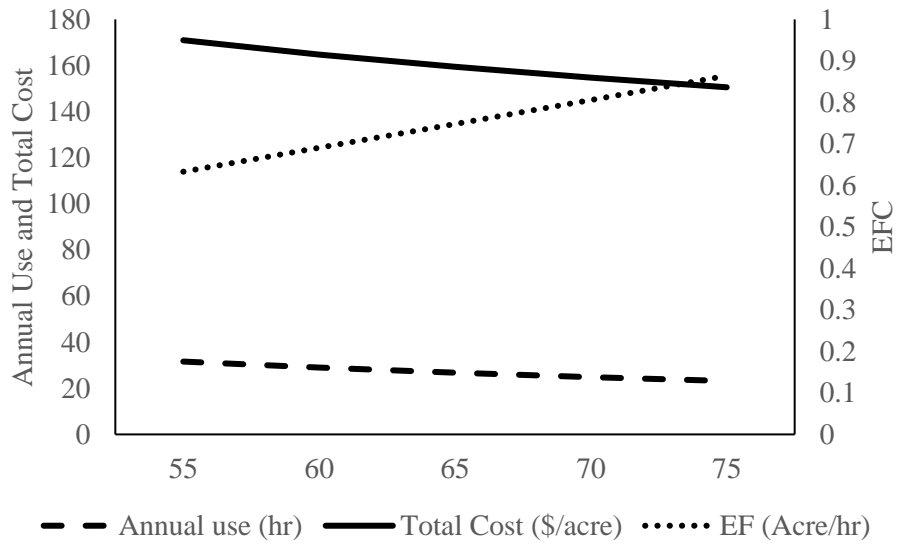


Figure 57. The effect of increasing field efficiency on machine total cost.

CHAPTER VI

CONCLUSIONS AND RECOMMENDATIONS

Conclusions

1. The designed control system was able to maintain flame temperature in between 100 to 1000°C and the LPG working pressure of $\pm 10\%$ from the set pressure. The sensor inputs were an analog pressure sensor and two K-type thermocouples. The system utilized microcontroller board from Arduino Uno to control a solid-state relay and AC solenoid valves.
2. A higher temperature range of 800-840°C was generated by a burner that had an 3/8" mixing tube. This temperature range was recorded at 5" from the burner flare and achieved using a working pressure of 20-30 PSI, air flow rate of 0.88 CF, LPG consumption of 3.4-4.3 lb/hour and an orifice discharge coefficient of 0.9.
3. The study of the effect of burner angle on the percentage of burned area and burned area uniformity for the burning machine prototype showed the burner angle of 67° burned more area (92.5%) compared to the other treatments. Furthermore, this angle gave a significantly higher burned uniformity (81.7%) than other treatments ($\alpha=0.05$). Conversely, burner angle of 22.5° gave both the lowest percentage of burned area and burned area uniformity, which was 48.2% and 26.2%, respectively.

4. Using a 67° of burner angle, a lower crop residue loading rate “3Low”, which had 1.9 mph and 2.9 ton/acre of travel speed and crop residue loading, respectively, gave the highest percentage of burned area. The higher crop residue loading treatments (3.5 ton/acre) gave inconsistent results on burned area percentages and uniformity. The flames experienced difficulties to burn the crop residues that were located underneath the surface. In addition, the slower travel speed at 2.2 ton/acre of loading rate significantly improved the percentage of burned area.
5. Gas emission study shows a high concentration of O₂ in the flue gas that suggests there was too much air was supplied for the combustion resulting in heat loss through flue gas. With the average combustion efficiency of 98.0±0.3%, the highest emission factor for CO, NO and NO₂ are 57, 3.7 and 0.5 lb/acre respectively.
6. Using a-20 acre burn scenario, the cost of burning using burning machine was \$164.78. This cost was slightly lower than the bed flamer (\$172.23). This primarily because of the difference in working pressure, which in turn affecting the fuel consumption. Using the assumption of a-5 feet working width of burning machine, the machine field efficiency of 60%, the travel speed of 1.9 mph, and a-20 acre of burn unit the total cost of burning practice using the developed burning machine was comparable to prescribed burning cost on 134 acres of burn unit.

Recommendations

There were several limitations to this study that needs further research and improvements as follows.

1. The flame length and width were not uniform among the burners. The flame generated from the burner closer to the LPG source generated a wider and shorter flame, while at the other end, it was longer and narrower. The uneven length and width of flame across the burners is

likely due to uneven distribution of air supply. The addition of an orifice and external air mixers in each individual burner line to improve the machine and combustion efficiency needs further study. This addition might also lower the high concentration of O₂ and CO that were found in the flue gas during the study.

2. The distance between the tray and the burner was not constant due to the limitation in burner design. Therefore, the results on burned area and burned area uniformity was not solely because of the burner angle difference but also the height of the burner. The improvement in burner design allowing the relatively constant height in every burner angle treatment is needed.
3. The two sets burner setting was not effectively reducing NO_x concentrations. The improvement in the design of the setting is needed so that fuel staging techniques to control NO_x concentrations could be optimized. In addition, the field experiment is needed to understand the effect of two burner settings on burned area percentage and uniformity.
4. EF results were difficult to compare against previous reports on biomass. Further improvements on methodology are recommended to quantify the mass of the burned crop residue allowing the tray to be weighed before and after burn. So that the EFs in weight of pollutant divided by the weight of burned crop residues can be determined.
5. The prototype was not equipped with the means of preventing escaped fire. Further study on the addition of chain skirt for mop up operation is recommended.

REFERENCES

- Allmaras, R. R., & Rasmussen, P. E. (1985). *Distribution of Small Grain Residue Produced* (Vol. 734, pp. 730–734). Vol. 734, pp. 730–734.
- Andreu, V., Rubio, J. L., Forteza, J., & Cerni, R. (1996). Postfire effects on soil properties and nutrient losses. *International Journal of Wildland Fire*, 6(2), 53–58.
<https://doi.org/10.1071/wf9960053>
- Ansley, R. J., & Rasmussen, G. A. (2005). Managing Native Invasive Juniper Species Using Fire. *Weed Technology*, 19(3), 517–522. <https://doi.org/10.1614/WT-04-098R1.1>
- ASAE. (1999). *American Society of Agricultural Engineers*. <https://doi.org/10.1590/S0100-69162014000100017>
- ASAE. (2015). *Agricultural Machinery Management Data* (No. ASAE D497.7 MAR2011 (R2015)). Retrieved from <https://elibrary.asabe.org/azdez.asp?JID=2&AID=36431&CID=s2000&T=2>
- Ascard, J. (1995). *Thermal Weed Control by Flaming: Biological and Technical Aspects*. Swedish University of Agricultural Science.
- Ascard, J. (1998). Flame weeding -effects of burner angle on weed control and temperature patterns. *Acta Agriculturae Scandinavica*, 48, 248–254.
<https://doi.org/10.1080/09064719809362505>
- Badía, D., & Martí, C. (2003). Plant Ash and Heat Intensity Effects on Chemical and Physical Properties of Two Contrasting Soils. *Arid Land Research and Management*, 17(February 2015), 23–41. <https://doi.org/10.1080/15324980301595>
- Baukal Jr, C. E. (2003). *Industrial Burner Handbook* (1st ed.). CRC Press.
- Bell, B. (1996). *Farm Machinery* (Fourth). Alexandria Bay, NY: Farming Press Books & Videos; Miller Freeman Professional Ltd.
- Berry, W. M., Brumbaugh, V., Moulton, F., & Shawn, B. (1921). Design of atmospheric gas burners. In *Technologic Papers of Bureau Standards* (No. 193).
[https://doi.org/10.1016/S0016-0032\(13\)90386-0](https://doi.org/10.1016/S0016-0032(13)90386-0)

- ABB. (2009). A beginner ' s guide to combustion optimization Improve efficiency , lower environmental impact , reduce downtime. Retrieved November 11, 2019, from <http://www.revbase.com/tt/sl.ashx?z=33b57d1d&dataid=209408>
- Allmaras, R. R., & Rasmussen, P. E. (1985). *Distribution of Small Grain Residue Produced* (Vol. 734, pp. 730–734). Vol. 734, pp. 730–734.
- Andreu, V., Rubio, J. L., Forteza, J., & Cerni, R. (1996). Postfire effects on soil properties and nutrient losses. *International Journal of Wildland Fire*, 6(2), 53–58. <https://doi.org/10.1071/wf9960053>
- Ansley, R. J., & Rasmussen, G. A. (2005). Managing Native Invasive Juniper Species Using Fire. *Weed Technology*, 19(3), 517–522. <https://doi.org/10.1614/WT-04-098R1.1>
- ASAE. (1999). *American Society of Agricultural Engineers*. <https://doi.org/10.1590/S0100-69162014000100017>
- ASAE. (2015). *Agricultural Machinery Management Data* (No. ASAE D497.7 MAR2011 (R2015)). Retrieved from <https://elibrary.asabe.org/azdez.asp?JID=2&AID=36431&CID=s2000&T=2>
- Ascard, J. (1995). *Thermal Weed Control by Flaming: Biological and Technical Aspects*. Swedish University of Agricultural Science.
- Ascard, J. (1998). Flame weeding -effects of burner angle on weed control and temperature patterns. *Acta Agriculturae Scandinavica*, 48, 248–254. <https://doi.org/10.1080/09064719809362505>
- Badía, D., & Martí, C. (2003). Plant Ash and Heat Intensity Effects on Chemical and Physical Properties of Two Contrasting Soils. *Arid Land Research and Management*, 17(February 2015), 23–41. <https://doi.org/10.1080/15324980301595>
- Baukal Jr, C. E. (2003). *Industrial Burner Handbook* (1st ed.). CRC Press.
- Bell, B. (1996). *Farm Machinery* (Fourth). Alexandria Bay, NY: Farming Press Books & Videos; Miller Freeman Professional Ltd.
- Berry, W. M., Brumbaugh, V., Moulton, F., & Shawn, B. (1921). Design of atmospheric gas burners. In *Technologic Papers of Bureau Standards* (No. 193). [https://doi.org/10.1016/S0016-0032\(13\)90386-0](https://doi.org/10.1016/S0016-0032(13)90386-0)
- Bidwell, T. G., Weir, J. R., Carlson, J. D., Masters, R. E., Fuhlendorf, S. D., Waymire, J., & Conrady, S. (2003). Using Prescribed Fire in Oklahoma. *Oklahoma Cooperative Extension Fact Sheets*, (E-927). Retrieved from <http://pods.dasn.okstate.edu/docushare/dsweb/Get/Document-2563/E927web.pdf>
- Bidwell, T. G., Weir, J. R., Masters, R. E., & Engle, D. M. (2018). Fire Prescriptions for Maintenance and Restoration of Native Plant Communities. *Oklahoma Cooperative Extension Fact Sheets*, (NREM-2878). Retrieved from <http://pods.dasn.okstate.edu/docushare/dsweb/Get/Document-2704/NREM-2878web-surv>
- Brandt, C. S. (1966). Agricultural burning. *Journal of the Air Pollution Control Association*, 16(2), 85–86. <https://doi.org/10.1080/00022470.1966.10468447>

- Brown, A. M. (2001). A step-by-step guide to non-linear regression analysis of experimental data using a Microsoft Excel spreadsheet. *Computer Methods and Programs in Biomedicine*, 65(3), 191–200. [https://doi.org/10.1016/S0169-2607\(00\)00124-3](https://doi.org/10.1016/S0169-2607(00)00124-3)
- Burgess, L. W., Backhouse, D., Swan, L. J., & Esdaile, R. J. (1996). Control of Fusarium crown rot of wheat by late stubble burning and rotation with sorghum. *Australasian Plant Pathology*, 25(4), 229–233. <https://doi.org/10.1071/AP96042>
- CA ARB. (2000). *Agricultural burning emission factors*. Retrieved from http://www.arb.ca.gov/ei/see/memo_ag_emission_factors.pdf
- Cadotte, M. W., Cardinale, B. J., & Oakley, T. H. (2008). Evolutionary history and the effect of biodiversity on plant productivity. *Proceedings of the National Academy of Sciences of the USA*, 105(44), 17012–17017. <https://doi.org/10.1073/pnas.0805962105>
- Carolan, J. E., Joshi, S. V., & Dale, B. E. (2007). Technical and Financial Feasibility Analysis of Distributed Bioprocessing Using Regional Biomass Pre-Processing Centers. *Journal of Agricultural & Food Industrial Organization*, 5(2), 1–29. <https://doi.org/10.2202/1542-0485.1203>
- Carter, L. M., Colwick, R. F., & Tavernetti, J. R. (1960). Evaluating Flame-Burner Design for Weed Control in Cotton. *Transactions-American Society of Agricultural Engineers*, 3(2), 125–128.
- Certini, G. (2005). Effects of fire on properties of forest soils: A review. *Oecologia*, 143(1), 1–10. <https://doi.org/10.1007/s00442-004-1788-8>
- Chen, L. W. A., Moosmüller, H., Arnott, W. P., Chow, J. C., Watson, J. G., Susott, R. A., ... Wei, M. H. (2007). Emissions from laboratory combustion of wildland fuels: Emission factors and source profiles. *Environmental Science and Technology*, 41(12), 4317–4325. <https://doi.org/10.1021/es062364i>
- Cheng, M. T., Horng, C. L., Su, Y. R., Lin, L. K., Lin, Y. C., & Chou, C. C. K. (2009). Particulate matter characteristics during agricultural waste burning in Taichung City, Taiwan. *Journal of Hazardous Materials*, 165(1–3), 187–192. <https://doi.org/10.1016/j.jhazmat.2008.09.101>
- Chou, C.-H., & Lin, H.-J. (1976). Autointoxication Mechanism of *Oryza sativa* I. Phytotoxic effects on Decomposing Rice Residues in Soil. *L Chem. EcoL*, 2(3), 353–367.
- Christiansen, J. E. (1942). Irrigation by Sprinkling. In *Bulletin* (Vol. 670).
- Cleaves, D. A., & Brodie, J. D. (1990). Economic analysis of prescribed burning. *Natural and Prescribed Fire in Pacific Northwest Forests*, 271–282.
- Cleaves, D. A., Martinez, J., & Haines, T. K. (1999). Influences on Prescribed Burning Activity and Costs in the National Forest System. *Proc. of the Symposium on Fire Economics, Planning, and Policy: Bottom Lines*, 277–287. <https://doi.org/http://www.srs.fs.usda.gov/pubs/gtr/gtr%5Fsr5037.pdf>
- CPNRD. (2019). Central Platte Natural Resource District: Prescribed Fire Program. Retrieved October 24, 2019, from <http://cpnrd.org/wp-content/uploads/2015/12/PF-Program-Brochure.pdf>

- Crowder, D. W., Northfield, T. D., Gomulkiewicz, R., & Snyder, W. E. (2012). Conserving and promoting evenness: organic farming and fire-based wildland management as a case studies. *Ecology*, *93*(9), 2001–2007.
- Dauve, J., & Flaim, S. J. (1979). *Agricultural Crop Residue Collection Costs*. Retrieved from <https://www.nrel.gov/docs/legosti/old/354.pdf>
- Dhammapala, R., Claiborn, C., Corkill, J., & Gullett, B. (2006). Particulate emissions from wheat and Kentucky bluegrass stubble burning in eastern Washington and northern Idaho. *Atmospheric Environment*, *40*(6), 1007–1015. <https://doi.org/10.1016/j.atmosenv.2005.11.018>
- Dhammapala, R., Claiborn, C., Simpson, C., & Jimenez, J. (2007). Emission factors from wheat and Kentucky bluegrass stubble burning: Comparison of field and simulated burn experiments. *Atmospheric Environment*, *41*(7), 1512–1520. <https://doi.org/10.1016/j.atmosenv.2006.10.008>
- DiTomaso, J. M. (2000). Invasive weeds in rangelands: Species, impacts, and management. *Weed Science*, *48*(2), 255–265. [https://doi.org/10.1614/0043-1745\(2000\)048\[0255:IWIRSI\]2.0.CO;2](https://doi.org/10.1614/0043-1745(2000)048[0255:IWIRSI]2.0.CO;2)
- DiTomaso, J. M., Kyser, G. B., Hastings, M. S., Science, S. W., Apr, N. M., DiTomaso, J. M., ... Hastings, M. S. (1999). *Native Plant Diversity Published by : Weed Science Society of America and Allen Press Linked references are available on JSTOR for this article : Prescribed burning for control of yellow starthistle (Centaurea soistitialis) and enhanced native plant div. 47*(2), 233–242.
- Dobermann, A., & Fairhurst, T. H. (2002). Rice straw management. *Better Crops International*, *16*(May), 7–11.
- Douglas, C. L., Rasmussen, P. E., & Allmaras, R. R. (1989). *Effects on Residue Distribution by Combines*. (8645), 1258–1262.
- Edward, W. (2015). *Estimating Farm Machinery Repair Costs* (No. Ag Decision maker PM710).
- EPA. (1995). *AP 42 : Open burning*. Retrieved from <http://www.epa.gov/ttn/chief/ap42/ch02/final/c02s05.pdf>
- EPA. (1999). Nitrogen oxides (NO_x), why and how they are controlled. *Epa-456/F-99-006R*, (November), 48. https://doi.org/EPA_456/F-99-006R
- Field, H. L., & Long, J. M. (2018). *Introduction to Agricultural Engineering Technology* (Fourth Edi). <https://doi.org/10.1007/978-3-319-69679-9>
- Fight, R., & Barbour, J. (2004). *Prescribed Fire Cost* (No. RMRS-RN-20-8-WWW). Portland, OR.
- Flamme, M. (2001). Low No_x combustion technologies for high temperature applications. *Energy Conversion and Management*, *42*(15–17), 1919–1935. [https://doi.org/https://doi.org/10.1016/S0196-8904\(01\)00051-6](https://doi.org/https://doi.org/10.1016/S0196-8904(01)00051-6)
- FSA. (2019). Oklahoma Farm Service Agency, USDA. Retrieved October 22, 2019, from <https://www.fsa.usda.gov/state-offices/Oklahoma/index>

- Fuentes-Dávila, G., Goates, B. J., Thomas, P., Nielsen, J., & Ballantyne, B. (2002). Smut Diseases. *Bread Wheat: Improvement and Production*, 567. Retrieved from <http://www.fao.org/docrep/006/Y4011e/y4011e0h.htm%5Chttp://www.fao.org/docrep/006/Y4011e/y4011e00.htm>
- Fuhlendorf, S. D., Engle, D. M., O’Meilia, C. M., Weir, J. R., & Cummings, D. C. (2009). Does herbicide weed control increase livestock production on non-equilibrium rangeland? *Agriculture, Ecosystems and Environment*, 132(1–2), 1–6. <https://doi.org/10.1016/j.agee.2009.02.015>
- Gaffney, P. (2000). *Agricultural burning emission factors*. Retrieved from http://www.arb.ca.gov/ei/see/memo_ag_emission_factors.pdf
- Glancey, J. L. (1997). *Analysis of Header Loss from Pod Stripper Combines in Green Peas*. 1–10.
- Gonzalez, R. C., Woods, R. E., & Eddins, S. L. (2009). *No Title* (Second Edi). Gatemark Publishing.
- Grass Seed Crops: Post Harvest Residue Management. (n.d.). Retrieved May 21, 2017, from http://cropandsoil.oregonstate.edu/system/files/classes/css460-560/Chapter_6.pdf
- Gupta, P. K., Krishna Prasad, V., Sharma, C., Sarkar, A. K., Kant, Y., Badarinath, K. V. S., & Mitra, A. P. (2001). Ch4 emissions from biomass burning of shifting cultivation areas of tropical deciduous forests - Experimental results from ground-based measurements. *Chemosphere - Global Change Science*, 3(2), 133–143. [https://doi.org/10.1016/S1465-9972\(01\)00003-4](https://doi.org/10.1016/S1465-9972(01)00003-4)
- Hancock, J. N., Swetnam, L. D., & Benson, F. J. (1991). Calculating Farm Machinery Field Capacities. *Agriculture Engineering Extension Publications*. Retrieved from https://uknowledge.uky.edu/cgi/viewcontent.cgi?article=1020&context=aen_reports
- Hardison, J R. (1976). Fire and Flame for Plant Disease Control. *Phytopathology*, 14, 355–379. <https://doi.org/Http://Dx.Doi.Org/10.1146/Annurev.Py.14.090176.002035>
- Hardison, John R. (1976). Fire and flame for plant disease control. *Annual Review of Phytopathology*, 14(1), 355–379. <https://doi.org/10.1146/annurev.py.14.090176.002035>
- Hays, M. D., Fine, P. M., Geron, C. D., Kleeman, M. J., & Gullett, B. K. (2005). Open burning of agricultural biomass: Physical and chemical properties of particle-phase emissions. *Atmospheric Environment*, 39(36), 6747–6764. <https://doi.org/10.1016/j.atmosenv.2005.07.072>
- Houshfar, E., Skreiberg, Ø., Todorović, D., Skreiberg, A., Løvås, T., Jovović, A., & Sørum, L. (2012). NO x emission reduction by staged combustion in grate combustion of biomass fuels and fuel mixtures. *Fuel*, 98(x), 29–40. <https://doi.org/10.1016/j.fuel.2012.03.044>
- Huhnke, R. L., & Bowers, W. (1990). HAYMACH\$ A Program to Estimate Equipment Costs. *An ASAE Meeting Presentation, Paper No. 901558*. St. Joseph, MI: American Society of Agricultural Engineers.
- Jain, N., Bhatia, A., & Pathak, H. (2014). Emission of air pollutants from crop residue burning in India. *Aerosol and Air Quality Research*, 14(1), 422–430. <https://doi.org/10.4209/aaqr.2013.01.0031>

- Jenkins, B., Baxter, L., & Miles, T. (1998). Combustion properties of biomass. *Fuel Processing Technology*, 54(1–3), 17–46. [https://doi.org/10.1016/S0378-3820\(97\)00059-3](https://doi.org/10.1016/S0378-3820(97)00059-3)
- Jenkins, B. M., Kennedy, I. M., Turn, S. Q., Williams, R. B., Hall, S. G., Teague, S. V, ... Raabe, O. G. (1993). Wind-tunnel modeling of atmospheric emissions from agricultural burning - Influence of operating configuration on flame structure and particle-emission factor for a spreading-type fire. *Environmental Science & Technology*, 27(9), 1763–1775. <https://doi.org/10.1021/es00046a002>
- Jenkins, B. M., Turn, S. Q., Williams, R. B., Goronea, M., & Abd-el-Fattah, H. (1996). *Atmospheric pollutant emission factors from open burning of agricultural and forest biomass by wind tunnel simulations. Volume 1. Final report (No. PB--97-133037/XAB)*. Davis, CA.
- Johnsson, J. E. (1994a). Formation and reduction of nitrogen oxides in fluidized-bed combustion. *Fuel*, 73(9), 1398–1415. [https://doi.org/10.1016/0016-2361\(94\)90055-8](https://doi.org/10.1016/0016-2361(94)90055-8)
- Johnsson, J. E. (1994b). *Formation and reduction of Nitrogen oxides in fluidized-bed combustion*. 73(9), 1398–1415.
- Johnston, W. J., Golob, C. T., Sitton, J. W., & Schultz, T. R. (1996). Effect of temperature and postharvest field burning of Kentucky bluegrass on germination of sclerotia of *Claviceps purpurea*. *Plant Disease*, Vol. 80, pp. 766–768.
- Jyothi, G., Sushma, C., & Veeresh, D. S. S. (2015). Luminance Based Conversion of Gray Scale Image to RGB Image. *International Journal of Computer Science and Information Technology Research*, 3(3), 279–283.
- Kang, W. S. (2001). Development of A Flame Weeder. *Transactions-American Society of Agricultural Engineers*, 44(5), 1065–1070.
- Kemmerer, B. (2012). Large square baling and bale handling efficiency—A case study. *Agricultural Sciences*, 03(02), 178–183. <https://doi.org/10.4236/as.2012.32020>
- Klemm, R. J., Mason, R. M., Heilig, C. M., Neas, L. M., & Dockery, D. W. (2000). Is daily mortality associated specifically with fine particles? Data reconstruction and replication of analyses. *Journal of the Air & Waste Management Association (1995)*, 50(7), 1215–1222. <https://doi.org/10.1080/10473289.2000.10464149>
- Klinner, W. E., Neale, M. A., Arnold, R. E., Geikie, A. A., & Hobson, R. N. (1987). *A new concept in combine harvester headers*. 37–45.
- Knezevic, S. Z., Datta, A., Bruening, C., & Gogos, G. (2014). Propane-fueled flame weeding in corn, soybean, and sunflower. Retrieved from Propane education and research council website: <https://lpg-apps.org/uploads/Modules/Library/propanefueledflameweeding.pdf>
- Kutiél, P., & Inbar, M. (1993). Fire impacts on soil nutrients and soil erosion in a Mediterranean pine forest plantation. *Catena*, 20(1–2), 129–139. [https://doi.org/10.1016/0341-8162\(93\)90033-L](https://doi.org/10.1016/0341-8162(93)90033-L)
- Lafond, G. P., Stumborg, M., Lemke, R., May, W. E., Holzapfel, C. B., & Campbell, C. A. (2009). Quantifying straw removal through baling and measuring the long-term impact on soil quality and wheat production. *Agronomy Journal*, 101(3), 529–537.

<https://doi.org/10.2134/agronj2008.0118x>

- Laguë, C., Gill, J., Lehoux, N., & Péloquin, G. (1997). Engineering Performances of Propane Flamers Used For Weed, Insect Pest, and Plant Disease Control. *Applied Engineering in Agriculture*, 13(1), 7–16.
- Langner, H.-R., Ehlert, D., Heisig, M., Potsdam-Bornim, Kirste, A., & Brandenburg. (2006). The Thermal Effect of Laser Radiation. *LANDTECHNIK*, 61(5), 252–253.
- Li, X., Wang, S., Duan, L., Hao, J., Li, C., Chen, Y., & Yang, L. (2007). Particulate and trace gas emissions from open burning of wheat straw and corn stover in China. *Environmental Science and Technology*, 41(17), 6052–6058. <https://doi.org/10.1021/es0705137>
- Loghavi, M. (2012). *Comparison of Uniform and Targeted Discrete-Flame Weeding Methods for Inter-row Weed Control in Maize Planting*. 7004(12).
- Loreau, M., Naeem, S., Inchausti, P., Bengtsson, J., Grime, J. P., Hector, A., ... Raffaelli, D. (2001). Biodiversity and ecosystem functioning: current knowledge and future challenges. *Science*, 294(5543), 804. Retrieved from <http://www.sciencemag.org.erl.lib.byu.edu/cgi/content/abstract/sci;294/5543/804>
- Marx, C., Barcikowski, S., Hustedt, M., Haferkamp, H., & Rath, T. (2012). Design and application of a weed damage model for laser-based weed control. *Biosystems Engineering*, 113(2), 148–157. <https://doi.org/10.1016/j.biosystemseng.2012.07.002>
- Mataix-Solera, J., Cerdà, A., Arcenegui, V., Jordán, A., & Zavala, L. M. (2011). Fire effects on soil aggregation: A review. *Earth-Science Reviews*, 109(1–2), 44–60. <https://doi.org/10.1016/j.earscirev.2011.08.002>
- Mathiassen, S. K., Bak, T., Christensen, S., & Kudsk, P. (2006). The Effect of Laser Treatment as a Weed Control Method. *Biosystems Engineering*, 95(4), 497–505. <https://doi.org/10.1016/j.biosystemseng.2006.08.010>
- McCarty, J. L., Korontzi, S., Justice, C. O., & Loboda, T. (2009). The spatial and temporal distribution of crop residue burning in the contiguous United States. *Science of the Total Environment*, 407(21), 5701–5712. <https://doi.org/10.1016/j.scitotenv.2009.07.009>
- McMaster, G. S., Aiken, R. M., & Nielsen, D. C. (2000). *Optimizing wheat harvest cutting height for harvest efficiency and soil and water conservation*. 1104–1108.
- McMeeking, G. R., Kreidenweis, S. M., Baker, S., Carrico, C. M., Chow, J. C., Collett, J. L., ... Cyle E., W. (2009). Emissions of trace gases and aerosols during the open combustion of biomass in the laboratory. *Journal of Geophysical Research Atmospheres*, 114(19), 1–20. <https://doi.org/10.1029/2009JD011836>
- Morris, N. L., Miller, P. C. H., Orson, J. H., & Froud-Williams, R. J. (2009). The effect of wheat straw residue on the emergence and early growth of sugar beet (*Beta vulgaris*) and oilseed rape (*Brassica napus*). *European Journal of Agronomy*. <https://doi.org/10.1016/j.eja.2008.09.002>
- Myers, R. J., Powell, W., & Megalos, M. (2012). Prescribed Burning Cost Recovery Analysis on Nonindustrial Private Forestland in North Carolina. *Proceedings of the 16th Biennial Southern Silvicultural Research Conference. e-Gen. Tech. Rep. SRS-156. Asheville, NC:*

U.S. Department of Agriculture Forest Service, Southern Research Station. 230-234, 230–234.

- NCFS. (2009). North Carolina Division Forest Resources: Prescribed Burning Rate. Retrieved from https://www.ncforestservice.gov/Managing_your_forest/pdf/Burning_rates.pdf
- Neilson, B. D., Bruening, C. A., Stepanovic, S., Datta, A., Knezevic, S., & Gogos, G. (2017). Design and Field Testing of a CombinedFlaming and Cultivation Implementfor Effective Weed Control. *Applied Engineering in Agriculture*, 33(1), 43–54. <https://doi.org/10.13031/aea.11719>
- NRCS. (2014). Scenario Cost: Firebreak Scenaria. Retrieved November 22, 2019, from <https://efotg.sc.egov.usda.gov/references/public/MO/MO394FirebreakFY15.pdf>
- NRCS. (2019). Oklahoma Payment Schedule. Retrieved October 30, 2019, from <https://www.nrcs.usda.gov/wps/portal/nrcs/detail/national/programs/financial/?cid=nrcseprd1328258>
- Nussbaumer, T. (2003). Combustion and Co-combustion of Biomass: Fundamentals, Technologies, and Primary Measures for Emission Reduction. *Energy and Fuels*, 17(6), 1510–1521. <https://doi.org/10.1021/ef030031q>
- Patil, S., & Bodhe, S. (2011). Betel leaf area measurement using image processing. *International Journal on Computer Science ...*, 3(7), 2656–2660. Retrieved from <http://www.enggjournals.com/ijcse/doc/IJCSE11-03-07-087.pdf>
- Peruzzi, A., Ginanni, M., Fontanelli, M., Raffaelli, M., & Bärberi, P. (2007). Innovative strategies for on-farm weed management in organic carrot. *Renewable Agriculture and Food Systems*, 22(04), 246–259. <https://doi.org/10.1017/S1742170507001810>
- Raffaelli, M., Frasconi, C., Fontanelli, M., Martelloni, L., & Peruzzi, A. (2015). LPG burners for weed control. *Applied Engineering in Agriculture*, 31(5), 717–731. <https://doi.org/10.13031/aea.31.10762>
- Raffaelli, M., Martelloni, L., Frasconi, C., Fontanelli, M., & Peruzzi, A. (2013). Development of machines for flaming weed control on hard surfaces. *Applied Engineering in Agriculture*, 29(5), 663–673. <https://doi.org/10.13031/aea.29.10143>
- Raffaelli, Michele, Fontanelli, M., Frasconi, C., Sorelli, F., Ginanni, M., & Peruzzi, A. (2011). Physical weed control in processing tomatoes in Central Italy. *Renewable Agriculture and Food Systems*, 26(2), 95–103. <https://doi.org/10.1017/S1742170510000578>
- Sahs, R. (2018). Current Report: Oklahoma Farm and Ranch Custom Rate, 2017-2018. *Oklahoma Cooperative Extension Fact Sheets*, CR-205. Retrieved from <http://factsheets.okstate.edu/documents/cr-205-oklahoma-farm-and-ranch-custom-rates-2017-2018/>
- Schwartz, J., Dockery, D. W., & Neas, L. M. (1996). Is daily mortality associated specifically with fine particles? *Journal of Air and Waste Management Association*, 46(10), 1996–1996. <https://doi.org/10.1080/10473289.1996.10467528>
- Shipp, B. E. (1971). *Patent No. 3,606,877*.

- Singh, T. P. (2016). *Farm Machinery*. Delhi: PHI Learning Private Limited.
- Soille, P. (1999). *Morphological Image Analysis: Principles and Applications*. Berlin: Springer-Verlag.
- Špokas, L., & Dainius Steponavičius. (2010). Impact of wheat stubble height on combine technological parameters. *Journal of Food, Agriculture and Environment*, 8(2), 464–468.
- Srivastava, A. K., Goering, C. E., & Rohrbach, R. P. (1993). *Engineering Principles of Agricultural Machines* (P. DeVore-Hansen, Ed.). St. Joseph, MI: American Society of Agricultural Engineers.
- Stevens, R., Aljoe, H., Forst, T. S., Motal, F., Shankles, K., Samuel, T., & Noble, R. (1996). *How Much Does It Cost to Burn*. 19(2), 16–19.
- Stone, R. E., & Coakley, R. D. (1974). *Patent No. 3,802,020*.
- Storeheier, K. J. (1994). Basic investigations into flaming for weed control. *Acta Horticulturae*, Vol. 372, pp. 195–204.
- Streets, D. G., Yarber, K. F., Woo, J.-H., & Carmichael, G. R. (2003). Biomass burning in Asia: Annual and seasonal estimates and atmospheric emissions. *Global Biogeochemical Cycles*, 17(4), 1099. <https://doi.org/10.1029/2003GB002040>
- Tado, C. J. M., Wacker, P., Kutzbach, H. D., & Suministrado, D. C. (1998). Development of Stripper Harvesters: A Review. *Journal of Agricultural Engineering Research*, 71(2), 103–112. <https://doi.org/10.1006/jaer.1998.0318>
- Tariq, A. S., & Purvis, M. R. I. (1996). NO_x emissions and thermal efficiencies of small scale biomass-fuelled combustion plant with reference to process industries in a developing country. *International Journal of Energy Research*, 20(1), 41–55. [https://doi.org/10.1002/\(SICI\)1099-114X\(199601\)20:1<41::AID-ER222>3.3.CO;2-7](https://doi.org/10.1002/(SICI)1099-114X(199601)20:1<41::AID-ER222>3.3.CO;2-7)
- Turmel, M.-S., Speratti, A., Baudron, F., Verhulst, N., & Govaerts, B. (2014). Crop residue management and soil health: A systems analysis. *Agricultural Systems*, 134, 6–16. <https://doi.org/10.1016/j.agsy.2014.05.009>
- US Bureau of Standards. (1931). *Design of gas burners for domestic use* (Circular o). Washington DC: US Government printing office.
- US EPA. (1992). *Prescribed burning background document and technical information document for prescribed burning best available control measures*. Retrieved from <https://nepis.epa.gov/Exe/ZyPDF.cgi/00001X20.PDF?Dockey=00001X20.PDF>
- US EPA. (1996). *AP 42 : Miscellaneous Sources*.
- Valzano, F. P., Greene, R. S. B., & Murphy, B. W. (1997). Direct effects of stubble burning on soil hydraulic and physical properties in a direct drill tillage system. *Soil and Tillage Research*, 42(3), 209–219. [https://doi.org/10.1016/S0167-1987\(96\)01101-4](https://doi.org/10.1016/S0167-1987(96)01101-4)
- Webster, R., Bolstad, J., Wick, C., & Hall, D. (1976). Vertical distribution and survival of sclerotium oryzae.pdf. *Phytopathology*, 66(1), 97–101.

- Weir, J. (2019). *Personal Communication*. Stillwater, OK.
- Weir, J. R. (2009). *Conducting prescribed fires: a comprehensive manual*. College Station, Texas: Texas A & M University Press.
- Weir, J. R., Bidwell, T. G., Stevens, R., & Mustain, J. (2017). Firebreaks for Prescribed Burning. *Oklahoma Cooperative Extension Fact Sheets*, (NREM-2890). Retrieved from <http://pods.dasnr.okstate.edu/docushare/dsweb/Get/Document-8542/NREM-2890web.pdf>
- Werther, J., Saenger, M., Hartge, E.-U., Ogada, T., & Siagi, Z. (2000). 00/02785 Combustion of agricultural residues. *Fuel and Energy Abstracts*, 41(5), 308. [https://doi.org/10.1016/S0140-6701\(00\)96698-0](https://doi.org/10.1016/S0140-6701(00)96698-0)
- Wöltjen, C., Haferkamp, H., Rath, T., & Herzog, D. (2008). Plant growth depression by selective irradiation of the meristem with CO₂ and diode lasers. *Biosystems Engineering*, 101(3), 316–324. <https://doi.org/10.1016/j.biosystemseng.2008.08.006>
- Wuest, S., & Skirvin, K. (1999). Crop Residue and Plant Health: Research Overview and Implications for No-Till. *Columbia Basin Agricultural Research Annual Report. Spec. Rpt.*, 999, 81–84.
- Xie, Y., Alleyne, A. G., Greer, A., & Deneault, D. (2011). Fundamental limits in combine harvester header height control. *Proceedings of the 2011 American Control Conference*, 135(May 2013), 5279–5285. <https://doi.org/10.1115/1.4023209>
- Yang, H. H., Tsai, C. H., Chao, M. R., Su, Y. L., & Chien, S. M. (2006). Source identification and size distribution of atmospheric polycyclic aromatic hydrocarbons during rice straw burning period. *Atmospheric Environment*, 40(7), 1266–1274. <https://doi.org/10.1016/j.atmosenv.2005.10.032>
- Yang, S., He, H., Lu, S., Chen, D., & Zhu, J. (2008). Quantification of crop residue burning in the field and its influence on ambient air quality in Suqian, China. *Atmospheric Environment*, 42(9), 1961–1969. <https://doi.org/10.1016/j.atmosenv.2007.12.007>
- Yoder, J. (2008). Liability, Regulation, and Endogenous Risk: The Incidence and Severity of Escaped Prescribed Fires in the United States. *The Journal of Law and Economics*, 51(2), 297–325. <https://doi.org/10.1086/589661>
- Yu, T. Y., Lin, C. Y., & Chang, L. F. W. (2012). Estimating air pollutant emission factors from open burning of rice straw by the residual mass method. *Atmospheric Environment*, 54, 428–438. <https://doi.org/10.1016/j.atmosenv.2012.02.038>
- Zevenhoven, R., & Kilpinen, P. (2001). Furnace Flue Gas. *Control of Pollutants in Flue Gases and Fuel Gases*, 2.1-2.12. Retrieved from <http://users.abo.fi/rzevenho/gases.PDF>

APPENDICES

Appendix A1. Arduino codes for temperature measurements

```
#include <MAX31856.h>

#include<SD.h>

#include<SPI.h>

#include <RTCLib.h>

#include <Wire.h>

#define SCK 3

#define CS0 4

#define CS1 5

#define CS2 6

#define CS3 7

#define SDI 8

#define SDO 9

#define NUM_MAX31856 4

const int sdpin =10;

File logfile;

String newfile;

RTC_DS1307 rtc;
```

```

int val;

int tempPin = 1;

File logFile;

File dataTemp;

String newFile;

int swOnoff = 2;

int readSw ;

int processRun = LOW;

int state = HIGH;

int prev = LOW;

// MAX31856 Initial settings (see MAX31856.h and the MAX31856 datasheet)

// The default noise filter is 60Hz, suitable for the USA

#define CR0_INIT (CR0_AUTOMATIC_CONVERSION +
CR0_OPEN_CIRCUIT_FAULT_TYPE_K /* + CR0_NOISE_FILTER_50HZ */)

#define CR1_INIT (CR1_AVERAGE_2_SAMPLES +
CR1_THERMOCOUPLE_TYPE_K)

#define MASK_INIT (~(MASK_VOLTAGE_UNDER_OVER_FAULT +
MASK_THERMOCOUPLE_OPEN_FAULT))

// Create the temperature object, defining the pins used for communication
MAX31856 *TemperatureSensor[NUM_MAX31856] = {
    new MAX31856(SDI, SDO, CS0, SCK),
    new MAX31856(SDI, SDO, CS1, SCK),
    new MAX31856(SDI, SDO, CS2, SCK),
    new MAX31856(SDI, SDO, CS3, SCK)
};

void error(char *str)
{
    Serial.print("error: ");

```

```

Serial.println(str);
while(1);
}
void setup() {
  // Display temperatures using the serial port
  Serial.begin(9600);
  Wire.begin();
  rtc.begin();
  pinMode(swOnoff,INPUT);
  pinMode(10, OUTPUT);
  delay(3000);
  Serial.println("Dual MAX31856 Sample application");
  // Initializing the MAX31855's registers
  for (int i=0; i<NUM_MAX31856; i++) {
    TemperatureSensor[i]->writeRegister(REGISTER_CR0, CR0_INIT);
    TemperatureSensor[i]->writeRegister(REGISTER_CR1, CR1_INIT);
    TemperatureSensor[i]->writeRegister(REGISTER_MASK, MASK_INIT);
  }
  Serial.print("Initializing SD card .....");
  if (!SD.begin(sdpin))
  {
    Serial.println (" sd card inzialization failed");
    return;
  }
  Serial.println("sd card inzialization done");
  // Wait for the first samples to be taken
  if(!rtc.isrunning()){

```

```

    Serial.println("RTC failde, or not present");
    rtc.adjust(DateTime(__DATE__, __TIME__));
}
delay(200);
}
void loop () {
    String dtTime = "";
    DateTime now = rtc.now();
    readSw = digitalRead(swOnoff);
    if (readSw == HIGH && prev == LOW)
    {
        Serial.print("SWITCH STATE =");
        Serial.println(readSw);
        // create a new file
        char filename[] = "LOGGER00.CSV";
        for (uint8_t i = 0; i < 500; i++) {
            filename[6] = i/10 + '0';
            filename[7] = i%10 + '0';
            if (! SD.exists(filename)) {
                // only open a new file if it doesn't exist
                logfile = SD.open(filename, FILE_WRITE);
                break;
            }
        }
        if (! logfile) {
            error("couldnt create file");
        }
    }
}

```

```

    Serial.print("Logging to: ");
    Serial.println(filename);
    logfile =SD.open(filename,FILE_WRITE);
    logfile.println("DATE, TIME, Cold Junction 0, Cold Junction 1, Thermocouple 0,
Thermocouple 1");
    logfile.close();
    newfile = filename;
    processRun = HIGH;
    prev =HIGH;
    Serial.print ("PREV INITIAL ");
    Serial.println (prev);
    Serial.print ("PROCESS RUN INITIAL ");
    Serial.println(processRun);
}
else if (readSw == LOW && prev == HIGH)
{
    Serial.println ("STOP LOGGING ");
    prev = LOW;
    processRun=LOW;
    Serial.print ("PREV sw off ");
    Serial.println (prev);
    Serial.print ("PROCESS RUN sw off ");
    Serial.println(processRun);
}
if (readSw == HIGH && processRun ==HIGH)
{
    String Yy = String(now.year(),DEC);

```



```

String Mm= String(now.month(),DEC);
String Dd = String(now.day(),DEC);
String Hh=String(now.hour(),DEC);
String Min=String(now.minute(),DEC);
String Sc=String(now.second(),DEC);
dtTime = String (Yy+"-"+Mm+"-"+Dd+", "+Hh+": "+Min+": "+Sc);
// Display the junction (IC) temperature first
// Sometimes the junction temperature is not provided until a thermocouple is attached
double temperature0 = TemperatureSensor[0]->readJunction(CELSIUS);
Serial.print("J");
Serial.print(0);
Serial.print("=");
printTemperature(temperature0);
// Display the thermocouple temperature
double temperature00 = TemperatureSensor[0]->readThermocouple(CELSIUS);
Serial.print("T");
Serial.print(0);
Serial.print("=");
printTemperature(temperature00);
delay (100);
double temperature1 = TemperatureSensor[1]->readJunction(CELSIUS);
Serial.print("J");
Serial.print(1);
Serial.print("=");
printTemperature(temperature1);
// Display the thermocouple temperature
double temperature11 = TemperatureSensor[1]->readThermocouple(CELSIUS);

```

```

Serial.print("T");
Serial.print(1);
Serial.print("=");
printTemperature(temperature11);
Serial.print("\t");
delay(100);
double temperature2 = TemperatureSensor[2]->readJunction(CELSIUS);
Serial.print("J");
Serial.print(2);
Serial.print("=");
printTemperature(temperature2);
// Display the thermocouple temperature
double temperature22 = TemperatureSensor[2]->readThermocouple(CELSIUS);
Serial.print("T");
Serial.print(2);
Serial.print("=");
printTemperature(temperature22);
double temperature3 = TemperatureSensor[3]->readJunction(CELSIUS);
Serial.print("J");
Serial.print(3);
Serial.print("=");
printTemperature(temperature3);
// Display the thermocouple temperature
double temperature33 = TemperatureSensor[3]->readThermocouple(CELSIUS);
Serial.print("T");
Serial.print(3);
Serial.print("=");

```

```

    printTemperature(temperature33);

    String dataString = String (Yy+"-"+Mm+"-"+Dd+", "+Hh+": "+Min+": "+Sc)+ "+", "+
String (temperature0)+", "+ String (temperature1) + ", " +
        String (temperature2) + ", " + String (temperature3)+ ", " +
        String (temperature00)+", "+ String(temperature11)+ ", " + String
(temperature22) + ", " + String (temperature33);

    File tempsData = SD.open(newfile, FILE_WRITE);

    if (tempsData)
    {
        tempsData.println(dataString);
        tempsData.close();
    }

    Serial.println();
    delay(1000);
}

// Print the temperature, or the type of fault
void printTemperature(double temperature) {
    switch ((int) temperature) {
        case FAULT_OPEN:
            Serial.print("FAULT_OPEN");
            break;
        case FAULT_VOLTAGE:
            Serial.print("FAULT_VOLTAGE");
            break;
        case NO_MAX31856:
            Serial.print("NO_MAX31856");
            break;
    }
}

```

```

    default:
      Serial.print(temperature);
      break;
  }
  Serial.print(" ");
}

```

Appendix A2. Arduino codes for safety fuel and control system

```

#include <MAX31856.h>
#include <RTCLib.h>
#include <SD.h>
#include <Wire.h>
RTC_DS1307 rtc;
unsigned long interval = (unsigned long) 1000*60*1;
unsigned long interval2 = (unsigned long) 1000*60*1;
unsigned long previousMillis=0;
unsigned long previousMillis1=0;
const int ssrSwitch = 8;
const int ssrSwitch1=9;
int ssrState;
int MaxError;
double temperature0;
double temperature00

double temperature1;
double temperature11;

double newtemp0=0;
double newtemp1=0;
#define SCK 3
#define CS0 4
#define CS1 5
#define SDI 6
#define SDO 7
int val;
int pressureSensor1 = A0 ;
int pressureSensor2 =A1;
int adcpresure1;
int adcpresure2;
float voltpresure1;
float voltpresure2;

```

```

float voltToPsi;
const int chipSelect=10;
File myFile;
int readSw ;
int processRun = LOW;
int prev = LOW;
#define NUM_MAX31856 2
#define CR0_INIT (CR0_AUTOMATIC_CONVERSION +
CR0_OPEN_CIRCUIT_FAULT_TYPE_K /* + CR0_NOISE_FILTER_50HZ */)
#define CR1_INIT (CR1_AVERAGE_2_SAMPLES +
CR1_THERMOCOUPLE_TYPE_K)
#define MASK_INIT (~(MASK_VOLTAGE_UNDER_OVER_FAULT +
MASK_THERMOCOUPLE_OPEN_FAULT))
MAX31856 *TemperatureSensor[NUM_MAX31856] = {
  new MAX31856(SDI, SDO, CS0, SCK),
  new MAX31856(SDI, SDO, CS1, SCK),
  //new MAX31856(SDI, SDO, CS2, SCK),
};
void error(char *str)
{
  Serial.print("error: ");
  Serial.println(str);
  while(1);
}
void setup() {
  // Display temperatures using the serial port
  Serial.begin(9600);
  Wire.begin();
  rtc.begin();
  pinMode(ssrSwitch,OUTPUT);
  pinMode(ssrSwitch1,OUTPUT);
  digitalWrite(ssrSwitch,HIGH);
  digitalWrite(ssrSwitch1, HIGH);
  ssrState=digitalRead(ssrSwitch);
  pinMode(10, OUTPUT);
  delay(1000);
  Serial.println("MAX31856 Sample application");
  // Initializing the MAX31855's registers
  for (int i=0; i<NUM_MAX31856; i++) {
    TemperatureSensor[i]->writeRegister(REGISTER_CR0, CR0_INIT);
    TemperatureSensor[i]->writeRegister(REGISTER_CR1, CR1_INIT);
    TemperatureSensor[i]->writeRegister(REGISTER_MASK, MASK_INIT);
  }
  // Wait for the first samples to be taken
  delay(200);
  if (!SD.begin(chipSelect)) {

```

```

    error("Card failed, or not present");
    return;
}
Serial.println("card initialized.");
if(!rtc.begin()){
    Serial.println ("could not find RTC");
    while(1);
}
else {
//    rtc.adjust(DateTime(F(__DATE__), F(__TIME__)));
}
if (! rtc.isrunning() ) {
    Serial.println ("RTC is not Running");
}
delay(200);
}
void loop () {
    adcpresure1 = analogRead(pressureSensor1);
    voltpresure1 = adcpresure1 * (5.0/1023.0);
    delay(50);
    adcpresure2 = analogRead(pressureSensor2);
    voltpresure2 = adcpresure2 * (5.0/1023.0);
    //voltToPsi = (voltpresure1 -0.3823)/0.1359;
    DateTime now = rtc.now();
    unsigned long currentMillis = millis();
    String Yy = String(now.year(),DEC);
    String Mm= String(now.month(),DEC);
    String Dd = String(now.day(),DEC);
    String Hh=String(now.hour(),DEC);
    String Min=String(now.minute(),DEC);
    String Sc=String(now.second(),DEC);
    String dtTime = String (Yy+"-"+Mm+"-"+Dd+", "+Hh+": "+Min+": "+Sc);
    delay(50);
    Serial.print (dtTime);
    Serial.print("\t");
    temperature0 = TemperatureSensor[0]->readJunction(CELSIUS);
    Serial.print("J");
    Serial.print(0);
    Serial.print("=");
    printTemperature(temperature0);
    // Display the thermocouple temperature
    temperature00 = TemperatureSensor[0]->readThermocouple(CELSIUS);
    Serial.print("T");
    Serial.print(0);
    Serial.print("=");
    printTemperature(temperature00);
}

```

```

Serial.print("\t");
delay(100);
temperature1 = TemperatureSensor[1]->readJunction(CELSIUS);
Serial.print("J");
Serial.print(1);
Serial.print("=");
printTemperature(temperature1);
// Display the thermocouple temperature
temperature11 = TemperatureSensor[1]->readThermocouple(CELSIUS);
Serial.print("T");
Serial.print(1);
Serial.print("=");
printTemperature(temperature11);
Serial.print("\t");
delay(100);
Serial.print ( "ADC 1= ");
Serial.print(adcpresure1);
Serial.print("\t");
delay(100);
Serial.print ("ADC 2 = ");
Serial.println(adcpresure2);
Serial.println();
delay(50);
  if (temperature00<100 || temperature11<100){
    unsigned long currentMillis = millis();
    if ((unsigned long)(currentMillis - previousMillis) >= interval) {
      Serial.println(currentMillis - previousMillis);
      digitalWrite (ssrSwitch,LOW);
      digitalWrite (ssrSwitch1,LOW);
      previousMillis =currentMillis ;
    }
  }
//-----
  if (temperature00>100 && temperature00 <=1000 || temperature11>100 &&
temperature11 <=1000 ){
    if (adcpresure1>=200 && adcpresure1<=900){

      unsigned long currentMillis1 = millis();
      if ((unsigned long) (currentMillis - previousMillis1)>= interval2)
      {
        previousMillis1 = currentMillis1;
        Serial.println(previousMillis1);
        newtemp0 = temperature00;
        newtemp1 = temperature11;
        Serial.print ("new temp 0= ");
        Serial.print (newtemp0);

```

```

        Serial.print ("new temp 1= ");
        Serial.println(newtemp1);
    }
    digitalWrite(ssrSwitch,HIGH);
    digitalWrite(ssrSwitch1,HIGH);
}
else {
    digitalWrite(ssrSwitch,LOW);
    digitalWrite(ssrSwitch1,LOW);
}
}
if (temperature00<newtemp0-100 || temperature11<newtemp1-100){
    digitalWrite(ssrSwitch,LOW);
    digitalWrite(ssrSwitch1,LOW);
    for(;;);
}
if (temperature00>1000 || temperature11>1000 || adcpresure1>900)
{
    digitalWrite(ssrSwitch,LOW);
    digitalWrite(ssrSwitch1,LOW);
    for(;;);
}
myFile = SD.open("TEMPLOG.csv", FILE_WRITE);
if (myFile) {
    myFile.print(dtTime);
    myFile.print(",");
    myFile.print(temperature0);
    myFile.print(",");
    myFile.print(temperature00);
    myFile.print(",");
    myFile.print(temperature1);
    myFile.print(",");
    myFile.print(temperature11);
    myFile.print(",");
    myFile.print(adcpresure1);
    myFile.print(",");
    myFile.println(adcpresure2);
    myFile.close();
}
else {
    Serial.println("error opening file csv");
}
delay(1000);
}
// Print the temperature, or the type of fault
void printTemperature(double temperature) {

```



```

switch ((int) temperature) {
case FAULT_OPEN:
    Serial.print("FAULT_OPEN");
    break;
case FAULT_VOLTAGE:
    Serial.print("FAULT_VOLTAGE");
    break;
case NO_MAX31856:
    Serial.print("NO_MAX31856");
    break;
default:
    Serial.print(temperature);
    break;
}
Serial.print(" ");
}

```

Appendix A3. MATLAB® codes for single burner temperature pattern

```

[x,y,z]=textread('20PSI.txt');

xres=100;

yres=100;

xmax=max(x);

ymax=max(y);

xmin=min(x);

ymin=min(y);

xv = linspace(xmin, xmax,xres);

yv = linspace(ymin, ymax,yres);

[xi,yi] = meshgrid(xv,yv);

zi = griddata(x,y,z,xi,yi,'cubic');

pcolor(xi,yi,zi);

shading interp;

colormap;

grid on;

```

```
colorbar;
```

Appendix A4. MATLAB® codes for the prototype machine temperature pattern

```
clc
```

```
clear all
```

```
[num, txt, raw] = xlsread ('testtemp.xlsx','Sheet1','B:E'); %reads the coordinate data
```

```
%defines variables
```

```
m = num(:,4); %temp
```

```
x = num(:,1); %Length
```

```
y = num(:,2); %Width
```

```
z = num(:,3); %Height
```

```
%define size
```

```
w = 5; %hood width
```

```
l = 13; %hood length
```

```
h = 4; %hood height
```

```
%define gridspace
```

```
x1 = linspace(0,l,25);
```

```
y1 = linspace(0,w,25);
```

```
z1 = linspace(0,h,25);
```

```
%define 3D grid
```

```
[xi,yi,zi] = meshgrid(x1,y1,z1);
```

```
%define the interpolant function
```

```
F = scatteredInterpolant(x,y,z,m);
```

```
V = F(xi,yi,zi);
```

```
%vertices are p1 to p8
```

```

%split into ....
%p1 p2 p6 p5 vertex
x =[0 4 9 13];
y = [0 0 0 0];
z = [0 4 4 0];
dt = [100 120 230 200];%temperature of 4 vertices

figure
fill3 (x,y,z, dt)
daspect ([ 1 1 1])
hold on
shading interp
colormap('jet')
colorbar
xlabel('x')
ylabel('y')
zlabel('z')
set(gca, 'YTick', []);
set(gca, 'XTick', []);
set(gca, 'ZTick', []);
%p4 p3 p7 p8 vertex
x1=[0 13 9 4];
y1=[5 5 5 5];
z1=[0 0 4 4];
dt1 =[200 230 100 120];
fill3 (x1,y1,z1, dt1)
%p1 p5 p8 p4 vertex
x2=[0 4 4 0];

```

```

y2=[0 0 5 5];
z2=[0 4 4 0];
dt2 =[100 90 120 200];
fill3 (x2,y2,z2, dt2)
%p2 p3 p7 p6 vertex
x3=[13 13 9 9];
y3=[0 5 5 0];
z3=[0 0 4 4];
dt3 =[120 230 100 120];
fill3 (x3,y3,z3, dt3)
%p5 p6 p7 p8 vertex
x4=[4 9 9 4];
y4=[0 0 5 5];
z4=[4 4 4 4];
dt4=[0 0 0 0];
fill3 (x4,y4,z4, dt4)
alpha (0.4)
% Thermocouple 1 (TA)
xa=5;
ya=0;
za=2;
% Thermocouple 2 (TB)
xb=5;
yb=0;
zb=1.5;
% Thermocouple 3 (TF)
xf=7.5;

```

```

yf=0;
zf=2.5;
% Thermocouple 4 (T2)
xt2=7.5;
yt2=0;
zt2=1.5;
% Thermocouple 5 (TC)
xc=5;
yc=3;
zc=2;
% Thermocouple 6 (TD)
xd=5;
yd=3;
zd=1.5;
% Thermocouple 7 (TE)
xe=7.5;
ye=3;
ze=2;
% Thermocouple 8 (T1)
xt1=7.5;
yt1=3;
zt1=1.5;
    y = 0:2;           % set cylinder length
    theta = linspace(0,2*pi,40);
    [y,theta]=meshgrid(y,theta);
    % calculate x and z
    x = cos(theta);

```

```

z = sin(theta);
% plot the mesh
hsp_a = surface(x/10+xa,y+ya,z/10+za);
hsp_b = surface(x/10+xb,y+yb,z/10+zb);
hsp_f = surface(x/10+xf,y+yf,z/10+zf);
hsp_2 = surface(x/10+xt2,y+yt2,z/10+zt2);
hsp_c = surface (x/10+xc,y+yc,z/10+zc);
hsp_d = surface (x/10+xd,y+yd,z/10+zd);
hsp_e = surface (x/10+xe,y+ye,z/10+ze);
hsp_1 = surface (x/10+xt1,y+yt1,z/10+zt1);
x_a = get(hsp_a,'XData');
y_a = get(hsp_a,'YData');
z_a = get(hsp_a,'ZData');
x_b = get(hsp_b,'XData');
y_b = get(hsp_b,'YData');
z_b = get(hsp_b,'ZData');
x_f = get(hsp_f,'XData');
y_f = get(hsp_f,'YData');
z_f = get(hsp_f,'ZData');
x_2 = get(hsp_2,'XData');
y_2 = get(hsp_2,'YData');
z_2 = get(hsp_2,'ZData');
x_c = get(hsp_c,'XData');
y_c = get(hsp_c,'YData');
z_c = get(hsp_c,'ZData');
x_d = get(hsp_d,'XData');
y_d = get(hsp_d,'YData');

```

```

z_d = get(hsp_d,'ZData');
x_e = get(hsp_e,'XData');
y_e = get(hsp_e,'YData');
z_e = get(hsp_e,'ZData');
x_1 = get(hsp_1,'XData');
y_1 = get(hsp_1,'YData');
z_1 = get(hsp_1,'ZData');

delete(hsp_a)

delete(hsp_b)

delete(hsp_f)

delete(hsp_2)

delete(hsp_c)

delete(hsp_d)

delete(hsp_e)

delete(hsp_1)

hslice_a = slice(xi,yi,zi,V,x_a,y_a,z_a);
set(hslice_a,'FaceColor','interp', 'EdgeColor','interp', ...
    'DiffuseStrength',1)

hslice_b = slice(xi,yi,zi,V,x_b,y_b,z_b);
set(hslice_b,'FaceColor','interp', 'EdgeColor','interp', ...
    'DiffuseStrength',1)

hslice_f = slice(xi,yi,zi,V,x_f,y_f,z_f);
set(hslice_f,'FaceColor','interp', 'EdgeColor','interp', ...
    'DiffuseStrength',1)

hslice_2 = slice(xi,yi,zi,V,x_2,y_2,z_2);
set(hslice_2,'FaceColor','interp', 'EdgeColor','interp', ...

```

```

'DiffuseStrength',1)
%----- other side -----
hslice_c = slice(xi,yi,zi,V,x_c,y_c,z_c);
set(hslice_c,'FaceColor','interp', 'EdgeColor','interp', ...
'DiffuseStrength',1)
hslice_d = slice(xi,yi,zi,V,x_d,y_d,z_d);
set(hslice_d,'FaceColor','interp', 'EdgeColor','interp', ...
'DiffuseStrength',1)
hslice_e = slice(xi,yi,zi,V,x_e,y_e,z_e);
set(hslice_e,'FaceColor','interp', 'EdgeColor','interp', ...
'DiffuseStrength',1)

hslice_1 = slice(xi,yi,zi,V,x_1,y_1,z_1);
set(hslice_1,'FaceColor','interp', 'EdgeColor','interp', ...
'DiffuseStrength',1)

```

Appendix A5. MATLAB® codes for image processing

```

clc
clear all
a='4ALOW3_crop.JPG';
info = imfinfo(a);
aaa = imread(a);
aa = rgb2gray(aaa);
level = 0.2; %before burn level = 0.1
bw1 = im2bw (aa,level);
bw2 = bwareaopen(bw1,100);
figure(1), imshow (a);

```



```

figure(2), imshow (bw1);
figure(3), imshow (bw2);
imwrite (bw2,['a','.jpg']);

% count white pixels
totalsum = sum(bw2(:) == 1);
labeledImage = bwlabel(bw2);
measurements = regionprops(labeledImage, 'Area');
allAreas = [measurements.Area]; % List of all the blob areas.
totalAreaOfAllBlobs = sum(allAreas); % Will be the same as pixelSum2
disp ('total sum');
disp (totalsum);
disp('total area all labels');
disp (totalAreaOfAllBlobs);
%-----uniformity for black pixels-----
%blacksum = sum(bw2(:) ==0);
%numBlackBinary = numel(bw2) - sum(bw2(:));
%disp ('total black');
%disp (blacksum);
%disp (numBlackBinary)

```

Appendix A6. Microsoft Visual Studio® codes for the machine cost estimation

Public Class Form1

Dim listprice As Single

Dim price As Long

Dim discFactor As Single

Public economiclife As Integer

Public RemainingValueFactor As Integer

Dim salvageValue As Single
Dim salvageValueFactor As Single
Dim AnnualDepreciation As Single
Dim TotalDepreciation As Single
Dim CapitalRecovery1 As Single
Dim OwnershipCostPercentages As Single
Dim AnnualOwnership1 As Single
Dim AnnualOwnership2 As Single
Dim THI As Single
Dim InterestRate As Single
Dim Q As Single
Dim loan As Single
Dim inflation As Single
Dim MachineWidth As Single
Dim MachineSpeed As Single
Dim FieldEfficiency As Single
Dim AgeOfMachine As Single
Dim RepairFactor1 As Single
Dim RepairFactor2 As Single
Dim PurchasedPriceVC As Single
Dim inflationVC As Single
Dim TractorRentCost As Single
Dim TractorRatedPower As Single
Dim TotalArea As Single
Dim Fuel1Consumption As Single
Dim Fuel2Consumption As Single
Dim Fuel1Price As Single

```

Dim Fuel2Price As Single
Dim LaborCost As Single
Dim MechanicalSitePrep As Single
Dim EffectiveCapacity As Single
Dim AnnualUse As Single
Dim AdjustedPriceForInflation As Single
Dim TotalTractorRent As Single
Dim AccumulatedRepairAndMaintenanceCost
Dim Fuel1Cost As Single
Dim Fuel2Cost As Single
Dim TotalFuelCost As Single
Dim TotalLaborCost As Single
Dim TotalMechanicalSitePrep As Single
Dim AnnualVariableCost As Single
Dim totalcost1 As Single
Dim totalcost2 As Single
Private Sub txtdiscfactor_KeyDown(sender As Object, e As KeyEventArgs)
    If e.KeyCode = Keys.Enter Then
        If txtdiscfactor.Text <> "" Then
            e.SuppressKeyPress = True
        End If
    End If
End Sub
Private Sub txtprice_KeyDown(sender As Object, e As KeyEventArgs)
End Sub
Private Sub Form1_Load(sender As Object, e As EventArgs) Handles MyBase.Load

```

```

lblFuel.Text = ""
For i As Integer = 1 To 20
    ComboBox1.Items.Add(i)
Next
txtlistprice.Focus()
cmbTractorRent.Items.Add("<100 HP")
cmbTractorRent.Items.Add("100-150 HP")
cmbFuel1Consumption.Items.Add("Gasoline")
cmbFuel1Consumption.Items.Add("Diesel")
End Sub

Private Sub btnloadtable_Click(sender As Object, e As EventArgs)
    FRMDATA.Show()
End Sub

Private Sub txteconomiclife_KeyDown(sender As Object, e As KeyEventArgs)
    If e.KeyCode = Keys.Enter Then
        e.SuppressKeyPress = True
        salvageValue = listprice * RemainingValueFactor
    End If
End Sub

Private Sub txtprice_KeyDown1(sender As Object, e As KeyEventArgs) Handles
txtprice.KeyDown
    If e.KeyCode = Keys.Enter Then
        If txtprice.Text <> "" Then
            e.SuppressKeyPress = True
            txtdiscfactor.Text = "0.9"
            txtdiscfactor.Focus()
        End If
    End If
End Sub

```

```

End If

End Sub

Private Sub txtdiscfactor_KeyDown1(sender As Object, e As KeyEventArgs) Handles
txtdiscfactor.KeyDown
    If e.KeyCode = Keys.Enter Then
        If txtdiscfactor.Text <> "" Then
            e.SuppressKeyPress = True
            ComboBox1.Focus()
        End If
    End If
End Sub

Private Sub ComboBox1_KeyDown(sender As Object, e As KeyEventArgs) Handles
ComboBox1.KeyDown
    If e.KeyCode = Keys.Enter Then
        If ComboBox1.Text <> "[Choose Year]" Then
            e.SuppressKeyPress = True
            txtRV.Focus()
            Select Case ComboBox1.Text
                Case 1
                    txtRV.Text = 69
                Case 2
                    txtRV.Text = 62
                Case 3
                    txtRV.Text = 56
                Case 4
                    txtRV.Text = 52
                Case 5

```

txtRV.Text = 48

Case 6

txtRV.Text = 45

Case 7

txtRV.Text = 42

Case 8

txtRV.Text = 40

Case 9

txtRV.Text = 37

Case 10

txtRV.Text = 35

Case 11

txtRV.Text = 33

Case 12

txtRV.Text = 31

Case 13

txtRV.Text = 29

Case 14

txtRV.Text = 28

Case 15

txtRV.Text = 26

Case 16

txtRV.Text = 25

Case 17

txtRV.Text = 24

Case 18

txtRV.Text = 22

Case 19

txtRV.Text = 21

Case 20

txtRV.Text = 20

End Select

End If

End If

End Sub

Private Sub ComboBox1_LostFocus(sender As Object, e As EventArgs) Handles
ComboBox1.LostFocus

End Sub

Private Sub ComboBox1_SelectedIndexChanged(sender As Object, e As EventArgs)
Handles ComboBox1.SelectedIndexChanged

Select Case ComboBox1.Text

Case 1

txtRV.Text = 69

Case 2

txtRV.Text = 62

Case 3

txtRV.Text = 56

Case 4

txtRV.Text = 52

Case 5

txtRV.Text = 48

Case 6

txtRV.Text = 45

Case 7

txtRV.Text = 42

Case 8

txtRV.Text = 40

Case 9

txtRV.Text = 37

Case 10

txtRV.Text = 35

Case 11

txtRV.Text = 33

Case 12

txtRV.Text = 31

Case 13

txtRV.Text = 29

Case 14

txtRV.Text = 28

Case 15

txtRV.Text = 26

Case 16

txtRV.Text = 25

Case 17

txtRV.Text = 24

Case 18

txtRV.Text = 22

Case 19

txtRV.Text = 21

Case 20

txtRV.Text = 20


```

    End Select

End Sub

Private Sub TabPage1_GotFocus(sender As Object, e As EventArgs) Handles
TABPAGE1.GotFocus

    txtprice.Focus()

End Sub

Private Sub txtRV_KeyDown(sender As Object, e As KeyEventArgs) Handles
txtRV.KeyDown

    If e.KeyCode = Keys.Enter Then

        If txtRV.Text <> "" Then

            e.SuppressKeyPress = True

            TXTINFLATION.Focus()

        End If

    End If

End Sub

Private Sub TXTINFLATION_KeyDown(sender As Object, e As KeyEventArgs)
Handles TXTINFLATION.KeyDown

    If e.KeyCode = Keys.Enter Then

        If TXTINFLATION.Text <> "" Then

            e.SuppressKeyPress = True

            TXT_LOAN.Focus()

        End If

    End If

End Sub

Private Sub TXTINFLATION_TextChanged(sender As Object, e As EventArgs)
Handles TXTINFLATION.TextChanged

End Sub

Private Sub TXT_LOAN_KeyDown(sender As Object, e As KeyEventArgs) Handles
TXT_LOAN.KeyDown

```

```

If e.KeyCode = Keys.Enter Then
    If TXT_LOAN.Text <> "" Then
        e.SuppressKeyPress = True
        TXTINTERESTRATE.Focus()
    End If

End If

End Sub

Private Sub TXTINTERESTRATE_KeyDown(sender As Object, e As KeyEventArgs)
Handles TXTINTERESTRATE.KeyDown
    If e.KeyCode = Keys.Enter Then
        If TXTINTERESTRATE.Text <> "" Then
            e.SuppressKeyPress = True
            TXTQ.Text = "1"
            TXTQ.Focus()
        End If
    End If

End Sub

Private Sub TXTINTERESTRATE_TextChanged(sender As Object, e As EventArgs)
Handles TXTINTERESTRATE.TextChanged

End Sub

Private Sub BTNCALCULATE_Click(sender As Object, e As EventArgs) Handles
BTNCALCULATE.Click

    Dim IRperQ As Single

    Dim loanQ As Single

    Dim OnePlusIRpreQLoanQ As Single

    Dim SvTimesIR As Single

    Dim OneMinusSVFperEconomicLife As Single

```

```

Dim OnePlusSVDFperTwoTimesIR As Single
discFactor = txtdiscfactor.Text
txtlistprice.Text = listprice
discFactor = txtdiscfactor.Text
txtSVF.Text = RemainingValueFactor
price = txtprice.Text
inflation = TXTINFLATION.Text
loan = TXT_LOAN.Text
InterestRate = TXTINTERESTRATE.Text
If ComboBox1.Text <> "[Choose Year]" Then
    economiclife = ComboBox1.Text
End If
listprice = price / discFactor
txtlistprice.Text = Format(listprice, "0.000")
THI = 0.02 * price
txtTHI.Text = Format(THI, "0.000")
salvageValue = (Val(txtRV.Text) / 100) * listprice
txtSV.Text = Format(salvageValue, "0.000")
salvageValueFactor = salvageValue / price
txtSVF.Text = Format(salvageValueFactor, "0.000")
AnnualDepreciation = (price - salvageValue) / economiclife
txtAnnualDep.Text = Format(AnnualDepreciation, "0.000")
TotalDepreciation = price - salvageValue
txtTotDep.Text = Format(TotalDepreciation, "0.000")
IRperQ = (InterestRate / 100) / Q
loanQ = loan * Q
OnePlusIRpreQLoanQ = (1 + IRperQ) ^ loanQ

```

```

SvTimesIR = (salvageValue * (InterestRate / 100)) / Q

CapitalRecovery1 = ((price - salvageValue) * ((IRperQ * OnePlusIRpreQLoanQ) /
(OnePlusIRpreQLoanQ - 1))) + (SvTimesIR)

txtCapitalRec.Text = Format(CapitalRecovery1, "0.000")

OneMinusSVFperEconomicLife = (1 - salvageValueFactor) / economiclife

OnePlusSVDFperTwoTimesIR = ((1 + salvageValueFactor) / 2) * (InterestRate /
100)

OwnershipCostPercentages = 100 * (OneMinusSVFperEconomicLife +
OnePlusSVDFperTwoTimesIR + 0.02)

txtOCP.Text = Format(OwnershipCostPercentages, "0.000")

AnnualOwnership1 = THI + CapitalRecovery1

txtAnnualOwn1.Text = Format(AnnualOwnership1, "0.000")

AnnualOwnership2 = OwnershipCostPercentages * 0.01 * price

txtAnnualOwn2.Text = Format(AnnualOwnership2, "0.000")

End Sub

Private Sub TXTQ_KeyDown(sender As Object, e As KeyEventArgs) Handles
TXTQ.KeyDown

    If e.KeyCode = Keys.Enter Then

        If TXTQ.Text <> "" Then

            e.SuppressKeyPress = True

            BTNCALCULATE.Focus()

            Q = TXTQ.Text

        End If

    End If

End Sub

Private Sub TXTQ_TextChanged(sender As Object, e As EventArgs) Handles
TXTQ.TextChanged

End Sub

```

Private Sub BTNCLEAR_Click(sender As Object, e As EventArgs) Handles
BTNCLEAR.Click

```
txtprice.Text = ""  
txtdisfactor.Text = ""  
ComboBox1.Text = "[Choose Year]"  
txtRV.Text = ""  
TXTINFLATION.Text = ""  
TXT_LOAN.Text = ""  
TXTINTERESTRATE.Text = ""  
TXTQ.Text = ""  
txtTHI.Text = ""  
txtlistprice.Text = ""  
txtSV.Text = ""  
txtSVF.Text = ""  
txtAnnualDep.Text = ""  
txtTotDep.Text = ""  
txtCapitalRec.Text = ""  
txtOCP.Text = ""  
txtAnnualOwn1.Text = ""  
txtAnnualOwn2.Text = ""  
txtprice.Focus()
```

End Sub

Private Sub ComboBox2_SelectedIndexChanged(sender As Object, e As EventArgs)

End Sub

Private Sub TabPage2_Click(sender As Object, e As EventArgs) Handles
TabPage2.Click

```
txtPurchasePrice.Text = price  
txtInflationVC.Text = inflation
```

```

End Sub

Private Sub txtMachineWidht_KeyDown(sender As Object, e As KeyEventArgs)
Handles txtMachineWidht.KeyDown

    If e.KeyCode = Keys.Enter Then

        If txtMachineWidht.Text <> "" Then

            e.SuppressKeyPress = True

            txtMachineSpeed.Focus()

        End If

    End If

End Sub

Private Sub txtMachineWidht_TextChanged(sender As Object, e As EventArgs)
Handles txtMachineWidht.TextChanged

End Sub

Private Sub txtMachineSpeed_KeyDown(sender As Object, e As KeyEventArgs)
Handles txtMachineSpeed.KeyDown

    If e.KeyCode = Keys.Enter Then

        If txtMachineSpeed.Text <> "" Then

            e.SuppressKeyPress = True

            txtFieldEfficiency.Focus()

        End If

    End If

End Sub

Private Sub txtFieldEfficiency_KeyDown(sender As Object, e As KeyEventArgs)
Handles txtFieldEfficiency.KeyDown

    If e.KeyCode = Keys.Enter Then

        If txtFieldEfficiency.Text <> "" Then

            e.SuppressKeyPress = True

            txtAgeOfMachine.Focus()

        End If

    End If

```

```

    End If
End Sub

Private Sub txtAgeOfMachine_KeyDown(sender As Object, e As KeyEventArgs)
Handles txtAgeOfMachine.KeyDown
    If e.KeyCode = Keys.Enter Then
        If txtAgeOfMachine.Text <> "" Then
            e.SuppressKeyPress = True
            txtrepairFactor1.Focus()
        End If
    End If
End Sub

Private Sub txtrepairFactor1_KeyDown(sender As Object, e As KeyEventArgs)
Handles txtrepairFactor1.KeyDown
    If e.KeyCode = Keys.Enter Then
        If txtrepairFactor1.Text <> "" Then
            e.SuppressKeyPress = True
            txtRepairFactor2.Focus()
        End If
    End If
End Sub

Private Sub txtrepairFactor1_TextChanged(sender As Object, e As EventArgs)
Handles txtrepairFactor1.TextChanged
End Sub

Private Sub txtRepairFactor2_KeyDown(sender As Object, e As KeyEventArgs)
Handles txtRepairFactor2.KeyDown
    If e.KeyCode = Keys.Enter Then
        If txtRepairFactor2.Text <> "" Then
            e.SuppressKeyPress = True
            cmbTractorRent.Focus()

```

```

        End If
    End If
End Sub

Private Sub cmbTractorRent_KeyDown(sender As Object, e As KeyEventArgs)
Handles cmbTractorRent.KeyDown
    If e.KeyCode = Keys.Enter Then
        If cmbTractorRent.Text <> "[Choose]" Then
            e.SuppressKeyPress = True
            txtTractorRent.Focus()
        End If
    End If
End Sub

Private Sub txtTractorRent_KeyDown(sender As Object, e As KeyEventArgs)
Handles txtTractorRent.KeyDown
    If e.KeyCode = Keys.Enter Then
        If txtTractorRent.Text <> "" Then
            e.SuppressKeyPress = True
            txtRatedPower.Focus()
        End If
    End If
End Sub

Private Sub txtTractorRent_TextChanged(sender As Object, e As EventArgs)
Handles txtTractorRent.TextChanged
End Sub

Private Sub txtRatedPower_KeyDown(sender As Object, e As KeyEventArgs)
Handles txtRatedPower.KeyDown
    If e.KeyCode = Keys.Enter Then
        If txtRatedPower.Text <> "" Then
            e.SuppressKeyPress = True

```



```

        txtTotalArea.Focus()
    End If
End If
End Sub

Private Sub txtRatedPower_TextChanged(sender As Object, e As EventArgs) Handles
txtRatedPower.TextChanged
    End Sub

Private Sub txtTotalArea_KeyDown(sender As Object, e As KeyEventArgs) Handles
txtTotalArea.KeyDown
    If e.KeyCode = Keys.Enter Then
        If txtTotalArea.Text <> "" Then
            e.SuppressKeyPress = True
            txtPurchasePrice.Focus()
            txtPurchasePrice.Text = price
        End If
    End If
End Sub

Private Sub txtPurchasePrice_KeyDown(sender As Object, e As KeyEventArgs)
Handles txtPurchasePrice.KeyDown
    If e.KeyCode = Keys.Enter Then
        If txtPurchasePrice.Text <> "" Then
            e.SuppressKeyPress = True
            txtInflationVC.Focus()
            txtInflationVC.Text = inflation
        End If
    End If
End Sub

Private Sub txtInflationVC_KeyDown(sender As Object, e As KeyEventArgs) Handles
txtInflationVC.KeyDown

```

```

If e.KeyCode = Keys.Enter Then
    If txtInflationVC.Text <> "" Then
        e.SuppressKeyPress = True
        cmbFuel1Consumption.Focus()
    End If
End If

End Sub

Private Sub cmbFuel1Consumption_KeyDown(sender As Object, e As KeyEventArgs)
Handles cmbFuel1Consumption.KeyDown
    If e.KeyCode = Keys.Enter Then
        If cmbFuel1Consumption.Text <> "[Choose]" Then
            e.SuppressKeyPress = True
            txtFuel1Consumption.Focus()
        End If
    End If
End Sub

Private Sub cmbFuel1Consumption_SelectedIndexChanged(sender As Object, e As
EventArgs) Handles cmbFuel1Consumption.SelectedIndexChanged
    If cmbFuel1Consumption.Text = "Gasoline" Then
        txtFuel1Price.Text = 2.5
        txtFuel1Consumption.Text = 0.06 * Val(txtRatedPower.Text)
    ElseIf cmbFuel1Consumption.Text = "Diesel" Then
        txtFuel1Price.Text = 2.8
        txtFuel1Consumption.Text = 0.044 * Val(txtRatedPower.Text)
    End If
End Sub

Private Sub txtFuel1Price_KeyDown(sender As Object, e As KeyEventArgs) Handles
txtFuel1Price.KeyDown

```

```

If e.KeyCode = Keys.Enter Then
    If txtFuel1Price.Text <> "" Then
        e.SuppressKeyPress = True
        txtFuel2Consumption.Focus()
    End If
End If

End Sub

Private Sub txtFuel2Price_KeyDown(sender As Object, e As KeyEventArgs) Handles
txtFuel2Price.KeyDown
    If e.KeyCode = Keys.Enter Then
        If txtFuel2Price.Text <> "" Then
            e.SuppressKeyPress = True
            txtLaborCost.Focus()
        End If
    End If
End Sub

Private Sub txtLaborCost_KeyDown(sender As Object, e As KeyEventArgs) Handles
txtLaborCost.KeyDown
    If e.KeyCode = Keys.Enter Then
        If txtLaborCost.Text <> "" Then
            e.SuppressKeyPress = True
            txtMechanicalSite.Focus()
        End If
    End If
End Sub

Private Sub txtMechanicalSite_KeyDown(sender As Object, e As KeyEventArgs)
Handles txtMechanicalSite.KeyDown
    If e.KeyCode = Keys.Enter Then

```

```

    If txtMechanicalSite.Text <> "" Then
        e.SuppressKeyPress = True
        btnCalculateVC.Focus()
    End If
End If
End Sub

Private Sub txtMechanicalSite_TextChanged(sender As Object, e As EventArgs)
Handles txtMechanicalSite.TextChanged
End Sub

Private Sub btnCalculateVC_Click(sender As Object, e As EventArgs) Handles
btnCalculateVC.Click
    MachineWidth = txtMachineWidht.Text
    MachineSpeed = txtMachineSpeed.Text
    FieldEfficiency = txtFieldEfficiency.Text
    AgeOfMachine = txtAgeOfMachine.Text
    RepairFactor1 = txtrepairFactor1.Text
    RepairFactor2 = txtRepairFactor2.Text
    TractorRentCost = txtTractorRent.Text
    TractorRatedPower = txtRatedPower.Text
    TotalArea = txtTotalArea.Text
    PurchasedPriceVC = txtPurchasePrice.Text
    inflationVC = txtInflationVC.Text
    Fuel1Consumption = txtFuel1Consumption.Text
    Fuel1Price = txtFuel1Price.Text
    Fuel2Consumption = txtFuel2Consumption.Text
    Fuel2Price = txtFuel2Price.Text
    LaborCost = txtLaborCost.Text
    MechanicalSitePrep = txtMechanicalSite.Text

```

```

EffectiveCapacity = MachineSpeed * MachineWidth * (FieldEfficiency / 100) / 8.25
txtEffectiveCapacity.Text = Format(EffectiveCapacity, "0.000")

AnnualUse = TotalArea / EffectiveCapacity
txtAnnualUse.Text = Format(AnnualUse, "0.000")

AdjustedPriceForInflation = PurchasedPriceVC * (1 + (inflationVC / 100)) ^
AgeOfMachine
txtAdjustedPriceForInflation.Text = Format(AdjustedPriceForInflation, "0.000")

TotalTractorRent = TractorRentCost * TractorRatedPower
txtTotalTractorRent.Text = Format(TotalTractorRent, "0.000")

'AccumulatedRepairAndMaintenanceCost = RepairFactor1 * () *
(AdjustedPriceForInflation / 1000) ^ RepairFactor2

AccumulatedRepairAndMaintenanceCost = RepairFactor1 *
AdjustedPriceForInflation * ((AnnualUse / 1000) ^ RepairFactor2)

txtAccumulatedRepair.Text = Format(AccumulatedRepairAndMaintenanceCost,
"0.000")

If cmbFuel1Consumption.Text = "Gasoline" Then
    Fuel1Cost = Fuel1Consumption * Fuel1Price * AnnualUse
    txtFuel1Cost.Text = Format(Fuel1Cost, "0.000")
ElseIf cmbFuel1Consumption.Text = "Diesel" Then
    Fuel1Cost = Fuel1Consumption * Fuel1Price * AnnualUse
    txtFuel1Cost.Text = Format(Fuel1Cost, "0.000")
End If

Fuel1Cost
Fuel2Cost = Fuel2Consumption * AnnualUse
txtFuel2Cost.Text = Format(Fuel2Cost, "0.000")

TotalFuelCost = Fuel1Cost + Fuel2Cost
txtTotalFuelCost.Text = Format(TotalFuelCost, "0.000")

TotalLaborCost = LaborCost * AnnualUse
txtTotalLaborCost.Text = Format(TotalLaborCost, "0.000")

```

```

TotalMechanicalSitePrep = MechanicalSitePrep * TotalArea
txtTotalMechanicalSitePrep.Text = Format(TotalMechanicalSitePrep, "0.000")

AnnualVariableCost = TotalTractorRent +
AccumulatedRepairAndMaintenanceCost + TotalFuelCost + TotalLaborCost +
TotalMechanicalSitePrep

txtAnnualVariableCost.Text = Format(AnnualVariableCost, "0.000")

totalcost1 = AnnualVariableCost + AnnualOwnership1
txttotalcost1.Text = Format(totalcost1, "0.000")

totalcost2 = AnnualVariableCost + AnnualOwnership2
txttotalcost2.Text = Format(totalcost2, "0.000")

lblFuel.Text = cmbFuel1Consumption.Text

End Sub

Private Sub txtFuel2Consumption_KeyDown(sender As Object, e As KeyEventArgs)
Handles txtFuel2Consumption.KeyDown

If e.KeyCode = Keys.Enter Then

If txtFuel2Consumption.Text <> "" Then

e.SuppressKeyPress = True

txtFuel2Price.Focus()

End If

End If

End Sub

Private Sub txtFuel2Consumption_TextChanged(sender As Object, e As EventArgs)
Handles txtFuel2Consumption.TextChanged

End Sub

Private Sub txtdiscfactor_TextChanged(sender As Object, e As EventArgs) Handles
txtdiscfactor.TextChanged

End Sub

Private Sub cmbTractorRent_SelectedIndexChanged(sender As Object, e As
EventArgs) Handles cmbTractorRent.SelectedIndexChanged

```

```

If cmbTractorRent.Text = "<100 HP" Then
    txtTractorRent.Text = 31.71
ElseIf cmbTractorRent.Text = "100-150 HP" Then
    txtTractorRent.Text = 32.16
End If
End Sub

Private Sub txtFuel1Price_TextChanged(sender As Object, e As EventArgs) Handles
txtFuel1Price.TextChanged
End Sub

Private Sub txtFuel1Consumption_KeyDown(sender As Object, e As KeyEventArgs)
Handles txtFuel1Consumption.KeyDown
    If e.KeyCode = Keys.Enter Then
        If txtFuel1Consumption.Text <> "" Then
            e.SuppressKeyPress = True
            txtFuel1Price.Focus()
        End If
    End If
End Sub

Private Sub txtFuel1Consumption_TextChanged(sender As Object, e As EventArgs)
Handles txtFuel1Consumption.TextChanged
End Sub

Private Sub btnClearVC_Click(sender As Object, e As EventArgs) Handles
btnClearVC.Click
    txtMachineWidht.Text = ""
    txtMachineSpeed.Text = ""
    txtFieldEfficiency.Text = ""
    txtAgeOfMachine.Text = ""
    txtrepairFactor1.Text = ""
    txtRepairFactor2.Text = ""

```

```
cmbTractorRent.Text = "[Choose]"
txtTractorRent.Text = ""
txtRatedPower.Text = ""
txtTotalArea.Text = ""
txtPurchasePrice.Text = ""
txtInflationVC.Text = ""
cmbFuel1Consumption.Text = "[Choose]"
txtFuel1Consumption.Text = ""
txtFuel2Consumption.Text = ""
txtFuel1Price.Text = ""
txtFuel2Price.Text = ""
txtLaborCost.Text = ""
txtMechanicalSite.Text = ""
txtEffectiveCapacity.Text = ""
txtAnnualUse.Text = ""
txtAdjustedPriceForInflation.Text = ""
txtTotalTractorRent.Text = ""
txtAccumulatedRepair.Text = ""
txtFuel1Cost.Text = ""
txtFuel2Cost.Text = ""
txtTotalFuelCost.Text = ""
txtTotalLaborCost.Text = ""
txtTotalMechanicalSitePrep.Text = ""
txtAnnualVariableCost.Text = ""
txtMachineWidht.Focus()
lblFuel.Text = ""
```

End Sub

Private Sub txtTotalArea_TextChanged(sender As Object, e As EventArgs) Handles txtTotalArea.TextChanged

End Sub

Private Sub TxtRV_TextChanged(sender As Object, e As EventArgs) Handles txtRV.TextChanged

End Sub

Private Sub Txtprice_TextChanged(sender As Object, e As EventArgs) Handles txtprice.TextChanged

End Sub

End Class

Appendix B1. Travel speed calibration

Reps	Distance (ft)	Time (s)	velocity (ft/s)	velocity (mph)
1	31	11.15	2.780	1.895
2	31	11.11	2.790	1.902
3	31	11.13	2.785	1.899
Average				1.899
SD				0.003
1	31	9.58	3.236	2.206
2	31	9.76	3.176	2.165
3	31	9.46	3.277	2.234
Average				2.202
SD				0.035

Appendix B2. Adjustable speed motor specification

Dayton adjustable speed motor specification	
#MFR	2Z846
Name Plate RPM	2500
HP	3/4
Shaft diameter	5/8"
Shaft length	1-7/8"
Motor bearing	Ball
Input voltage	115AC
Motor type	Permanent magnet DC
Max. Torque	18.9 in.-lb
Motor application	Variable speed

For a complete description of the motor specifications can be found [here](#).

Appendix B3. Blower motor specification

Baldor Reliance blower motor specification	
CAT. NO	CEM3610T
Spec.	35L113Q060G1
HP	3
Volts (V)	230/460
Amps	7.2/3.6
RPM	3450
Frequency (Hz)	60

For a complete description of the blower can be found [here](#).

Appendix B4. Variable frequency drive specification

Dayton variable frequency drive specification	
#MFR	13E658
Max.HP	5
Input Voltage	480 VAC
Max. output Amps	8.3
Input phase AC	3
Output phase AC	3
Input Frequency	50/60 Hz
Output frequency range	0 to 240 Hz

For a complete description of the blower can be found [here](#).

Appendix B5. Air compressor performance

Compressor performance	
Max. tank pressure	200 PSI
Air flowrate	5.4 SCFM @90 PSI
Motor	1.8 HP
Tank capacity	15 Gal

Appendix C1. LPG pressure readings during the determination of the best burner angle study

Treatments	Reps	ADC readings	P (PSI)	LPG tank pressure (PSI)
22.5	R1	635.74	20.03	23
	R2	636.34	20.05	23
	R3	635.00	20.01	23
30	R1	635.78	20.03	23

Treatments	Reps	ADC readings	P (PSI)	LPG tank pressure (PSI)
	R2	634.97	20.00	23
	R3	635.07	20.01	23
45	R1	636.25	20.05	23
	R2	635.00	20.01	23
	R3	635.12	20.01	23
67	R1	635.19	20.01	23
	R2	635.70	20.03	23
	R3	635.24	20.01	23

Appendix C2. LPG pressure readings during the determination of the best crop loading rate study

Treatments	Reps	ADC readings	P (PSI)	LPG tank pressure (PSI)
	R1	635.02	20.01	23
3 LOW	R2	635.00	20.01	23
	R3	634.87	20.00	23
4 LOW	R1	635.19	20.01	23
	R2	635.21	20.01	23
	R3	636.07	20.04	23
3 HIGH	R1	634.78	20.00	23
	R2	635.00	20.01	23
	R3	635.00	20.01	23
4 HIGH	R1	636.02	20.04	23
	R2	635.27	20.01	23
	R3	635.27	20.01	23

Appendix C3. Air flowrate during the determinations of the best burner angle study

Treatments	Reps	Air flowrate (CFH)	Air pressure (PSI)
	R1	260.00	22.00
22.5	R2	250.00	20.00
	R3	260.00	23.00
30	R1	260.00	23.00
	R2	260.00	22.00
	R3	260.00	22.00

Treatments	Reps	Air flowrate (CFH)	Air pressure (PSI)
45	R1	250.00	22.00
	R2	260.00	23.00
	R3	260.00	20.00
67	R1	260.00	23.00
	R2	260.00	23.00
	R3	260.00	22.00

Appendix C4. Air flow rate during the determinations of the best crop loading rate study.

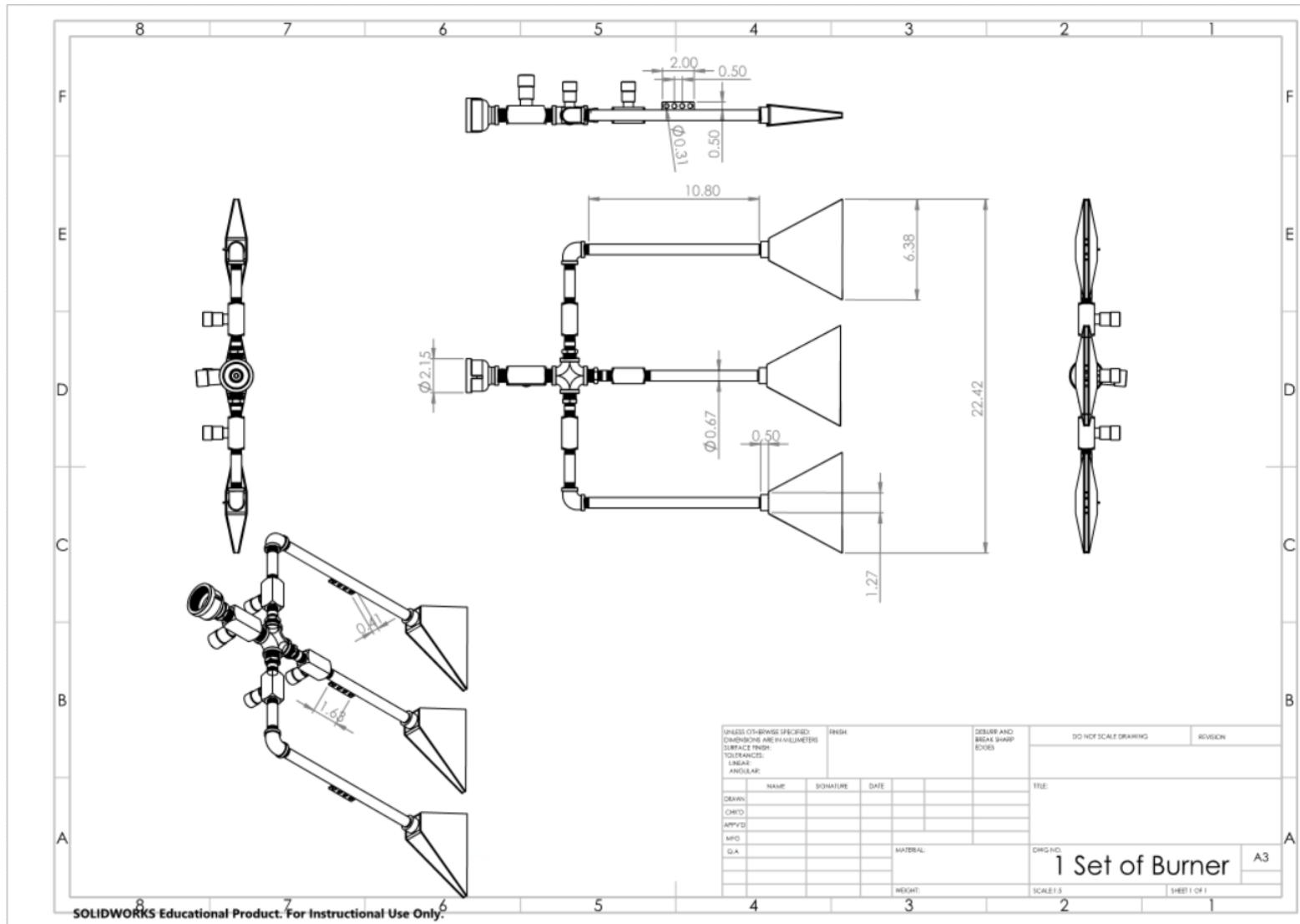
Treatments	Reps	Air flowrate (CFH)	Air Pressure (PSI)
3 LOW	R1	260.00	23.00
	R2	260.00	22.00
	R3	260.00	23.00
4 LOW	R1	250.00	23.00
	R2	260.00	23.00
	R3	260.00	23.00
3 HIGH	R1	250.00	22.00
	R2	260.00	23.00
	R3	260.00	23.00
4 HIGH	R1	260.00	23.00
	R2	260.00	23.00
	R3	250.00	23.00

Appendix C5. Stack flowrate and velocity data

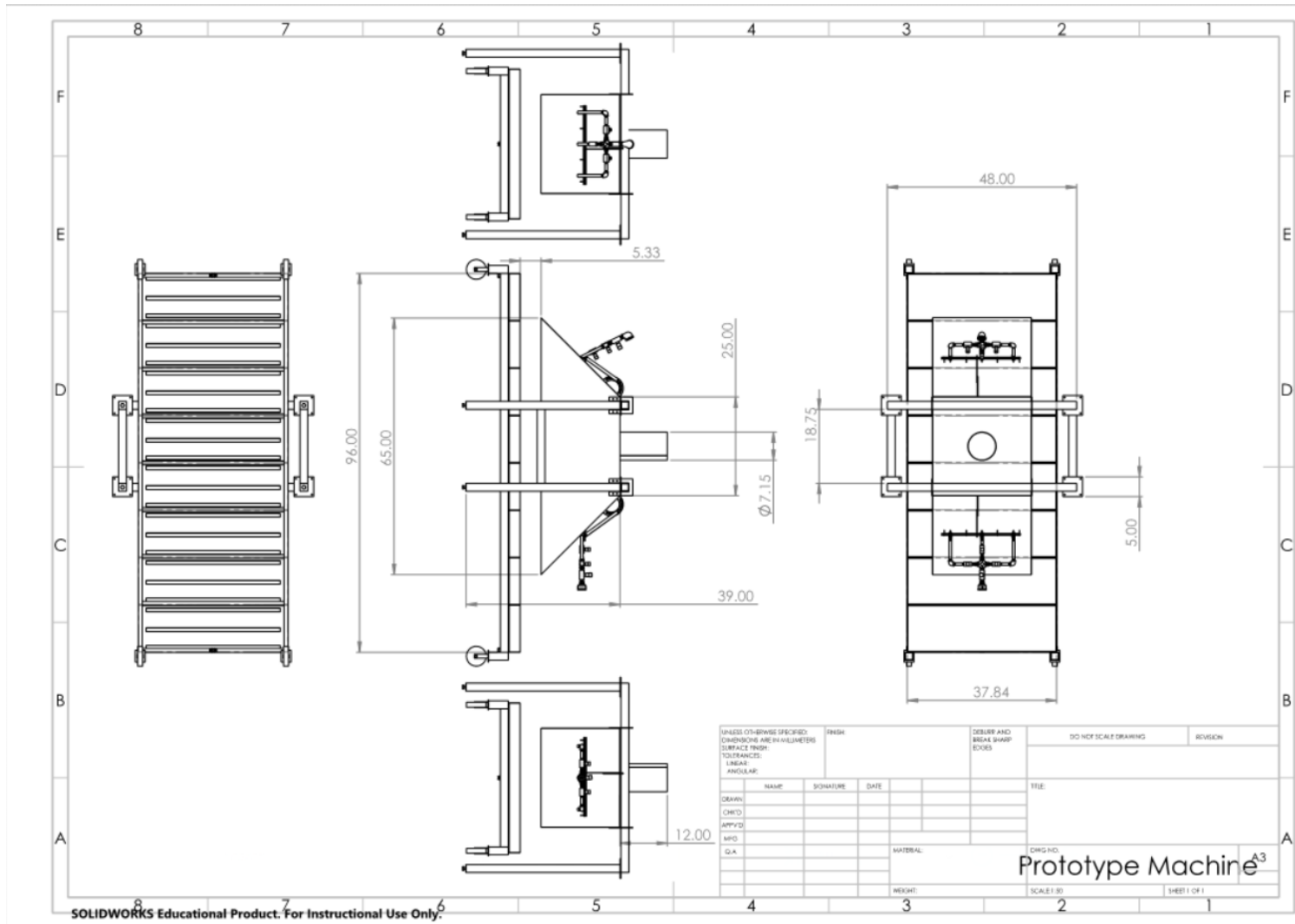
Treatments	Reps	Stack gas flow (scfm)	Stack gas velocity (ft/s)	Static Pressure (in H ₂ O)	
1 SET	Moving	R1	61.00	15.91	0
		R2	55.00	17.89	0
		R3	55.00	16.78	0
	Standstill	R1	77.00	17.44	0
		R2	68.00	15.73	0
		R3	61.00	16.16	0
2 SET	Moving	R1	126.00	19.92	0
		R2	125.00	18.45	0

Treatments	Reps	Stack gas flow (scfm)	Stack gas velocity (ft/s)	Static Pressure (in H ₂ O)
	R3	115.00	17.59	0
	R1	84.00	18.72	0
Standstill	R2	83.00	18.91	0
	R3	96.00	18.61	0

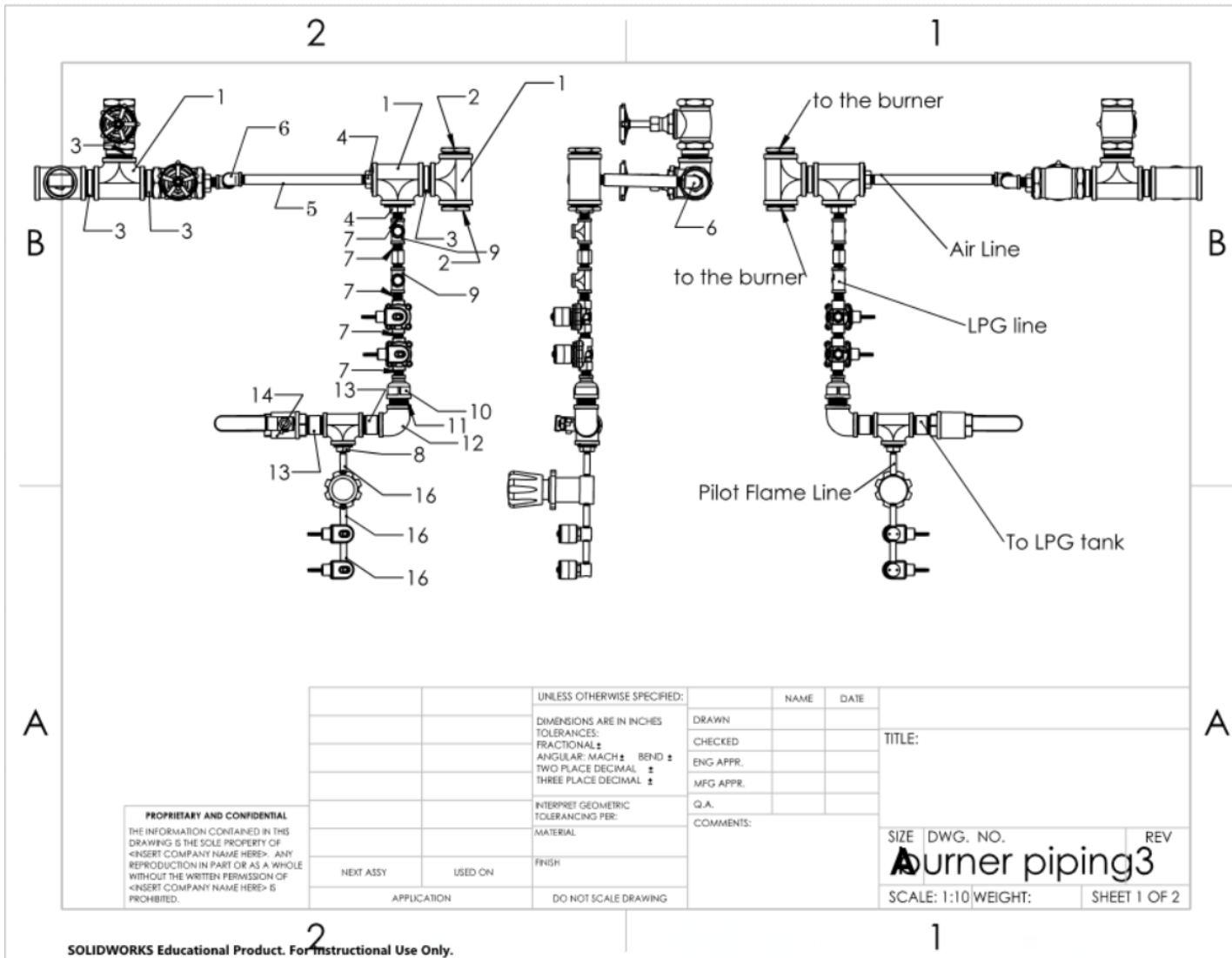
Appendix D1. One set of burner with 3/8" mixing tube



Appendix D2. The prototype crop residue burning machine



Appendix D3. Burner plumbing drawing



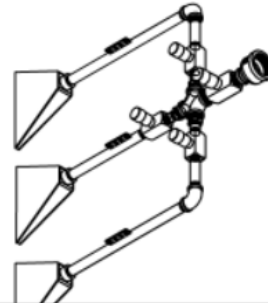
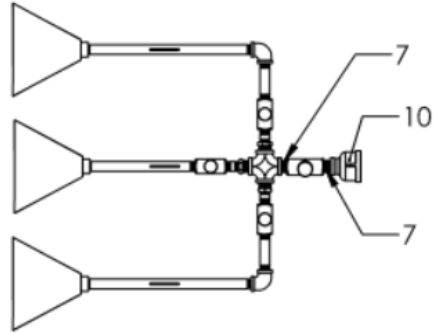
SOLIDWORKS Educational Product. For Instructional Use Only.

2

1

B

B



A

A

PROPRIETARY AND CONFIDENTIAL
 THE INFORMATION CONTAINED IN THIS DRAWING IS THE SOLE PROPERTY OF <INSERT COMPANY NAME HERE>. ANY REPRODUCTION IN PART OR AS A WHOLE WITHOUT THE WRITTEN PERMISSION OF <INSERT COMPANY NAME HERE> IS PROHIBITED.

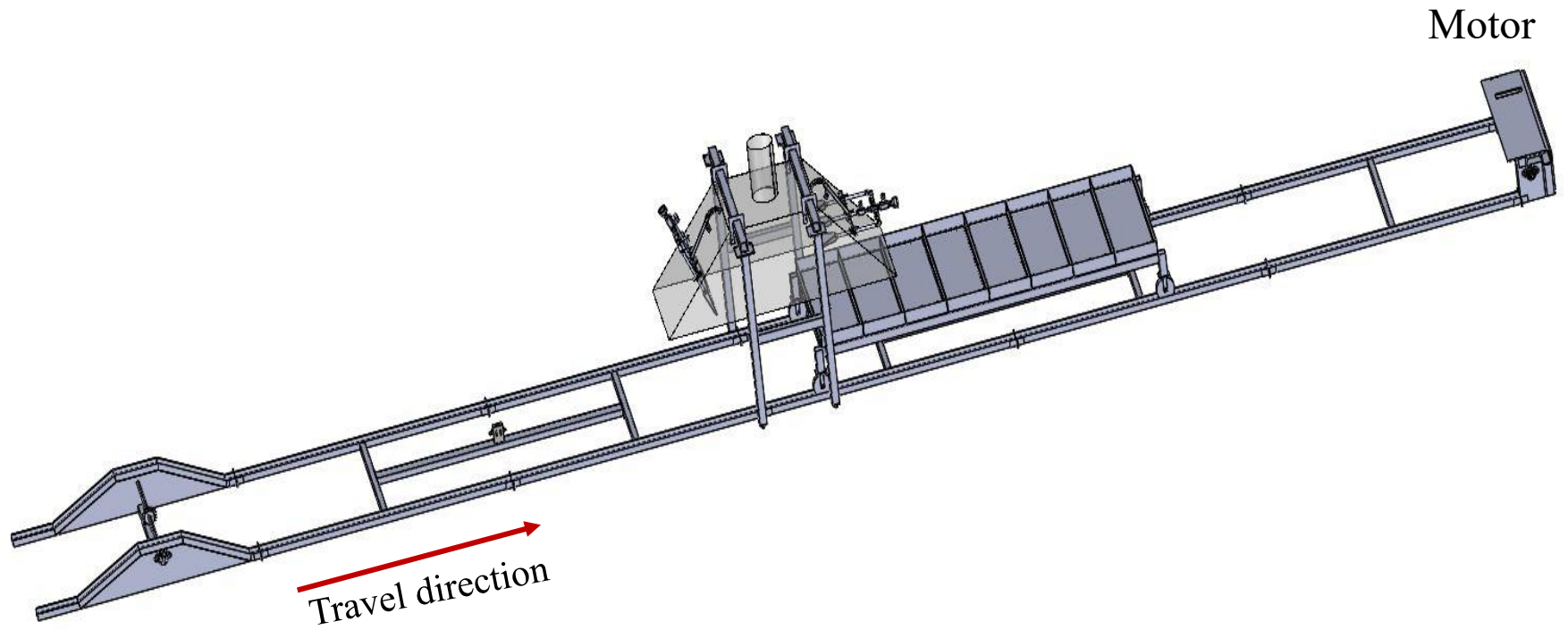
		UNLESS OTHERWISE SPECIFIED:		NAME	DATE	
		DIMENSIONS ARE IN INCHES		DRAWN		TITLE:
		TOLERANCES:		CHECKED		
		FRACTIONAL ±		ENG APPR.		
		ANGULAR: MACH ± BEND ±		MFG APPR.		
		TWO PLACE DECIMAL ±		Q.A.		
		THREE PLACE DECIMAL ±		COMMENTS:		
		INTERPRET GEOMETRIC TOLERANCING PER:				SIZE DWG. NO. REV
		MATERIAL				Turner piping3
NEXT ASSY	USED ON	FINISH				SCALE: 1:10 WEIGHT: SHEET 2 OF 2
		APPLICATION	DO NOT SCALE DRAWING			

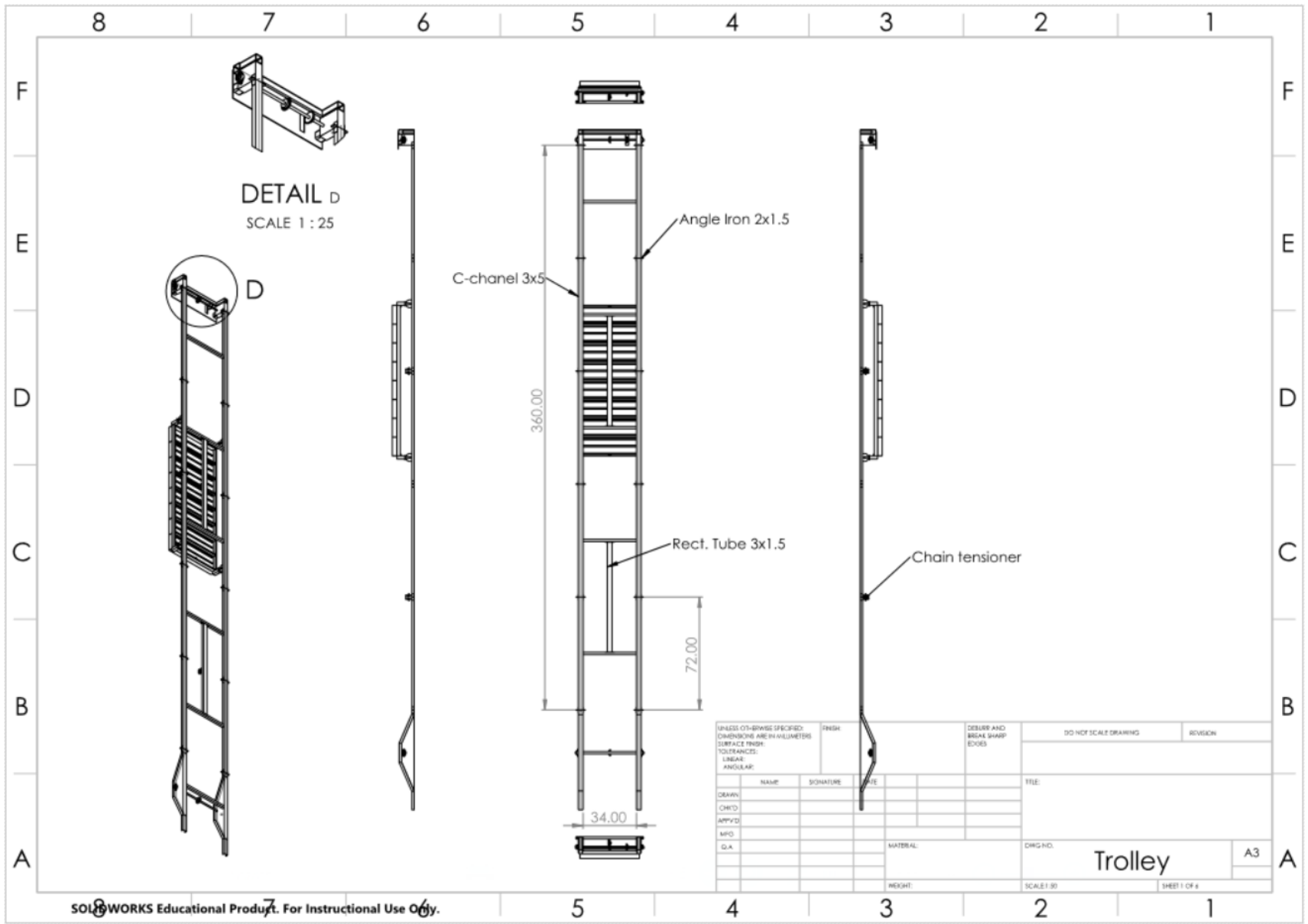
2

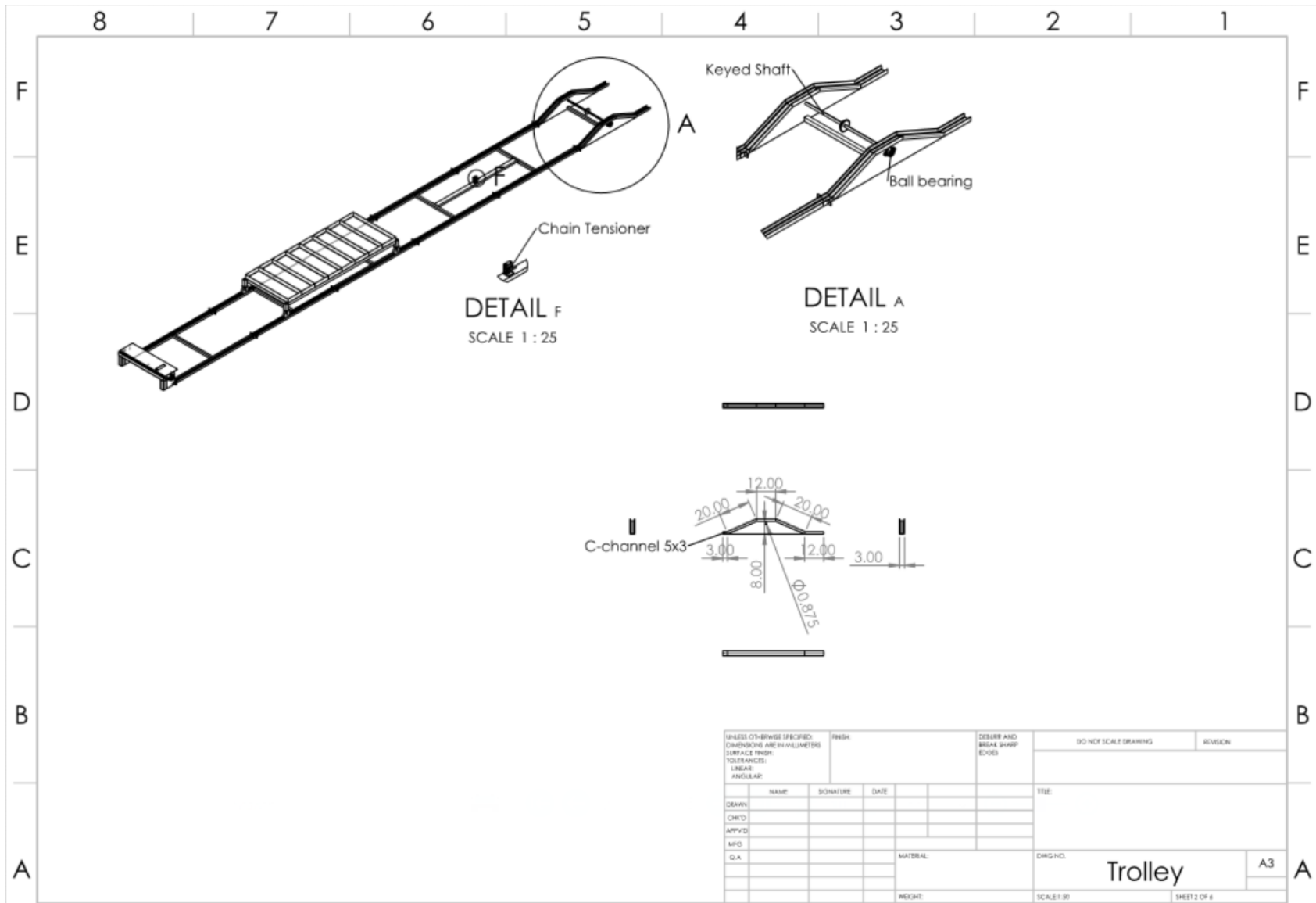
1

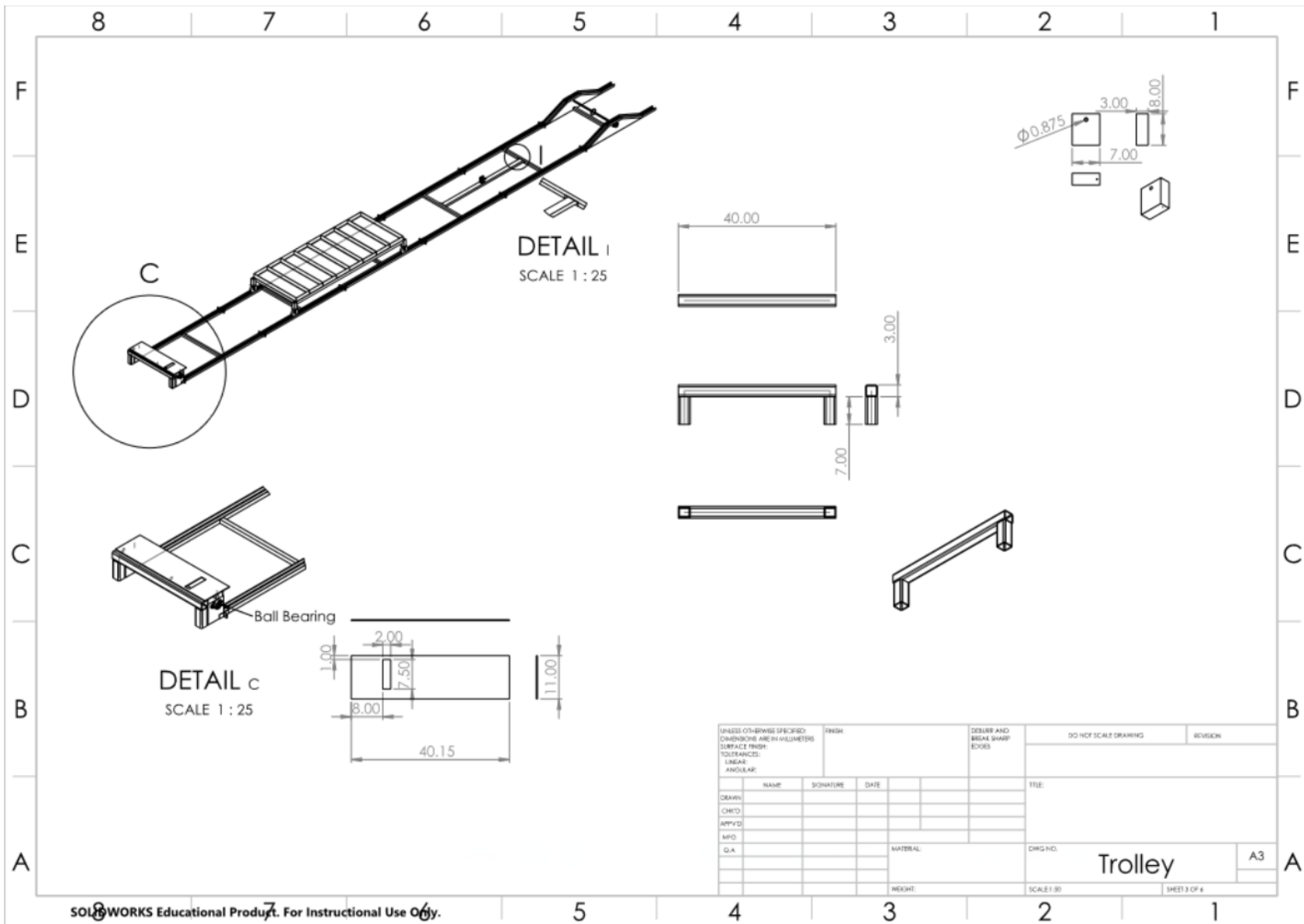
No	Parts	Descriptions	Quantity
1	Tee Connector 2" FNPT	https://www.mcmaster.com/44605k159	3
2	Hex Bushing 2"MNPTx1-1/4"FNPT	https://www.mcmaster.com/44605k626	2
3	Pipe Nipple 2" MNPT (L. 2-1/2")	https://www.mcmaster.com/44615k449	4
4	Hex Bushing 2" MNPT x1/2" FNPT	https://www.mcmaster.com/44605k719	2
5	Pipe Nipple 1/2" MNPT (L.12")	https://www.mcmaster.com/44615k544	1
6	Elbow 1/2" NPT	https://www.mcmaster.com/44605k114	2
7	Pipe Nipple 1/2" MNPT (L.1-1/2")	https://www.mcmaster.com/44615k424	7
8	Hex Bushing 2" MNPT x1/4" FNPT	https://www.mcmaster.com/44605k722	2
9	Tee Connector 1/2" FNPT	https://www.mcmaster.com/44605k154	2
10	Straight Reducer 1-1/4"x1/2" FNPT	https://www.mcmaster.com/44605k323	2
11	Pipe Nipple 1-1/4" MNPT (L. 2")	https://www.mcmaster.com/44615k437	1
12	Elbow 1-1/4 FNPT	https://www.mcmaster.com/44605k117	1
13	Pipe Nipple 1-1/4" MNPT (L. 3")	https://www.mcmaster.com/44615k457	2
14	On/Off Valve 1-1/4"x1-1/4" FNPT	https://www.mcmaster.com/47865k26	1
15	Hex Bushing 1-1/4" MNPTx1/4"FNPT	https://www.mcmaster.com/44605k714	1
16	Pipe Nipple 1/4" MNPT (L.3")	https://www.mcmaster.com/44615k452	3

Appendix D4. The trolley system drawing

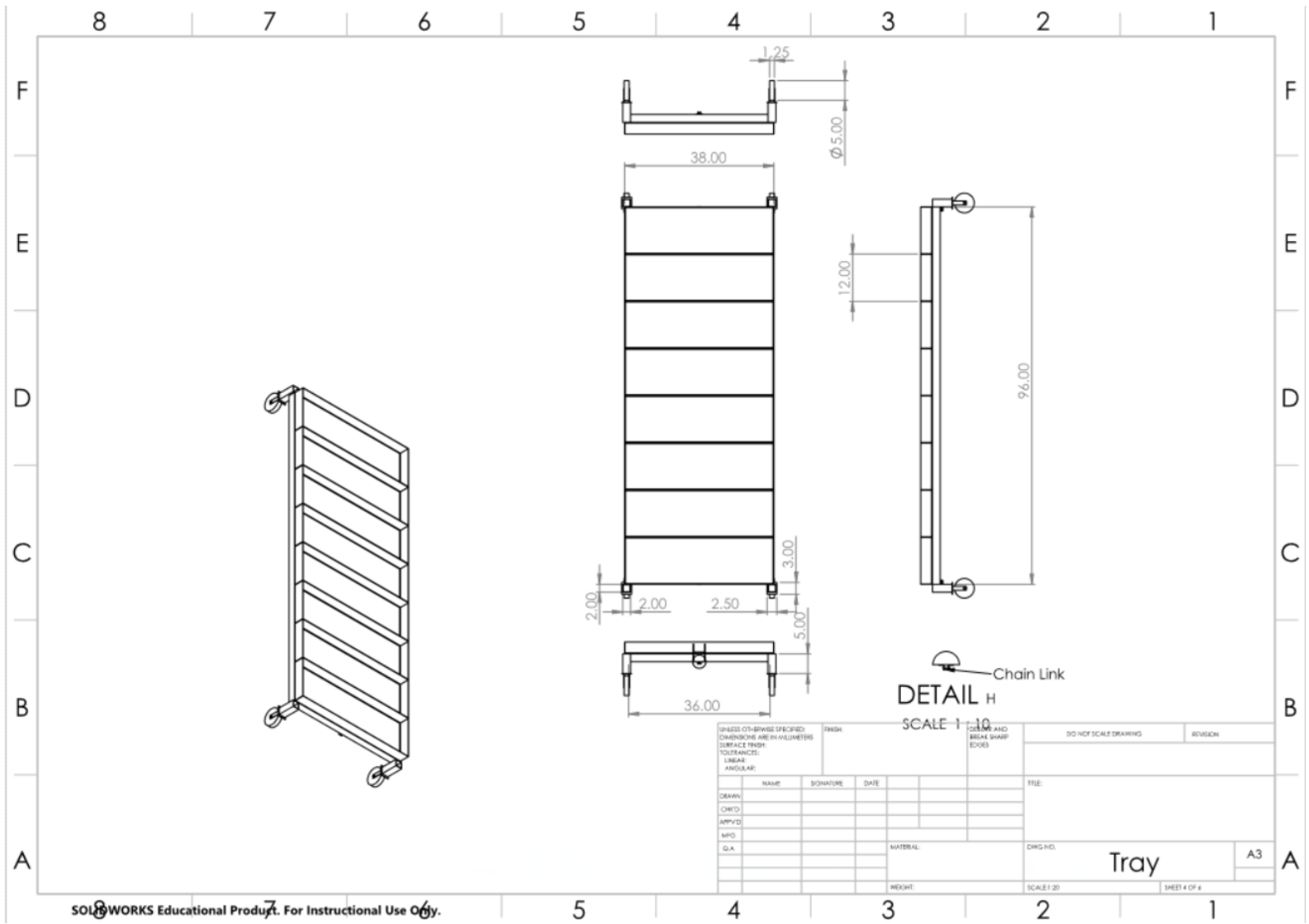




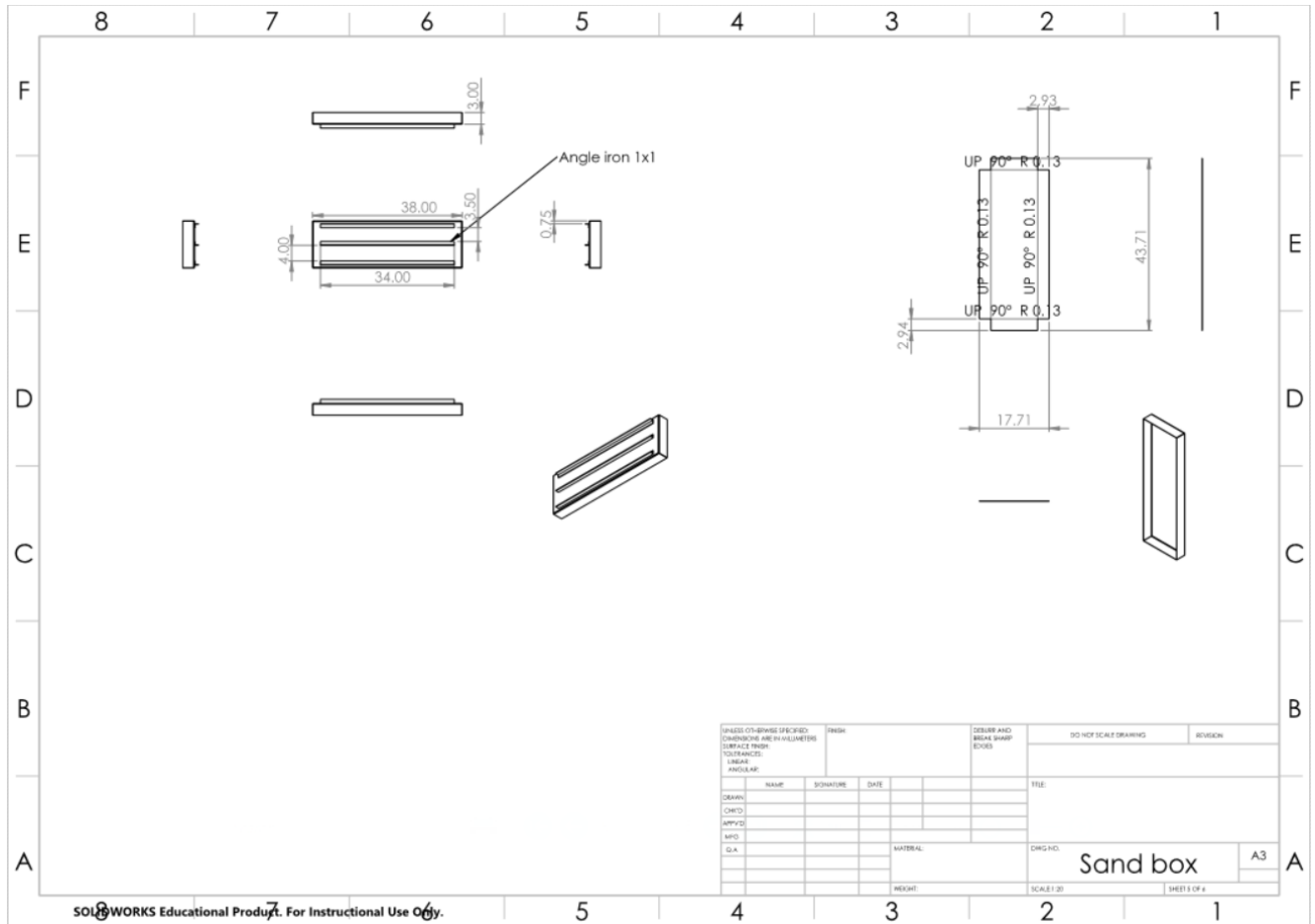




Appendix D5. Rectangular tray drawing



Appendix D6. Individual box drawing



VITA

Ni Nyoman Sulastri

Candidate for the Degree of

Doctor of Philosophy

Dissertation: THE DEVELOPMENT OF A PROTOTYPE CROP RESIDUE
BURNING MACHINE

Major Field: Biosystems Engineering

Biographical:

Education:

Completed the requirements for the Doctor of Philosophy in Biosystems Engineering at Oklahoma State University, Stillwater, Oklahoma in December 2019.

Completed the requirements for the Master of Agriculture in Environmental and Agricultural Science at Tokyo University of Agriculture and Technology/International Environmental and Agricultural Science, Tokyo, Japan in 2010

Completed the requirements for the Bachelor of Science in Agricultural Engineering at Universitas Gadjah Mada/Agriculture Technology, Yogyakarta, Indonesia in 2004

Experience: A junior staff in Udayana University, Bali, Indonesia for mentoring undergraduate students in some courses, especially in irrigation and natural resources conservations.

Professional Memberships: American Society of Biological and Agricultural Engineering (ASABE).